UNIVERSIDADE ESTADUAL PAULISTA
"JÚLIO DE MESQUITA FILHO"
FACULDADE DE MEDICINA

Felipe Cantore Tibúrcio

Aspectos morfológicos, funcionais e moleculares da interação neuromuscular após neurorrafia associada ao biopolímero heterólogo de fibrina

Tese apresentada à Faculdade de Medicina, Universidade Estadual Paulista "Júlio de Mesquita Filho", Câmpus de Botucatu, para obtenção do título de Doutor em Cirurgia e Medicina Translacional, Área de Morfologia.

Orientadora: Profa. Associada Selma Maria Michelin Matheus
Coorientadora: Profa. Dra. Cintia Yuri Matsumura

Botucatu - SP
2024

Felipe Cantore Tibúrcio

Aspectos morfológicos, funcionais e moleculares da interação neuromuscular após neurorrafia associada ao biopolímero heterólogo de fibrina

Tese apresentada à Faculdade de Medicina, Universidade Estadual Paulista “Júlio de Mesquita Filho”, Câmpus de Botucatu, para obtenção do título de Doutor em Cirurgia e Medicina Translacional, Área de Morfologia.

Orientadora: Profa. Associada Selma Maria Michelin Matheus
Coorientadora: Profa. Dra. Cintia Yuri Matsumura

Botucatu - SP
2024

FICHA CATALOGRÁFICA ELABORADA PELA SEÇÃO TÉC. AQUIS. TRATAMENTO DA INFORM.
DIVISÃO TÉCNICA DE BIBLIOTECA E DOCUMENTAÇÃO - CÂMPUS DE BOTUCATU - UNESP

BIBLIOTECÁRIA RESPONSÁVEL: MARIA CAROLINA A. CRUZ E SANTOS-CRB 8/10188

Tibúrcio, Felipe Cantore.
Aspectos morfológicos, funcionais e moleculares da interação neuromuscular após neurorrafia associada ao biopolímero heterólogo de fibrina / Felipe Cantore Tibúrcio. - Botucatu, 2024

Tese (doutorado) - Universidade Estadual Paulista (UNESP), Faculdade de Medicina, Botucatu
Orientador: Selma Maria Michelin Matheus
Coorientador: Cintia Yuri Matsumura
Capes: 20600003

1. Biopolímeros - Adesivo tecidual de fibrina. 2. Junção Neuromuscular. 3. Traumatismos dos Nervos Periféricos. 4. Músculo esquelético. 5. Regeneração Nervosa.

Palavras-chave: Biopolímero de fibrina; Junção neuromuscular; Lesão nervosa periférica; Músculo esquelético; Regeneração nervosa.

UNIVERSIDADE ESTADUAL PAULISTA

Câmpus de Botucatu

ATA DA DEFESA PÚBLICA DA TESE DE DOUTORADO DE FELIPE CANTORE TIBÚRCIO, DISCENTE DO PROGRAMA DE PÓS-GRADUAÇÃO EM CIRURGIA E MEDICINA TRANSLACIONAL, DA FACULDADE DE MEDICINA.

Aos 16 dias do mês de agosto do ano de 2024, às 09:00 horas, por meio de Videoconferência, realizou-se a defesa de TESE DE DOUTORADO de FELIPE CANTORE TIBÚRCIO, intitulada **Aspectos morfológicos, funcionais e moleculares da interação neuromuscular após neurorrafia associada ao biopolímero heterólogo de fibrina**. A Comissão Examinadora foi constituida pelos seguintes membros: Profa. Dra. SELMA MARIA MICHELIN MATHEUS (Orientador(a) - Participação Virtual) do(a) Depto. de Biologia Estrutural e Funcional / IB/Botucatu - Unesp, Profa. Dra. LUCIANA POLITTI CARTAROZZI (Participação Virtual) do(a) Depto. de Biologia Estrutural e Funcional / IB/Campinas - Unicamp, Prof. Dr. RENATO FERRETTI (Participação Virtual) do(a) Depto. de Biologia Estrutural e Funcional / IB/Botucatu - Unesp. Após a exposição pelo doutorando e arguição pelos membros da Comissão Examinadora que participaram do ato, de forma presencial e/ou virtual, o discente recebeu o conceito final: APROVADO . Nada mais havendo, foi lavrada a presente ata, que após lida e aprovada, foi assinada pelo(a) Presidente(a) da Comissão Examinadora.

gov.br
Documento assinado digitalmente
SELMA MARIA MICHELIN MATHEUS
Data: 19/08/2024 14:46:39-0300
Verifique em https://validar.iti.gov.br

Profa. Dra. SELMA MARIA MICHELIN MATHEUS

IMPACTO ESPERADO NA SOCIEDADE

O tratamento das lesões de nervo, sendo eficaz, tem um impacto significativo e positivo na sociedade, possibilitando melhorias substanciais na qualidade de vida dos pacientes afetados. Lesões nervosas, que podem resultar de traumas, acidentes, cirurgias ou doenças, frequentemente levam a dor crônica, perda de movimentos e sensibilidade, e comprometimento da capacidade de realizar atividades diárias. Com avanços na neurociência e nas técnicas de regeneração nervosa, como terapias com células-tronco, enxertos, medicamentos neuroprotetores e biomateriais, como o biopolímero heterólogo de fibrina, espera-se uma recuperação mais rápida e completa dos pacientes. Isso não apenas reduz a carga sobre os sistemas de saúde, devido a tratamentos prolongados e reabilitação, mas também promove a reintegração social e profissional dos indivíduos afetados, contribuindo para uma sociedade mais inclusiva, saudável e produtiva.

Esta tese está em acordo com o Objetivo de Desenvolvimento Sustentável 3 (ODS - ONU): Saúde e Bem-Estar, que busca garantir o acesso à saúde de qualidade e promover o bem-estar para todos, em todas as idades.

EXPECTED IMPACT ON SOCIETY

Effective treatment of nerve injuries has a significant and positive impact on society, offering substantial improvements in the quality of life of affected patients. Nerve injuries, which can result from trauma, accidents, surgery, or illness, often lead to chronic pain, loss of movement and sensation, and impaired ability to perform daily activities. With advances in neuroscience and nerve regeneration techniques, such as stem cell therapies, grafts, neuroprotective medications, and biomaterials, such as heterologous fibrin biopolymer, faster and more complete recovery for patients is expected. This reduces the burden on healthcare systems due to prolonged treatments and rehabilitation and promotes the social and professional reintegration of affected individuals, contributing to a more inclusive, healthy, and productive society.

This thesis is in accordance with Sustainable Development Goal 3 (SDG - UN): Health and Well-Being, which seeks to guarantee access to quality healthcare and promote well-being for everyone, at all ages.

DEDICATÓRIA

A Todos Os Pacientes Acometidos Por Lesões Nervosas Periféricas:

Que a Ciência e a Medicina um dia encontrem um tratamento que garanta a recuperação total e a devolução de uma vida justa e digna a eles.

"A medicina é uma luta pela vida boa, da qual a morte faz parte"

Rubem Alves.

AGRADECIMENTOS

A **Deus**, por ser meu refúgio, minha fortaleza e meu guia nos momentos bons e ruins desta jornada. Por me permitir sempre ir mais além e nunca desistir.

"Vosso é o reino, o poder e a glória para sempre"

A minha **família**, aos meus pais **Rosemeire Cantore** e **Osvaldo Tibúrcio**, aos meus avós **Maria Neuza Cantore** e **Deonísio Cantore** (*in memoriam*), a minha tia **Ana Cristina Cantore**, aos meus "primos-irmãos" **Caio Cantore**, **Maria Laura Cantore** e **Maria Beatriz Cantore**, e a minha "sobrinha" **Amora Cantore** (que ainda nem nasceu, mas que já traz consigo todo o amor e alegria para completar essa família). Obrigado estarem sempre ao meu lado, me apoiarem, confiarem e acreditarem em mim. Obrigado por todo o amor, carinho e união, que estejamos sempre juntos para o que der e vier.

A minha orientadora e "mãe científica" **Profa. Dra. Selma Matheus**, por ser uma orientadora excepcional e a melhor que eu poderia ter, apaixonada pelo que faz, um exemplo pessoal e profissional no qual eu me espelho. Por todas as oportunidades, aprendizados, conhecimento e experiência compartilhados, pela paciência, confiança e dedicação. Por todos os risos e choros e por estarmos sempre juntos na saúde e na doença, literalmente. Por me apoiar e me auxiliar em todas as minhas decisões acadêmicas e pessoais, que me permitiram chegar até aqui. Por sempre me encorajar a seguir a carreira da docência como anatomista e por despertar cada vez mais o meu amor pelo estudo e ensino da Anatomia.

"Minha decisão de ser anatomista foi para servir à humanidade através do meu trabalho não só como cientista, mas também como educador"

Liberato DiDio

A minha coorientadora **Profa. Dra. Cintia Matsumura**, por toda ajuda que possibilitaram o desenvolvimento deste trabalho. Por todo apoio e ensinamentos, amizade, carinho e dedicação. Por ser também minha orientadora didática, um exemplo pessoal e profissional, obrigado por toda ajuda, dicas e conhecimentos anatômicos compartilhados, que foram imprescindíveis para que eu pudesse chegar até aqui.

Ao meu companheiro de laboratório e amigo **Kevin Muller** e as minhas ICs e amigas **Manuela Silva** e **Stephanye Moreira**, por toda amizade, parceria e ajuda na realização de todas as etapas deste trabalho, sem vocês eu não teria conseguido, muito obrigado.

E a minha ex-parceira de laboratório amiga **Ana Paula Leite**, que mesmo já tendo terminado suas atividades e estando longe, me auxiliou na realização das análises de JNM. Obrigado por toda experiência e conhecimento compartilhados e por toda ajuda e dedicação.

Aos alunos, docentes e técnicos do **Setor de Anatomia** do Departamento de Biologia Estrutural e Funcional do IBB/Unesp/Botucatu, por todo auxílio, companheirismo, incentivo e amizade.

Em especial ao **Rinaldo Ortiz** e **Gelson Rodrigues**, técnicos do laboratório de histologia; e ao **Luciano Cunha**, **Paulo Silva** e **Marcos Pavan**, técnicos do laboratório didático de Anatomia, por todo o apoio técnico e aprendizado, e por toda a amizade construída ao longo desses anos.

E a todos os **Professores do Setor de Anatomia** que de alguma forma contribuíram para minha formação como anatomista, obrigado por todo aprendizado, confiança e oportunidade de ser Professor Bolsista durante os meus 3 anos de Doutorado.

"*Ao cadáver que, jacente na fria lousa do laboratório, me permitiu aprender Anatomia*"

Valdemar de Freitas

A todos os **meus alunos** dos cursos de Graduação do IBB e da FMB da Unesp. Em especial aos meus alunos da disciplina de Anatomia Humana do curso de Nutrição turma XXVI, minha última turma como Professor e como doutorando da Unesp. Quando assumimos o papel de professor devemos não só ensinar, mas também aprender, e eu aprendi muito com vocês.

Ao **Jorge Barros**, meu companheiro de vida, obrigado por todos os momentos que vivemos e que ainda vamos viver e por estar sempre comigo nas alegrias e tristezas, na saúde e na doença, literalmente. Por toda convivência, dedicação e por me apoiar sempre. Por sempre me ajudar e me aguentar, e por fazer os meus dias e a minha vida mais feliz. Que em nosso novo ciclo que iniciaremos em breve, nunca deixemos de lembrar que nosso lar será sempre onde estivermos juntos.

"Então o destino trouxe sua recompensa, um novo mundo para chamarmos de casa"

A minha amiga **Fernanda France**, que acabou se tornando uma irmã que Botucatu me deu, obrigado por todo apoio, companheirismo, preocupação, paciência, diversão... Obrigado por todos os momentos que vivemos juntos nesses quase 10 anos de amizade e pelos outros mais que ainda vamos viver. Sou muito grato e honrado por ter você em minha vida.

As minhas amigas **Lorraine Requena, Victória Mokarzel** e **Joyce Rizzi**, amizades especiais que começaram em Botucatu e vou levar para a vida toda. Obrigado por todo apoio e companheirismo, pelas infinitas risadas e conversas, pelos cafés e reflexões, por me entenderem e me ajudarem a sempre a seguir em frente nesta jornada chamada pós-graduação.

A minha amiga **Thamiris Figueiredo**, que passou de amiga, a vizinha, a colega de casa, e agora é uma das saudades que Botucatu nos deixa. Obrigado por todo companheirismo e apoio, pelos momentos divertidos, conversas e risadas que tivemos e que ainda teremos nesses vastos anos da nossa vida.

Aos **Profs. Drs. José de Anchieta Horta-Júnior** e **Carla Machado**, pela participação em minhas Bancas de Acompanhamento e em minha Qualificação, que permitiram melhorar substancialmente este trabalho. E por serem meus grandes mestres da Neuroanatomia, obrigado por todo ensinamento, parceria e por acentuarem ainda mais minha paixão pelo estudo do Sistema Nervoso.

"Provavelmente, o mais bonito, elegante, e complexo sistema do corpo"

Hal Blumenfeld

Ao **Dr. André Luís Bombeiro**, obrigado pela dedicação e paciência para aprovação da minha bolsa de doutorado sanduíche no exterior, mesmo não tendo sido implementada.

Aos **Profs. Drs. Renato Ferretti** e **Luciana Cartarozzi**, membros titulares da minha banca de defesa, e aos **Profs. Drs. Tais Harumi de Castro Sasahara**, **Patrícia Villela e Silva** e **Bruno Cesar Schimming**, membros suplentes, por terem aceitado este convite e pelas contribuições.

Aos **animais** que doaram involuntariamente suas vidas para a realização deste trabalho e para o desenvolvimento da Ciência.

Ao **Programa de Pós-Graduação em Cirurgia e Medicina Translacional** da FMB/Unesp, que me permitiu realizar este Doutorado.

Em especial a **Márcia Cruz**, secretária do Programa, por todo auxílio burocrático e por estar sempre pronta a nos atender e ajudar.

E a minha colega de pós-graduação **Mariana Santesso**, por toda amizade e parceria nesses anos de representação discente, pelas conversas burocráticas e pessoais. Sobrevivemos juntos a essa etapa.

A **Unidade de Pesquisa Experimental (Unipex)** da FMB/Unesp e seus servidores, pela estrutura e auxílio físico e instrumental, que foram indispensáveis para realização deste estudo.

Em especial aos técnicos do Laboratório de Cirurgia Experimental, **Zé** e **Bardella**; aos bioteristas, **Robson** e **Sílvio**; ao veterinário responsável, **Diego Generoso**; e ao técnico do Laboratório de Microscopia Confocal, **Leandro Alves**.

Ao **Centro de Microscopia Eletrônica** do IBB/Unesp, pelo uso dos equipamentos. Em especial a **Shelly Carvalho**, técnica do microscópio confocal, por todo auxílio com a obtenção das imagens, e pelas longas conversas, amizade e parceria de sempre.

Ao **Centro de Estudos de Venenos e Animais Peçonhentos (CEVAP)** e ao **Centro de Ciência Translacional e Desenvolvimento de Biofármacos (CTS)** da Unesp de Botucatu, pela colaboração científica e por ceder o biopolímero de fibrina para a realização deste trabalho.

As agências de fomento **Coordenação de Aperfeiçoamento de Pessoal de Nível Superior (CAPES)**, pela concessão da bolsa de Doutorado; a **Fundação de Amparo à Pesquisa do Estado de São Paulo (FAPESP)**, pela concessão da bolsa de iniciação científica vinculada a este estudo (processo nº 23/16239-4); e a **Coordenadoria de Permanência Estudantil (COPE-UNESP)**, pela bolsa COPE Conecta vinculada a este trabalho.

A todos que fizeram parte da minha vida acadêmica e pessoal nesses quase 10 anos de UNESP, que agora me recordo e que não cabem nestas poucas linhas, mas que sempre estarão nas entrelinhas da minha vida.

RECORDAR: do latim "re-cordis", voltar a passar pelo coração...
Eduardo Galeano

Muito Obrigado!

EPÍGRAFE

"Dos nossos medos nascem as nossas coragens,
e em nossas dúvidas, vivem as nossas certezas.
Os sonhos anunciam outra realidade possível, e
os delírios, outra razão"

Eduardo Galeano

LISTA DE ILUSTRAÇÕES

Figura 1. Representação esquemática de um nervo em corte transversal (página 18).

Figura 2. Representação esquemática da inervação do músculo estriado esquelético (página 19).

Figura 3. Representação dos compartimentos da junção neuromuscular (pré-sináptico, fenda sináptica e pós-sináptico) (página 20).

Figura 4. Estrutura do receptor nicotínico de acetilcolina (página 21).

Figura 5. Representação dos compartimentos da junção neuromuscular, AChR e proteínas associadas (Agrina/Lrp4/MusK/Rapsina) (página 22).

Figura 6. Representação da classificação das lesões nervosas periféricas de acordo com Seddon (1943) e Sunderland (1951) (página 23).

Figura 7. Representação esquemática da degeneração Walleriana (página 24).

Figura 8. Representação esquemática das repercussões da lesão nervosa periférica na junção neuromuscular (página 25).

Figura 9. Fotografias das técnicas cirúrgicas realizadas em todos os grupos experimentais (página 33).

Figura 10. Embalagem e frascos do biopolímero heterólogo de fibrina (página 34).

Figura 11. Polimerização do biopolímero heterólogo de fibrina, formando um biocomplexo constituído por uma rede de fibrina (página 34).

Figura 12. Equipamento para análise funcional da marcha (CatWalk XT) (página 36).

Figura 13. Fluxograma da análise da JNM e dos AChR utilizando o plugin NMJ-morph (página 39).

Figura 14. Ilustrações e gráficos da análise funcional da marcha (CatWalk XT) para os grupos experimentais nos diferentes momentos de avaliação (página 42).

Figura 15. Gráficos de peso corpóreo e peso do músculo sóleo (página 43).

Figura 16. Fotomicrografias de secções transversais e gráficos da morfometria do nervo isquiático de acordo com os grupos experimentais (página 45).

Figura 17. Fotomicrografias de cortes transversais e gráficos da morfometria do músculo sóleo de acordo com os grupos experimentais (página 47).

Figura 18. Microscopia confocal dos receptores de acetilcolina e terminais nervosos (página 49).

Figura 19. Gráficos das análises da JNM por meio do NMJ-morph (página 50).

LISTA DE ABREVIATURAS E SIGLAS

ACh – Acetilcolina

AChE – Acetilcolinesterase

ANOVA – Análise de variância

BHF – Biopolímero Heterólogo de Fibrina

C – Grupo Controle

CEVAP – Centro de Estudos de Venenos e Animais Peçonhentos

D – Grupo Desnervado

FMB – Faculdade de Medicina de Botucatu

HE – Hematoxilina e Eosina

IFF – Índice funcional do Fibular

IBB – Instituto de Biociências de Botucatu

IR – Índice de Regularidade

JNM – Junção neuromuscular

LNP – Lesão nervosa periférica

LRP4 – Receptor lipoproteico relacionado a proteína 4

MMP3 – Metaloproteinase de matriz 3

MRFs – Fatores de regulação miogênica

MuSK – Receptor tirosina quinase músculo-específico

N – Grupo Neurorrafia

AChR – Receptores nicotínicos de acetilcolina

NB – Grupo Neurorrafia + BHF

NCAMs – Moléculas de adesão de células neurais

NSSP – Número de padrões normais de sequência de passos

PBS – Tampão fosfato salino

PP – Número total de colocações de patas

SEM – Erro padrão da média

SN – Sistema nervoso

SNC – Sistema nervoso central

SNP – Sistema nervoso periférico

TBS-T – Tampão tris salino com Tween 20

UNESP – Universidade Estadual Paulista

v – Versão

RESUMO

Os nervos são estruturas frágeis propensas a danos causados por traumas que interrompem a condução nervosa. As lesões nervosas periféricas (LNPs) afetam, além do nervo, os músculos inervados e as junções neuromusculares (JNMs) a eles associadas, levando a diversas alterações morfofuncionais e moleculares. Apesar dos avanços nas técnicas cirúrgicas, a neurorrafia (sutura) ainda é considerada o "padrão ouro", mas a recuperação após LNP raramente é completa. Métodos adjuvantes vêm sendo utilizados para acelerar a regeneração e melhorar a recuperação neuromuscular, entre eles, o biopolímero heterólogo de fibrina (BHF). O objetivo deste estudo foi avaliar os efeitos da neurorrafia associada ao BHF na regeneração nervosa e nos aspectos morfofuncionais da interação neuromuscular. Foram utilizados 60 ratos Wistar machos adultos (CEUA-FMB: 1402/2021), distribuídos em quatro grupos (n=15/grupo): Grupo Controle (C): dissecção e localização do nervo isquiático direito. Grupo Desnervado (D): transecção do nervo (neurotmese) e remoção de fragmento de 6 mm, com os cotos nervosos invertidos e fixados na tela subcutânea adjacente. Grupo Neurorrafia (N): neurotmese seguida de neurorrafia término-terminal. Grupo Neurorrafia + BHF (NB): neurotmese seguida de neurorrafia, com adição do BHF. Um dia antes e 120 dias após as cirurgias, foi realizada a análise funcional da marcha (CatWalk XT) de todos os animais. Aos 120 dias após a cirurgia, os animais foram eutanasiados, e os nervos isquiáticos e músculos sóleos foram coletados para análises morfológicas e morfométricas. Na análise funcional, o grupo NB foi o único a apresentar resultados semelhantes ao grupo C e diferentes do grupo D em relação a parâmetros de coordenação (índice de regularidade e número de passos). Em relação ao peso do músculo sóleo, os grupos N e NB apresentaram valores intermediários, maiores que o grupo D e menores que o grupo C, mas iguais entre si. Na morfometria do nervo, todos os parâmetros foram menores nos grupos reconstruídos (N e NB), semelhantes entre si e diferentes do grupo C. A morfometria das fibras musculares mostrou no grupo NB resultados mais próximos do grupo C, nos parâmetros de área, perímetro e diâmetro das fibras. Quanto à porcentagem de colágeno intramuscular, o grupo NB foi o único semelhante ao grupo C, sendo diferente dos grupos N e D. A análise morfométrica das JNMs e AChR evidenciou que o grupo NB apresentou resultados semelhantes ao grupo C e diferentes dos grupos N e D em relação à área dos AChR e da placa motora e número de clusters; nos demais parâmetros, o grupo NB mostrou maior proximidade ao grupo C. Esses resultados demonstram que o BHF contribuiu para a recuperação funcional parcial, a restauração morfológica das JNMs e dos AChR aos padrões normais, além de promover a reinervação das placas motoras e a regeneração das fibras musculares. Esses efeitos contribuem para uma melhora global na regeneração neuromuscular. Em conclusão, a combinação de neurorrafia e BHF surge como uma abordagem médica emergente e economicamente viável, vantajosa no reparo de nervos periféricos.

Palavras-chave: biopolímero heterólogo de fibrina, junção neuromuscular, lesão nervosa periférica, músculo esquelético, neurorrafia, regeneração nervosa.

ABSTRACT

Nerves are fragile structures prone to damage caused by trauma that interrupts nerve conduction. Peripheral nerve injuries (PNIs) affect, in addition to the nerve, the innervated muscles and associated neuromuscular junctions (NMJs), leading to several morpho-functional and molecular alterations. Despite advances in surgical techniques, neurorrhaphy (suture) is still considered the “gold standard”, but recovery after PNI is rarely complete. Adjuvant methods have been used to accelerate regeneration and improve neuromuscular recovery, including heterologous fibrin biopolymer (HFB). This study aimed to evaluate the effects of neurorrhaphy associated with HFB on nerve regeneration and the morphofunctional aspects of neuromuscular interaction. Sixty adult male Wistar rats (CEUA-FMB: 1402/2021) were distributed into four groups (n = 15/group): Control Group (C): dissection and location of the right sciatic nerve. Denervated Group (D): nerve transection (neurotmesis) and removal of a 6 mm fragment, with the nerve stumps inverted and fixed to the adjacent subcutaneous tissue. Neurorrhaphy Group (N): neurotmesis followed by end-to-end neurorrhaphy. Neurorrhaphy + HFB Group (NB): neurotmesis followed by neurorrhaphy, with the addition of HFB. One day before and 120 days after surgeries, functional gait analysis (CatWalk XT) was performed on all animals. At 120 days after surgery, the animals were euthanized, and the sciatic nerves and soleus muscles were collected for morphological and morphometric analyses. In the functional analysis, the NB group was the only one to present results like group C and different from group D concerning coordination parameters (regularity index and number of steps). Regarding the weight of the soleus muscle, groups N and NB presented intermediate values, greater than group D and smaller than group C, but equal. In the nerve morphometry, all parameters were lower in the reconstructed groups (N and NB), like each other, and different from group C. The morphometry of the muscle fibers showed that group NB obtained results closer to group C, in terms of the fibers' area, perimeter, and diameter. Regarding the percentage of intramuscular collagen, group NB was the only one like group C, being different from groups N and D. The morphometric analysis of the NMJs and AChR showed that group NB presented results like group C and different from groups N and D about the area of the AChR and motor endplate and number of clusters; In the other parameters, the NB group showed greater proximity to group C. These results demonstrate that HFB contributes to partial functional recovery, and morphological restoration of NMJs and AChRs to normal patterns, in addition to promoting reinnervation of motor endplates and regeneration of muscle fibers. These effects contribute to an overall improvement in neuromuscular regeneration. In conclusion, the combination of neurorrhaphy and HFB emerges as an emerging and economically viable medical approach advantageous in peripheral nerve repair.

Keywords: heterologous fibrin biopolymer, neuromuscular junction, peripheral nerve injury, neurorrhaphy, nerve regeneration, skeletal muscle.

SUMÁRIO

Introdução 17

Justificativa 29

Objetivos 31

Material e Métodos 32

Resultados 42

Discussão 52

Conclusões 58

Referências 59

Artigo (Manuscrito em Inglês) 66

Anexo I (Certificado CEUA) 93

Anexo II (Artigo de Revisão) 96

INTRODUÇÃO

ORGANIZAÇÃO GERAL DO SISTEMA NERVOSO PERIFÉRICO

O sistema nervoso (SN) é formado por uma complexa rede de células altamente especializadas que transmitem sinais elétricos (impulsos nervosos) de e para as diferentes regiões do corpo, coordenando todas as suas funções (HUSSAIN et al., 2020). Este sistema pode ser dividido anatomicamente em duas partes: sistema nervoso central (SNC), constituído pelo encéfalo e pela medula espinal; e o sistema nervoso periférico (SNP), composto por nervos, gânglios e terminações nervosas (BEAR; CONNORS; PARADISO, 2020; MURTAZINA; ADAMEYKO, 2023).

As células que compõe o SN são divididas em dois grupos: neurônios e células da glia (neuroglia). Os neurônios são constituídos por um corpo celular, do qual tem origem os dendritos e o axônio. Estas células são responsáveis pela recepção, processamento e transmissão de estímulos, por meio da geração e condução de impulsos nervosos. As células da glia possuem papel de sustentação e defesa dos neurônios, e incluem, no SNP, células de Schwann e células satélites (BEAR; CONNORS; PARADISO, 2020; MURTAZINA; ADAMEYKO, 2023).

Os axônios, no SNP, associam-se a células de Schwann, que emitem projeções da sua membrana plasmática, envolvendo os axônios. Essa associação pode formar as bainhas de mielina, cuja função é o isolamento elétrico, visando o aumento da velocidade de condução do impulso nervoso. Os axônios mais o seu envoltório glial são denominados de fibras nervosas, que podem ser mielinizadas ou não (BEAR; CONNORS; PARADISO, 2020; MURTAZINA; ADAMEYKO, 2023).

A maioria das fibras nervosas do SNP é mielinizada, nas quais a célula de Schwann se enrola em volta do axônio e da origem à bainha de mielina (Figura 1), um complexo lipoproteico constituído por diversas camadas de membrana celular modificada, possuindo maior quantidade de lipídeos do que as membranas celulares em geral. A bainha de mielina não se estende continuamente ao longo de todo o comprimento do axônio, essa bainha se interrompe em intervalos regulares formando espaços sem mielinização, denominados de nodos de Ranvier. Esses nodos são recobertos por expansões laterais das células de Schwann, que vão garantir a condição saltatória dos sinais elétricos, aumentado a velocidade de condução do impulso nervoso (GEUNA et al., 2009; BEAR; CONNORS; PARADISO, 2020; MURTAZINA; ADAMEYKO, 2023).

NERVOS PERIFÉRICOS

Os nervos, principais constituintes do SNP, são formados por feixes de fibras nervosas, e possuem a função de associar diferentes partes do corpo ao sistema nervoso central (SNC). Os sinais sensoriais são transmitidos ao SNC por meio das fibras nervosas sensitivas (aferentes), e a resposta gerada é conduzida pelas fibras nervosas motoras (eferentes) até os órgãos-alvo. Assim, uma via de comunicação mútua é estabelecida entre o SNC e áreas periféricas do corpo (HUSSAIN et al., 2020; MURTAZINA; ADAMEYKO, 2023).

Morfologicamente, cada nervo (Figura 1) é constituído externamente pelo epineuro, uma camada de tecido conjuntivo denso fibroso que reveste o nervo e envolve os feixes de fibras nervosas, denominados de fascículos nervosos. O epineuro possui um arranjo mais espaçado de fibras colágenas, e ainda inclui células adiposas, além de ser vascularizado por capilares fenestrados, ou seja, que possuem orifícios (fenestras) em sua camada de células endoteliais. Cada fascículo nervoso é revestido pelo perineuro, formado por várias camadas de células robustas, achatadas e justapostas (células perineurais), unidas por junções oclusivas e interpostas por lâmina basal. O perineuro é permeado por pequenos vasos sanguíneos, que irrigam o tecido nervoso, denominados de *vasa nervorum* ou vaso dos nervos, cujas células endoteliais são unidas por junções oclusivas. Devido a isso, o perineuro é uma das camadas que constitui a barreira hematoneural (ou hematonervosa), uma barreira que previne a passagem de muitas macromoléculas e agentes nocivos, sendo assim, um importante mecanismo de defesa para o SNP. Dentro de cada fascículo encontram-se os axônios, cada um envolvido pelas células de Schwann, com sua lâmina basal, e um envoltório de tecido conjuntivo frouxo, o endoneuro. O endoneuro é constituído principalmente por células endoneurais, fibras colágenas, fibras reticulares sintetizadas pelas células de Schwann, além de outros elementos da matriz extracelular. O endoneuro é permeado por capilares sanguíneos que provêm dos *vasa nervorum*, e com isso, suas células endoteliais também formam junções oclusivas impermeáveis, estabelecendo efetivamente a barreira hematoneural (KERNS, 2008; GEUNA et al., 2009).

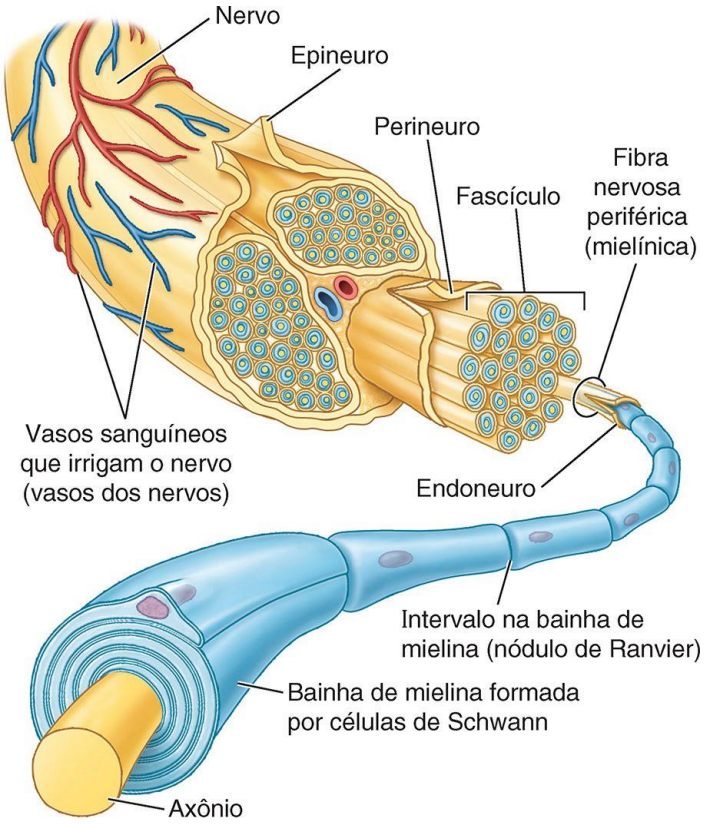


Figura 1. Representação esquemática de um nervo em corte transversal. Organização e formação da bainha nas fibras nervosas mielínicas. Os nervos são formados por feixes de fibras nervosas, as camadas de tecido conjuntivo que os unem e os vasos sanguíneos (*vasa nervorum*) que os irrigam. Todos os nervos, exceto os menores, estão organizados em feixes denominados fascículos. Adaptado de Moore, Dalley & Agur (2019).

Os nervos podem ser classificados anatomicamente, de acordo com a sua origem, em cranianos e espinais, e funcionalmente em sensitivos, motores e mistos. Os nervos espinais, em sua origem, são todos mistos, formados por fibras nervosas sensitivas e motoras, mas que podem apresentar ramos periféricos predominantemente sensitivos ou motores.(HUSSAIN et al., 2020; MURTAZINA; ADAMEYKO, 2023).

Os axônios das fibras nervosas motoras dos nervos espinais são projeções de neurônios, cujos corpos celulares estão localizados na coluna anterior (ventral) da medula espinal (Figura 2), para função motora somática. Entre as fibras nervosas motoras temos o neurônio motor inferior (Figura 2), uma célula altamente especializada e com uma arborização dendrítica desenvolvida. Esse neurônio consiste em um dos principais pontos de conexão do SNC com o SNP, e ao alcançar seu órgão-alvo, o músculo estriado esquelético, forma uma região morfofuncional e molecularmente especializada denominada de junção neuromuscular (JNM). Neste local, ocorre a transmissão e a transdução de um sinal elétrico (impulso nervoso) e químico (neurotransmissores) do neurônio motor para a fibra muscular (Figura 2), promovendo a contração muscular. Essa junção representa a principal classe de sinapse química no sistema nervoso dos mamíferos, crítica para a transferência de informações entre

o sistema nervoso e o músculo esquelético. Também representa uma sinapse "modelo" convenientemente acessível dentro do SNP (JONES et al., 2017; BOEHM et al., 2020; ARNOLD; CLARK, 2023).

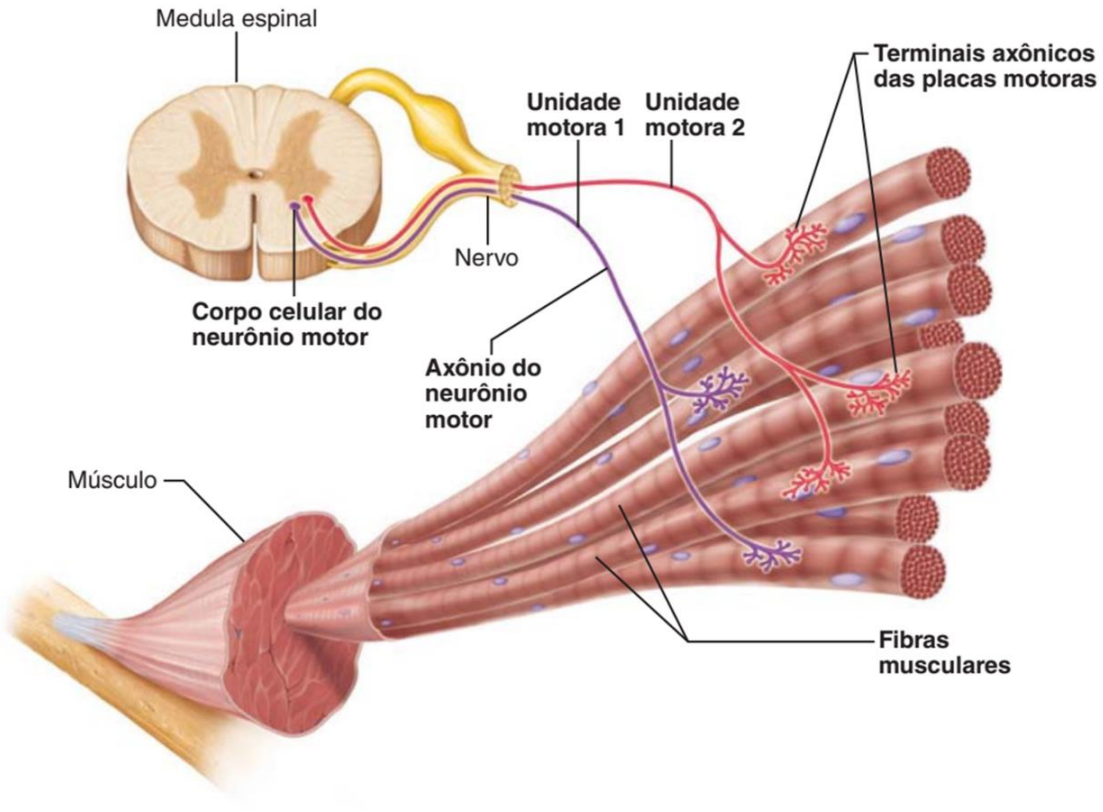


Figura 2. Representação esquemática da inervação do músculo estriado esquelético, desde a origem do neurônio motor inferior na coluna anterior da medula espinal até sua conexão com a fibra muscular, formando a junção neuromuscular (placa motora). Adaptado de Marieb et al (2014).

JUNÇÃO NEUROMUSCULAR

Morfologicamente, as JNMs são formadas por três compartimentos: o compartimento pré-sináptico, onde estão presentes o terminal nervoso do neurônio motor inferior, com as vesículas sinápticas contendo o neurotransmissor acetilcolina (ACh), e as células de Schwann terminais, específicas desta região; o compartimento extracelular ou fenda sináptica, preenchido pela lâmina basal; e o compartimento pós-sináptico ou placa motora, que compreende a membrana plasmática da fibra muscular (sarcolema) com as dobras juncionais, onde se encontram os receptores nicotínicos de acetilcolina (AChR) e o citoplasma da fibra muscular (sarcoplasma) (Figura 3) (LEPORE et al., 2019; BOEHM et al., 2020; DESCHENES et al., 2022)

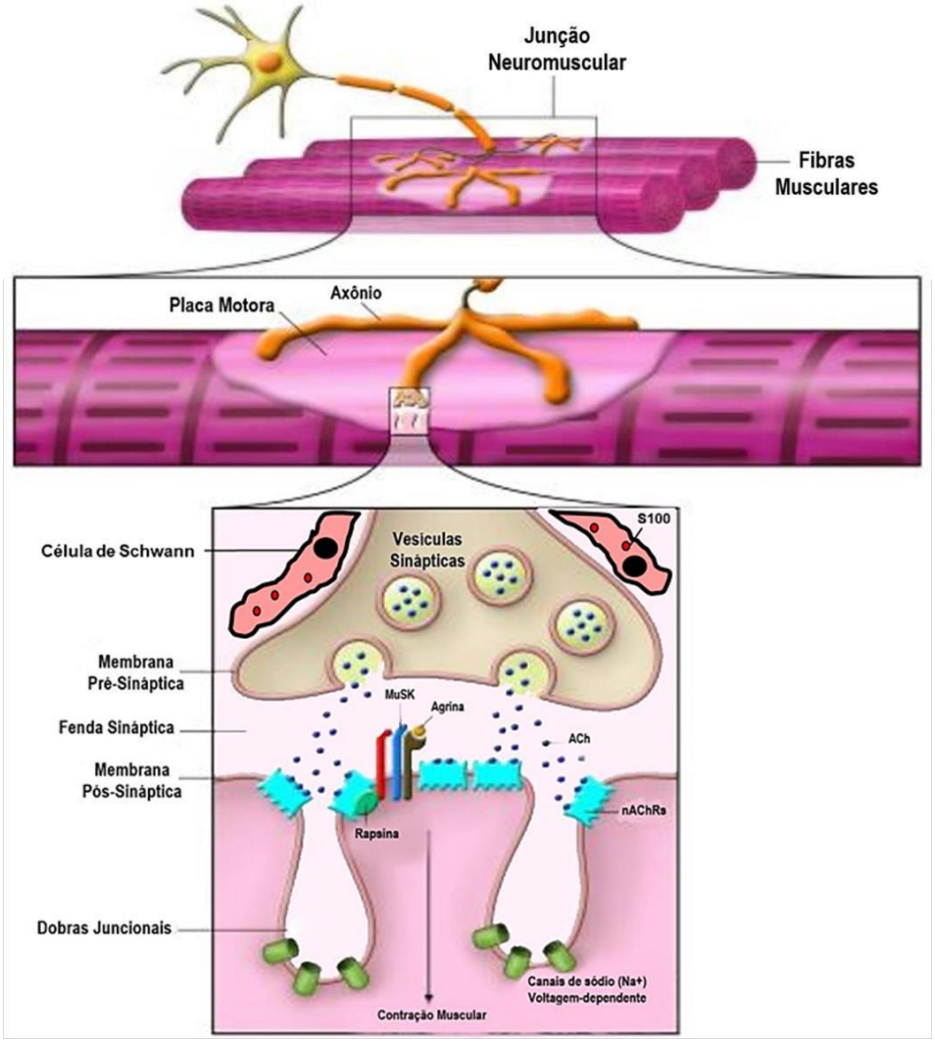


Figura 3. Representação dos compartimentos da junção neuromuscular: compartimento ou membrana pré-sináptica, compartimento extracelular ou fenda sináptica, compartimento ou membrana pós-sináptica. Adaptado de Conti-Fine et al (2006).

No compartimento pré-sináptico, o terminal nervoso também contém diversas organelas citoplasmáticas, substâncias orgânicas e íons metálicos (SANES; LICHTMAN, 1999; HUGHES; KUSNER; KAMINSKI, 2006). As células de Schwann terminais ou peri-sinápticas (Figura 3) são células da glia não mielinizantes, cujos prolongamentos recobrem os terminais nervosos, protegendo-os de lesões químicas e mecânicas, além de serem as principais células responsáveis pela plasticidade estrutural das JNMs, por meio da percepção de possíveis alterações na transmissão sináptica (SUGIURA; LIN, 2011; KO; ROBITAILLE, 2015; BARIK et al., 2016).

O compartimento extracelular ou fenda sináptica (Figura 3) é preenchido pela lâmina basal sináptica, que contém diversas proteínas importantes para o desenvolvimento, função e estabilidade da JNM; bem como agregação dos AChR no sarcolema, entre elas agrina, lamininas-4, 9 e 11, metaloproteinase de matriz 3 (MMP3), colágeno IV e a enzima

acetilcolinesterase (AChE), responsável pela degradação da ACh após a contração muscular (PATTON, 2003; SANES, 2003; ENGEL, 2008; RODRÍGUEZ CRUZ et al., 2020).

No compartimento pós-sináptico (placa motora) (Figura 3), as dobras juncionais do sarcolema apresentam duas regiões: o ápice ou crista, onde estão agrupados os AChR e outras proteínas, como a rapsina, utrofina e α-distrobrevina-1; e o fundo ou vale, onde estão presentes as proteínas α-distrobrevina-2, distrofina, moléculas de adesão de células neurais (NCAMs) e os canais de sódio, responsáveis pela geração do potencial de ação (RUFF, 2003; CONTI-FINE; MILANI; KAMINSKI, 2006; RODRÍGUEZ CRUZ et al., 2020).

Os AChR são proteínas integrais de membrana que têm como função manter e facilitar a transmissão sináptica (SHEN et al., 2006; WU et al., 2014). São compostos por cinco subunidades arranjadas em forma de rosácea, formando canais iônicos (MA et al., 2007). Estes receptores são distribuídos em duas formas: extrajuncional imatura, presente na fibra muscular embrionária, constituída pelas subunidades: duas alfa (α), beta (β), delta (δ) e gama (γ); e juncional madura, no qual se mantem α (2), β e δ, e a subunidade γ é substituída pela épsilon (ε) (Figura 4) (RODRÍGUEZ CRUZ et al., 2020). A ligação simultânea de 2 moléculas de ACh na interface das subunidades αδ e αε inicia a mudança conformacional dos AChR para a abertura do poro iônico (Figura 4) (ENGEL, 2008; RODRÍGUEZ CRUZ et al., 2020).

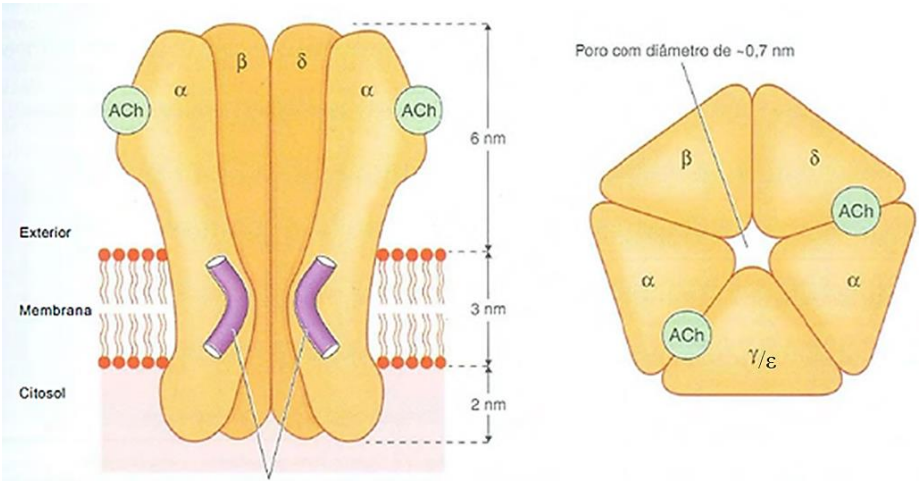


Figura 4. Estrutura do receptor nicotínico de acetilcolina (AChR). Adaptado de Rang & Dale (2004).

A agregação e manutenção das subunidades dos AChR na região da placa motora requer ações coordenadas de moléculas derivadas do nervo e do músculo, caracterizadas como vias de sinalização envolvidas na manutenção da estrutura da JNM (RODRÍGUEZ CRUZ et al., 2020). Dentre as vias de sinalização, a mais bem caracterizada é a via da Agrina / receptor lipoproteico relacionado a proteína 4 (LRP4) / receptor tirosina quinase músculo-específico

(MuSK) / Rapsina, cuja interação promove a concentração dos AChR na região sináptica (Figura 5) (WALKER et al., 2021; LEITE et al., 2023). As proteínas envolvidas nessa via são consideradas mecanismos moleculares chaves, necessárias para o desenvolvimento e manutenção da JNM (RODRÍGUEZ CRUZ et al., 2020).

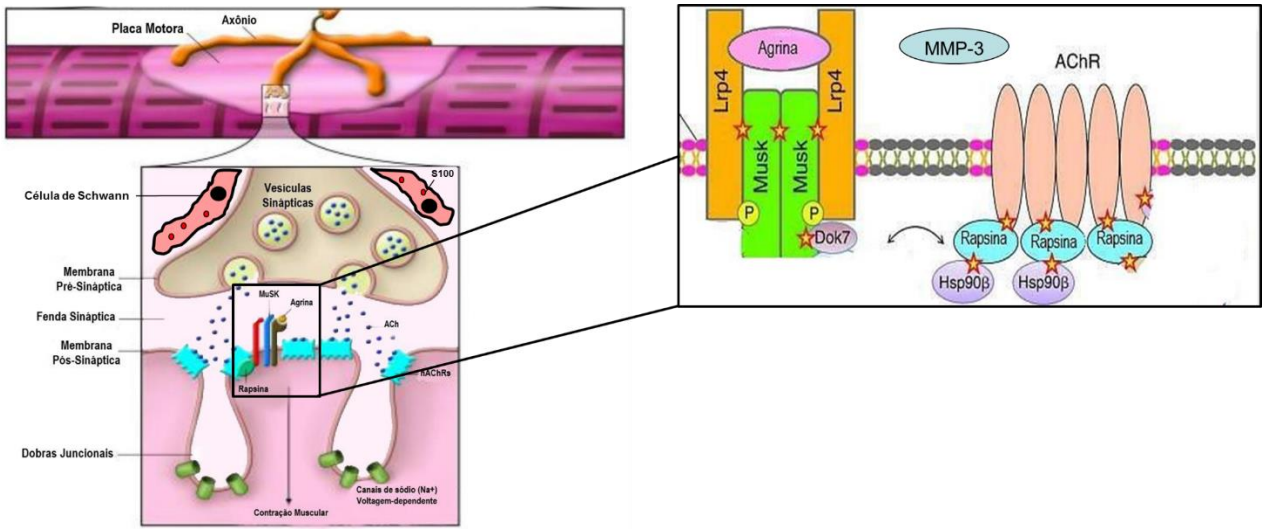


Figura 5. Representação dos compartimentos da junção neuromuscular, destaque para região pós-sináptica, as dobras juncionais com ápice contendo os AChR e outras proteínas incluindo Agrina, MuSK, Rapsina, que estão envolvidas no agrupamento dos AChR e estão presentes no sarcolema próximo aos receptores, e no fundo os canais de sódio voltagem-dependente. Detalhe em ampliação: interação específica das proteínas Agrina/Lrp4/MusK/Rapsina com o agrupamento dos AChR no sarcolema da fibra muscular. Adaptado de Conti-Fine et al (2006) e Wu et al (2014).

LESÃO NERVOSA PERIFÉRICA

Por serem estruturas frágeis, os nervos são propensos a serem danificados por traumas que causam a interrupção da condução nervosa, e geram um obstáculo na comunicação do SNC com as demais áreas do corpo (HUSSAIN et al., 2020; LOPES et al., 2022).

As lesões nervosas periféricas (LNPs) são um quadro clínico comum (DIVAC et al., 2021), afetando mundialmente cerca de 18 em cada 100 mil indivíduos por ano (JONES; EISENBERG; JIA, 2016). As principais causas de lesão nervosa são: acidentes automobilísticos, traumas por arma de fogo e arma branca, e lacerações com materiais perfurocortantes (ROBINSON, 2000; WALDRAM, 2003). As LNPs podem afetar a sensibilidade e a motricidade, e também resultar em retrações teciduais, edema, dor crônica, atrofias e encurtamentos musculares, bem como incapacidades para o resto da vida (SULLIVAN et al., 2016; HUSSAIN et al., 2020; LOPES et al., 2022).

A classificação das LNPs é baseada na extensão e gravidade dos danos, e permite a correlação entre as alterações microscópicas do nervo e a sintomatologia do paciente (RAZA et al., 2020; LOPES et al., 2022). Seddon (1942) as classificou em 3 graus, ao passo que Sunderland (1951) expandiu essa classificação para 5 graus, a fim de distinguir a dimensão

do dano nos envoltórios conjuntivos. A lesão denominada neurotmese por Seddon é análoga ao grau 5 de Sunderland, e consiste no bloqueio da condução nervosa devido à secção total do nervo; não apresenta recuperação funcional espontânea, sendo necessária uma intervenção cirúrgica, e assim, considerada a forma mais grave de lesão (Figura 6) (CHHABRA et al., 2014; HUSSAIN et al., 2020; RAZA et al., 2020; LOPES et al., 2022).

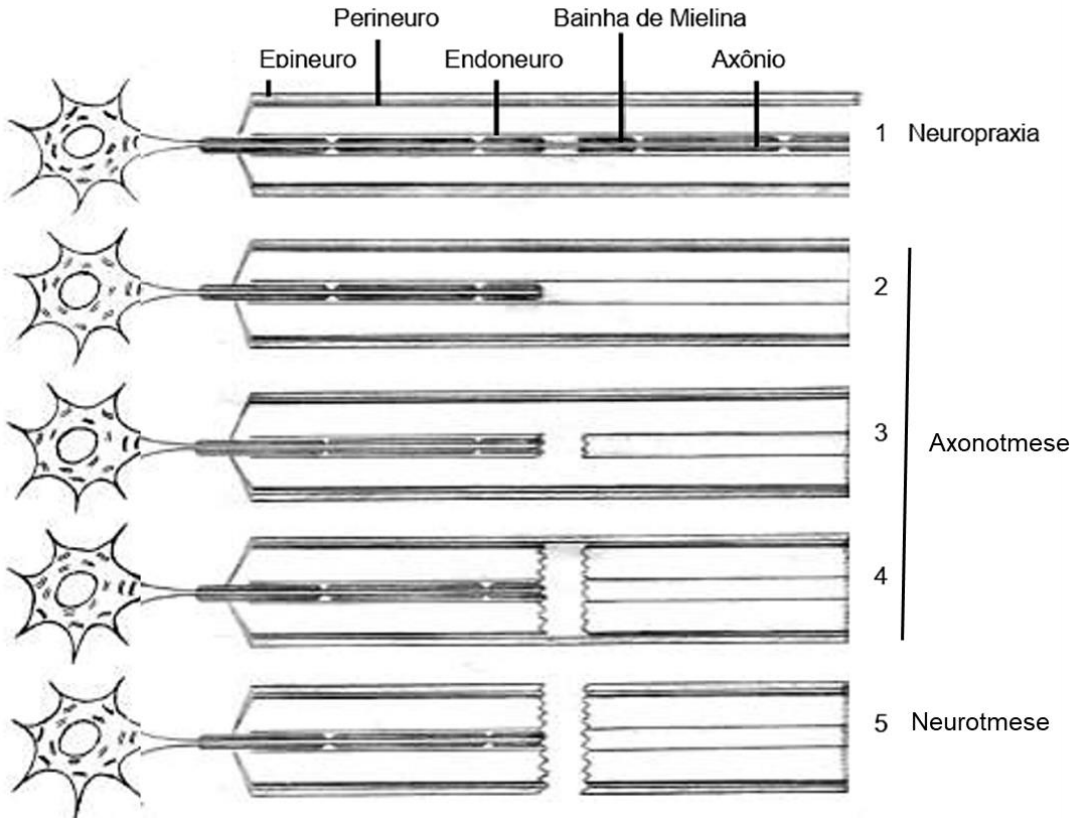


Figura 6. Representação da classificação das lesões nervosas periféricas de acordo com Seddon (1943) e Sunderland (1951). Detalhe para a dimensão do dano na bainha de mielina e nos envoltórios conjuntivos. Adptado de Oscar Colli (1993).

Entre 4 e 24h após LNP, inicia-se a degeneração Walleriana (Figura 7) (STOLL; JANDER; MYERS, 2002; GAUDET; POPOVICH; RAMER, 2011; ZHANG; JIANG; FANG, 2021), um processo que consiste na fragmentação da parte distal dos axônios e das bainhas de mielina, com isso, a continuidade axonal é perdida e a condução de impulsos não é mais possível (HUSSAIN et al., 2020). Esse processo pode perdurar por cerca de 10 a 14 dias (PERRIN et al., 2005), e ainda resulta na proliferação e reprogramação gênica das células de Schwann, promovendo um retorno a seu estágio imaturo (NOCERA; JACOB, 2020). Essas células atuam na secreção de fatores de crescimento e remielinização, além de protegerem o crescimento dos axônios (SULLIVAN et al., 2016; NOCERA; JACOB, 2020). A regeneração

axonal é altamente influenciada por células não neuronais, principalmente as células de Schwann (ZIGMOND; ECHEVARRIA, 2019).

Quando as LNPs ocorrem nos neurônios motores, comprometem o sistema neuromuscular, levando a diversas alterações morfofuncionais e moleculares, no nervo (DIVAC et al., 2021; BUENO et al., 2023), no músculo inervado (GORDON, 2020; CHEN et al., 2021; TERESHENKO et al., 2024) e nas junções neuromusculares associadas (PINTO et al., 2021; LEITE et al., 2023; TIBÚRCIO et al., 2023a) (Figura 7). Como o músculo estriado esquelético possui alta plasticidade, há tentativas de remodelação após desnervação (SAKUMA et al., 2016). No entanto, quando não são eficientes, levam a quadros de fibrose e atrofia, e a consequente diminuição da capacidade de contração (Figura 7) (GORDON, 2020; CHEN et al., 2021).

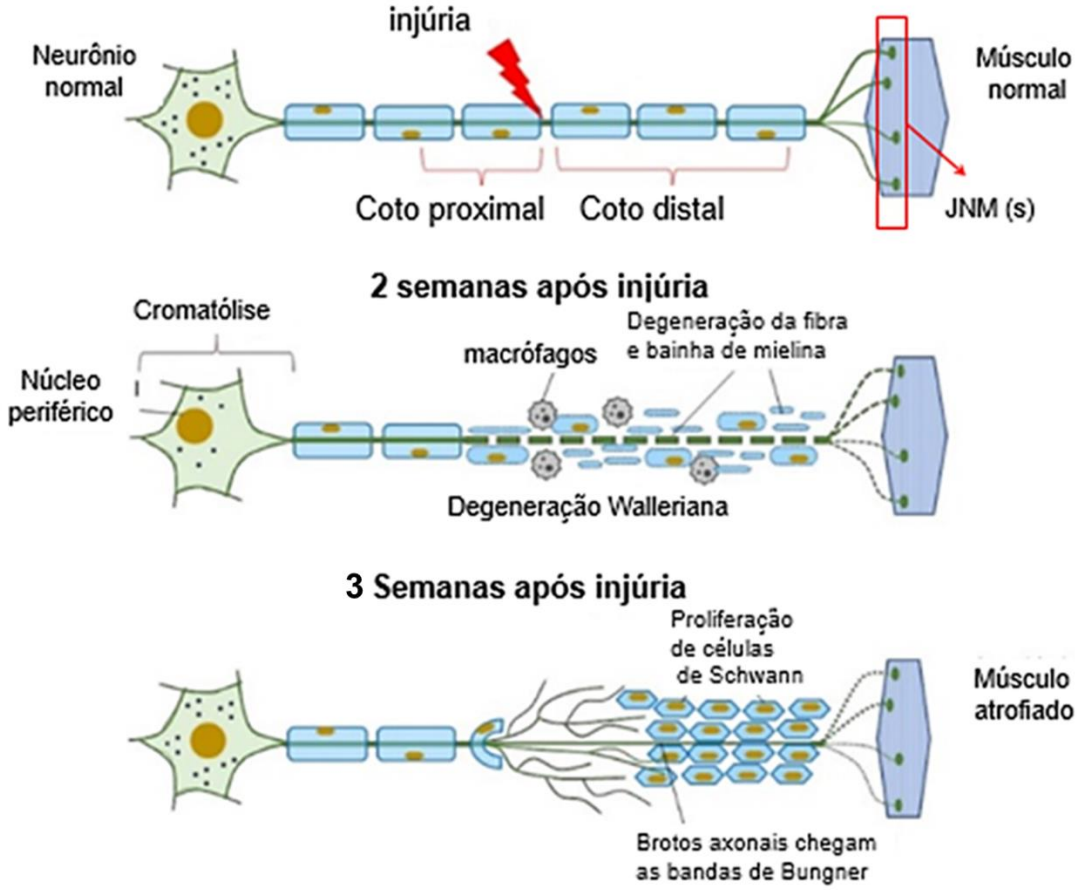


Figura 7. Representação esquemática da degeneração Walleriana. Detalhe para a fragmentação do axônio e bainhas de mielina e presença de macrófagos na extremidade distal do axônio. Adaptado de Arslantunali et al (2014).

Dentre as alterações que o correm na JNM após desnervação destacam-se: a fragmentação e modificação nos níveis das proteínas associadas as vias de sinalização,

principalmente a via da agrina, que resultam na desagregação dos AChR, havendo redistribuição através da fibra muscular (Figura 8) e alterações em suas subunidades, com o retorno para o padrão embrionário e aumento na expressão das subunidades γ e α (PINTO et al., 2021; LEITE et al., 2023) , sendo o mesmo acompanhado de um aumento dos fatores de regulação miogênica (MRFs), principalmente MyoD e miogenina (MA et al., 2007; LEITE et al., 2023).

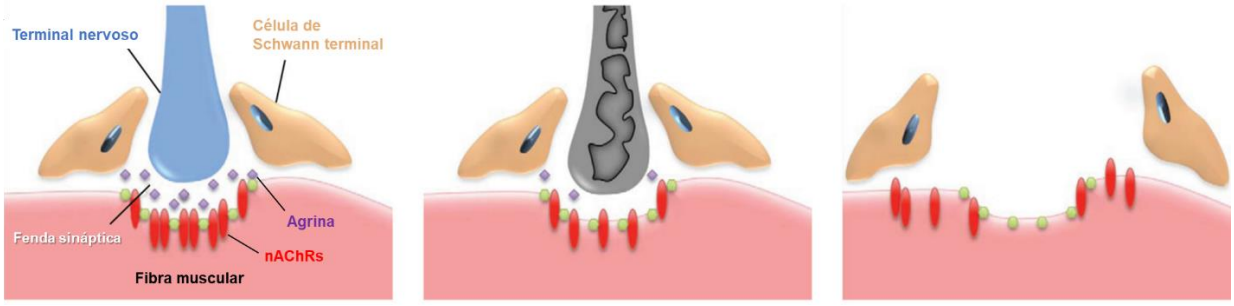


Figura 8. Representação esquemática das repercussões da lesão nervosa periférica na junção neuromuscular, com ênfase na degeneração do terminal nervoso, diminuição dos níveis de agrina, e desagregação e dispersão dos AChR através da fibra muscular. Adaptado de Kang et al (2011).

Dentre as técnicas de reparo das LNPs, a neurorrafia término-terminal ainda é o “padrão-ouro” da atualidade (PINTO et al., 2021; TIBÚRCIO et al., 2023a; BUENO et al., 2023, 2024). Entretanto, esse tratamento cirúrgico nem sempre restabelece a força e destreza muscular anterior à lesão (SAKUMA et al., 2016; GORDON, 2020). Assim, mesmo com os avanços nos procedimentos cirúrgicos, as neurorrafias resultam apenas em torno de 51% de recuperação funcional (SAKUMA et al., 2016). Com isso, várias estratégias vêm sendo utilizadas a fim de melhorar a regeneração nervosa (RAY; MACKINNON, 2010; HUSSAIN et al., 2020), entre elas: neurorrafia término-lateral (VITERBO et al., 2017; PAIVA et al., 2021; VITERBO; MAGNANI; NUNES, 2022; BRAGA SILVA et al., 2022; LEMOS et al., 2024), enxertos e conduítes (RODRÍGUEZ-SÁNCHEZ et al., 2021; LEITE et al., 2023), fotobiomodulação (BUCHAIM et al., 2022; BUENO et al., 2023, 2024), terapia celular (CARTAROZZI et al., 2015; SULLIVAN et al., 2016; ARAÚJO et al., 2017; ALVITES et al., 2020) e adjuvantes (LEITE et al., 2023; PINTO et al., 2021; TIBÚRCIO et al., 2023a)

Os adjuvantes são uma importante abordagem utilizada no reparo de LNPs, entre eles os selantes de fibrina ou colas de fibrina (ISAACS et al., 2008; BHATNAGAR et al., 2017). De modo geral, os selantes de fibrina de uso comercial são produzidos a partir de trombina bovina e fibrinogênio humano, que apresentam desvantagens e riscos, de modo que podem ser transmissores de doenças infecciosas, gerar fibrose, toxicidade e necrose (HUSSAIN et al.,

2020). E ainda podem acarretar no desenvolvimento de anticorpos contra a trombina bovina, além outras reações adversas (BARROS et al., 2009; BISCOLA et al., 2017; FERREIRA JR et al., 2017).

BIOPOLÍMERO HETERÓLOGO DE FIBRINA

O Centro de Estudos de Venenos e Animais Peçonhentos (CEVAP) da Universidade Estadual Paulista (UNESP), Câmpus de Botucatu, desenvolveu o Biopolímero Heterólogo de Fibrina (BHF), antes denominado de selante heterólogo de fibrina ou cola de fibrina (Figura 10A) (BUCHAIM et al., 2019; TIBÚRCIO et al., 2023a; VIGLIAR et al., 2024).

O BHF é composto por um crioprecipitado, contendo fibrinogênio em altas concentrações e outros fatores de coagulação, provenientes do sangue de bubalinos (*Bubalus bubalis)*, e a enzima giroxina, uma serinoprotease trombina-like extraída a partir da peçonha da cascavel (*Crotalus durissus terrificus*), que possui a capacidade de converter fibrinogênio em fibrina (FERREIRA JR et al., 2017; ABBADE et al., 2021; TIBÚRCIO et al., 2023a). Considerado uma cola biológica, biodegradável e bioabsorvível, o BHF possui grande capacidade adesiva e não produz reações adversas, além de ser atóxico (ABBADE et al., 2021; TIBÚRCIO et al., 2023a; VIGLIAR et al., 2024).

Por não possuir sangue humano, é considerada a única fibrina heteróloga do mundo, e devido a isso, não é transmissor de doenças infecciosas, podendo ser utilizado na clínica médica e em diversos procedimentos cirúrgicos (BUCHAIM et al., 2019; ABBADE et al., 2021; VIGLIAR et al., 2024).

O uso do BHF, principalmente como adjuvante na reconstrução de nervos periféricos, vem apresentando resultados promissores (BISCOLA et al., 2017; BUCHAIM et al., 2019; LEITE et al., 2019; PINTO et al., 2021; RODRÍGUEZ-SÁNCHEZ et al., 2021; BUENO et al., 2023, 2024; LEITE et al., 2023; TIBÚRCIO et al., 2023a). Nesse contexto, Leite e colaboradores (2019) evidenciaram que aos 60 dias após reconstrução do nervo isquiático, o BHF quando associado à neurorrafia, potencializou a regeneração axonal, e ainda permitiu a redução do número de pontos quando comparado a neurorrafia isolada, resultando na diminuição do tempo de cirurgia. Bueno e colaboradores (2023) observaram melhora significativa na recuperação do nervo facial após a utilização do BHF associado à fotobiomodulação.

Em outros estudos, também buscando tratamento para LNPs, o BHF apresentou desempenho similar, ou melhor, quando comparado com sutura tradicional (BUCHAIM et al., 2015), mostrou ter característica de fácil utilização com boa capacidade adesiva e boa biocompatibilidade com outros materiais (POMINI et al., 2023; VIGLIAR et al., 2024).

Em ensaios clínicos de fase I/II em humanos, o BHF demonstrou bons resultados no processo de cicatrização, como no tratamento de úlceras venosas crônicas, devido às suas

propriedades seguras e de fácil aplicação, levando à redução da dor após oito semanas de uso. O produto também mostrou-se seguro e com boa eficácia preliminar (ABBADE et al., 2021).

O BHF também demonstrou efeitos positivos quando associado à biomateriais (BUCHAIM et al., 2022; REIS et al., 2022; POMINI et al., 2023; VIGLIAR et al., 2024) e a fármacos, com o aumento de 50% da função motora e um efeito imunomodulatório quando associado ao dimetil fumarato, no tratamento de lesão do SNC em ratos (KEMPE et al., 2020, 2023).

Além disso, o BHF possui as vantagens de ter rápido processo de produção, baixo custo e o potencial para atuar como um arcabouço para células-tronco (BUCHAIM et al., 2019; RODRÍGUEZ-SÁNCHEZ et al., 2021). Estudos experimentais em ratos evidenciaram que a associação de células-tronco mesenquimais e BHF permitiu: melhora na regeneração axonal e recuperação motora após reparo do nervo isquiático (CARTAROZZI et al., 2015; RODRÍGUEZ-SÁNCHEZ et al., 2021), melhora na regeneração óssea, além da diferenciação de células-tronco mesenquimais (ORSI et al., 2017; CRESTE et al., 2020), e atividade neuroprotetora após lesão do SNC (SPEJO et al., 2018). Já a associação do BHF a células-tronco embrionárias também promoveu neuroproteção após lesão no SNC (ARAÚJO et al., 2017), e facilitou a regeneração do nervo isquiático de ratos (MOZAFARI et al., 2018).

Inúmeros estudos, incluindo do nosso grupo de pesquisa, demonstraram que o BHF, isolado ou associado a diferentes técnicas e componentes, em lesões do SNC e SNP, produz efeitos neuroprotetores, angiogênicos e imunomodulatórios que potencializam a regeneração nervosa (LEITE et al., 2019, 2023; PINTO et al., 2021; TIBÚRCIO et al., 2023a). Além disso, o BHF facilita a reinervação e gera uma consequente melhorar na recuperação do músculo e das junções neuromusculares, bem como auxilia na recuperação funcional após LNPs (LEITE et al., 2019, 2023). A recuperação funcional/motora efetiva envolve diferentes fatores, entre eles a interação entre nervo e músculo, bem como as junções neuromusculares associadas.

JUSTIFICATIVA

Nosso grupo de pesquisa vem trabalhando em um estudo cronológico utilizando BHF em LNPs, com ênfase na recuperação neuromuscular, e tem encontrado resultados promissores. Aos 7 e 30 dias após reparo, o BHF demostrou efeitos imunomodulatório, angiogênico e pró-regenerativos, além de auxiliar na recuperação morfológica parcial das JNMs e previnir degeneração severa do músculo (TIBÚRCIO et al., 2023a). Aos 60 dias, após reparo tardio, o BHF potencializou a regeneração axonal e ainda permitiu a redução do número de pontos quando comparado a neurorrafia isolada, com a consequente diminuição do tempo de procedimento cirúrgico (LEITE et al., 2019); ainda, potencializou a recuperação morfológica e molecular das JNMs, com retorno ao seu padrão molecular maduro (PINTO et al., 2021). Aos 90 dias, após lesão nervosa grave, o BHF resultou na estabilização dos AChR, que apresentaram distribuição normal após reparo, o que potencializa a regeneração neuromuscular, além de uma recuperação parcial da função motora (marcha) (LEITE et al., 2023).

Estudos em roedores indicam que somente a partir de 90 dias após reconstrução nervosa com neurorrafia isolada, que as placas motoras estão completamente reinervadas, com retorno da morfologia das JNMs aos padrões normais. No entanto, esses animais, 120 dias após reparo, ainda não apresentam recuperação motora, concluindo que a falta de recuperação funcional não é causada apenas pela incapacidade das fibras nervosas em reinervar o músculo, o que pode refletir em um possível defeito na transmissão sináptica. Isto sugere que o reparo por neurorrafia (sutura) isolada resulta em falha na restauração das JNMs funcionais (SAKUMA et al., 2016).

Embora haja avanços nos procedimentos cirúrgicos que envolvem diferentes técnicas, as neurorrafias resultam apenas em aproximadamente 51% de recuperação motora, sendo que cerca de um terço de todas as LNPs apresenta recuperação funcional incompleta. Muitos trabalhos demonstram que há recuperação morfológica do nervo e do músculo, mas ainda não está associada à recuperação funcional após LNP. Mesmo havendo regeneração axonal e as JNMs em aparência morfológica normal, a falha na ativação elétrica do músculo persiste, sendo a principal causa da falha na recuperação motora (SAKUMA et al., 2016).

A adição de substâncias à neurorrafia abre novas possibilidades de pesquisa. Nesse contexto, o uso do biopolímero heterólogo de fibrina (BHF) associado à neurorrafia surge como uma terapia biológica economicamente viável e isenta de reações adversas. Essa abordagem tem o potencial de melhorar o microambiente para o crescimento axonal, favorecendo a regeneração nervosa e a reinervação muscular, além de promover uma recuperação funcional e motora mais eficaz após lesão. O BHF também oferece perspectivas

promissoras para sua aplicação futura como estratégia de reparo de lesões nervosas periféricas e outras terapias em ensaios clínicos.

Com isso, neste estudo, buscamos avaliar a regeneração nervosa e a recuperação neuromuscular prolongada, 120 dias após reparo do nervo isquiático, empregando associação do BHF a neurorrafia.

OBJETIVOS

OBJETIVO GERAL

Avaliar os efeitos da neurorrafia associada ao biopolímero heterólogo de fibrina na regeneração nervosa e nos aspectos morfológicos e funcionais da interação neuromuscular, aos 120 dias após reparo do nervo isquiático de ratos.

OBJETIVOS ESPECÍFICOS

- Avaliar se o BHF auxilia na recuperação da função motora (CatWalk XT);
- Avaliar se o BHF acelera a regeneração do nervo isquiático (histomorfometria);
- Avaliar se o BHF potencializa a regeneração das junções neuromusculares, das fibras musculares e da matriz extracelular do músculo sóleo (histomorfometria);
- Avaliar se o BHF auxilia na recuperação dos receptores de acetilcolina da junção neuromuscular (NMJ-morph)

MATERIAL E MÉTODOS

ANIMAIS DE EXPERIMENTAÇÃO

Foram utilizados 60 ratos Wistar machos adultos, com 90 dias de idade e peso corporal médio entre 300 e 350 g, provenientes do Biotério Central da Unesp, Câmpus de Botucatu. Durante todo o período experimental, os animais foram mantidos no Biotério de Roedores 1 da Unidade de Pesquisa Experimental (Unipex) da Faculdade de Medicina de Botucatu (FMB/Unesp). Eles foram alojados em caixas de polietileno (40 x 30 x 15 cm), com fundos sólidos revestidos de maravalha, sob condições controladas de luminosidade (12 h claro/12 h escuro) e temperatura (22 ± 2 ºC). Água filtrada e ração Presence® foram fornecidas *ad libitum*. Este estudo foi aprovado pela Comissão de Ética no Uso de Animais (CEUA) da FMB/Unesp, sob o protocolo nº 1402/2021.

Os animais foram distribuídos aleatoriamente em 4 grupos experimentais (n=15/grupo):

1. Controle (C)
2. Desnervado (D)
3. Neurorrafia (N)
4. Neurorrafia + BHF (NB)

CÁLCULO DO TAMANHO AMOSTRAL

De acordo com os estudos realizados pelo nosso grupo de pesquisa, para determinar diferenças estatísticas significativas na morfologia e morfometria das junções neuromusculares, do músculo e do nervo, é necessário utilizar 5 animais por grupo experimental. No entanto, devido às variações nas técnicas de coleta e fixação das amostras teciduais, são necessários 5 animais para análise do músculo e do nervo, e outros 5 para a análise das junções neuromusculares. Além disso, para a análise funcional da marcha, que é uma avaliação comportamental com alta variabilidade, são necessários mais 5 animais por grupo para minimizar o desvio padrão. Assim, cada grupo experimental requer um total de 15 animais: 5 para análise das junções neuromusculares (PINTO et al., 2021; LEITE et al., 2023; TIBÚRCIO et al., 2023b), 5 para histologia do músculo e do nervo (GUIDI PINTO et al., 2018; LEITE et al., 2019, 2023; TIBÚRCIO et al., 2023a), e 5 para a análise funcional da marcha (PINTO et al., 2021; LEITE et al., 2023). Vale destacar que todos os 15 animais foram submetidos à análise funcional da marcha (LEITE et al., 2019, 2023).

PROCEDIMENTO CIRÚRGICO

Antes do início do procedimento cirúrgico, foi realizada profilaxia antimicrobiana com aplicação subcutânea de enrofloxacino (10 mg/kg). Trinta minutos após a profilaxia, os animais foram anestesiados com uma injeção intraperitoneal de ketamina (Dopalen, 90 mg/kg) e xilazina (Anasedan, 10 mg/kg).

Após a tricotomia do membro pélvico direito, os animais foram posicionados em decúbito ventral, com as patas dianteiras e traseiras em abdução. Foi aplicada lidocaína (7 mg/kg) no local da incisão, seguida de antissepsia com álcool iodado. A incisão foi feita sobre a face lateral da coxa, desde a altura do trocânter maior até o joelho, expondo os nervos isquiáticos direitos.

Nos animais do grupo C, foi realizada apenas a localização e dissecção do nervo isquiático, seguido de sutura dos tecidos moles e da pele (nylon 5-0). Nos animais dos grupos D, N e NB, foi realizada uma lesão nervosa por transecção do nervo isquiático (neurotmese) cerca de 3 mm proximal à sua trifurcação.

Nos animais do grupo D, para evitar a regeneração espontânea, foi removido um fragmento de 6 mm do nervo, e os cotos nervosos proximais e distais foram invertidos a 180º e fixados na tela subcutânea adjacente com pontos duplos (nylon 10-0). Nos grupos N e NB, imediatamente após a neurotmese, os cotos nervosos foram reconectados por meio de neurorrafia término-terminal (anastomose epineural) com dois pontos duplos (nylon 10-0) (Figura 9). Além disso, no grupo NB, após a neurorrafia, foi aplicado um volume de 250 µL do BHF, cedido pelo CEVAP, UNESP Botucatu, SP, Brasil (Figura 9).

Os componentes do BHF foram fornecidos separadamente em três microtubos armazenados a -20°C: uma enzima semelhante à trombina (giroxina) extraída do veneno de serpente, um crioprecipitado rico em fibrinogênio extraído do sangue de búfalo e o diluente cloreto de cálcio (Figura 10B). Inicialmente, a enzima semelhante à trombina foi misturada com o diluente; esses componentes e o crioprecipitado foram então depositados na área de reparo do nervo à temperatura ambiente. Após a mistura, ocorreu a polimerização, formando um biocomplexo constituído por uma rede de fibrina densa e estável, semelhante a uma substância gelatinosa (Figura 11a, b) (TIBÚRCIO et al., 2023a).

Após a realização da reconstrução nervosa, os tecidos moles foram suturados com nylon 5-0. Foi administrado tramadol (5 mg/kg) via subcutânea, e os animais foram mantidos sob aquecimento até o retorno da consciência.

O protocolo pós-cirúrgico consistiu na administração de enrofloxacino (10 mg/kg) por via subcutânea durante 3 dias, e tramadol (5 mg/kg) por via subcutânea a cada 12 horas por 5 dias. Durante o período de cicatrização, foi utilizado spray Rifocina (uso tópico) no local da incisão

OBS.: Devido à complexidade dos procedimentos cirúrgicos e pós-cirúrgicos, bem como às consequências naturais do protocolo de anestesia, houve uma taxa média de 10% de perda dos animais durante o experimento, os quais foram repostos. No período pós-cirúrgico, observou-se autotomia dos dedos em dois animais dos grupos lesionados e autotomia da pele e musculatura do membro pélvico em um animal; esses animais foram eutanasiados e substituídos.

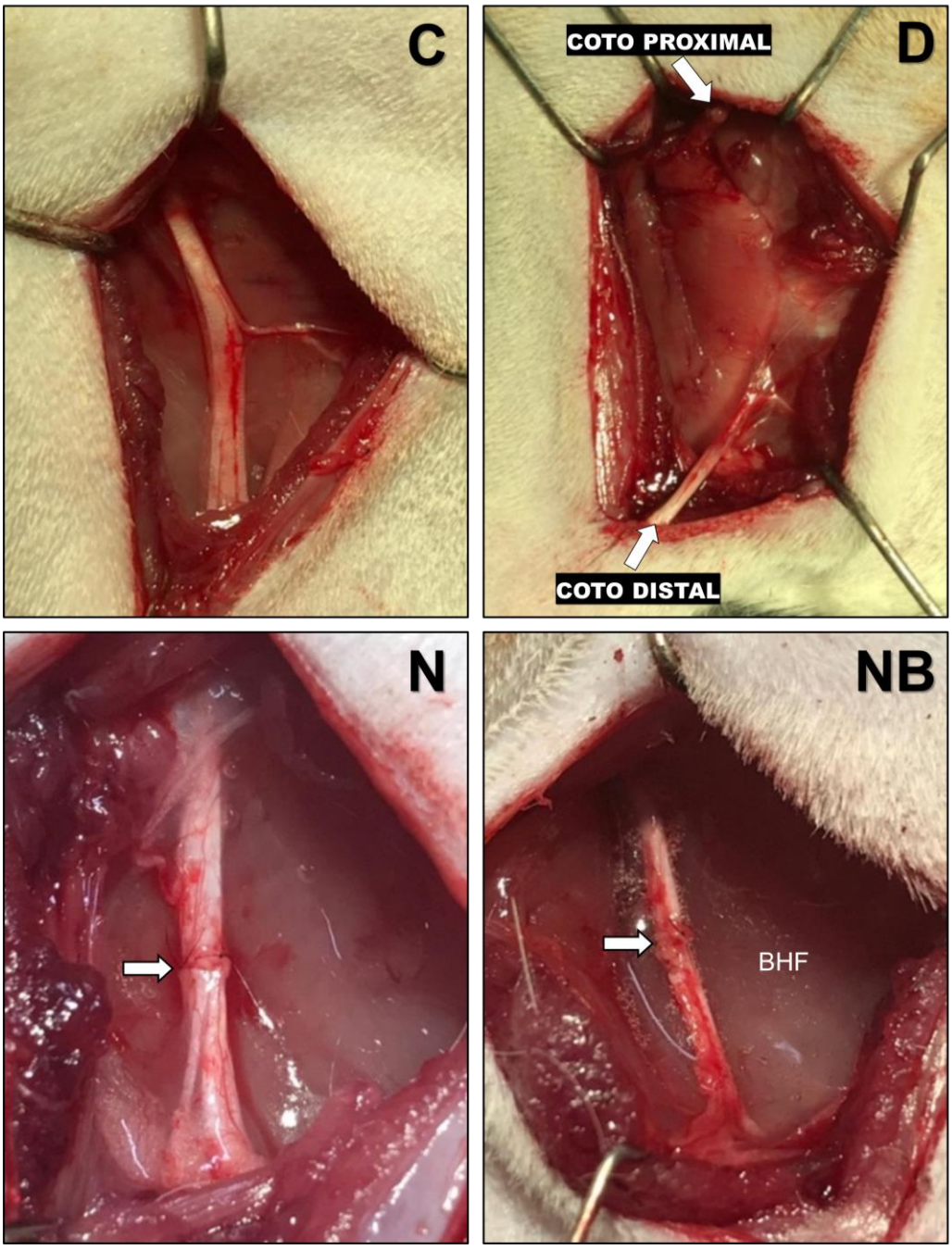


Figura 9. Fotografias das técnicas cirúrgicas realizadas em todos os grupos experimentais. C: Grupo controle, localização do nervo isquiático. D: Grupo desnervado, neurotmese e fixação dos cotos nervosos proximal e distal na tela subcutânea adjacente. N: Grupo neurorrafia, seta: detalhe da neurorrafia (➔). NB: Grupo neurorrafia + biopolímero heterólogo de fibrina (BHF), seta: detalhe da neurorrafia (➔). Arquivo pessoal.

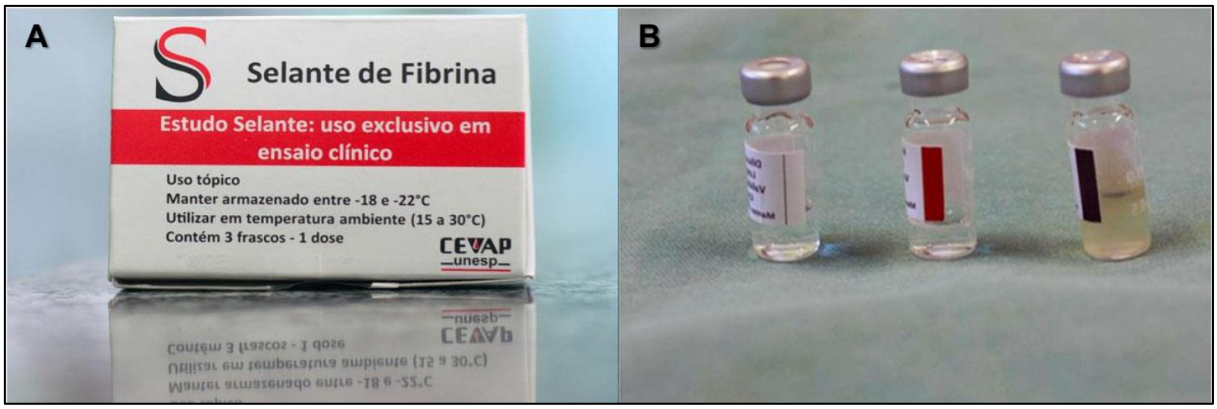


Figura 10. Embalagem e frascos do biopolímero heterólogo de fibrina. A: Embalagem (contendo o nome antigo "Selante de Fibrina"). B: Frascos contendo as frações I (giroxina extraída do veneno de serpente), II (crioprecipitado rico em fibrinogênio extraído do sangue de búfalo) e diluente (cloreto de cálcio). Adaptado de Ferreira et al (2017).

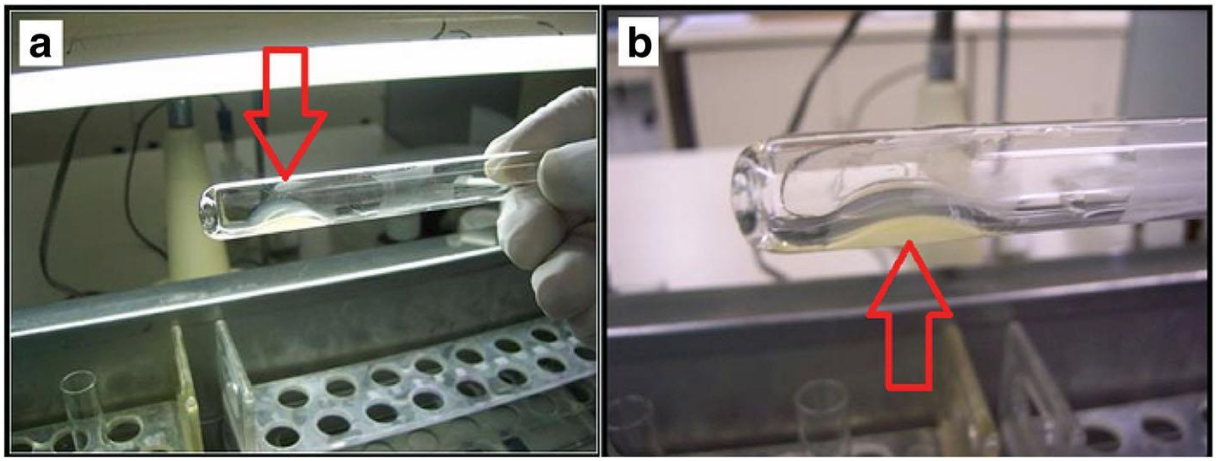


Figura 11. Polimerização do biopolímero heterólogo de fibrina, formando um biocomplexo, constituído por uma rede de fibrina densa e estável, semelhante a uma substância gelatinosa, devido a atividade coagulante da giroxina. a e b: Coágulo de fibrina formado após diluição de fibrinogênio com giroxina. Seta: Detalhe da rede de fibrina. Adaptado de Ferreira et al (2017).

ANÁLISE FUNCIONAL DA MARCHA

Um dia antes e 120 dias após as cirurgias, foi realizada análise funcional da marcha de todos os animais de acordo com os grupos experimentais, por meio do CatWalk XT, um sistema de análise de marcha para avaliação quantitativa de passos e locomoção em roedores (Figura 12A) (HEINZEL et al., 2020; TIMOTIUS et al., 2023).

Inicialmente, para aclimatação, uma semana antes do procedimento cirúrgico, todos os animais foram treinados 3 vezes a caminhar no dispositivo. O estudo se baseou nas pegadas e marcha do animal, de forma estática e dinâmica, baseadas em duração, orientação e coordenação dos movimentos entre as patas. Trata-se de um sistema de análise automatizado da marcha, no qual os animais foram colocados para andar em uma plataforma de vidro iluminada (Figura 12B), o contato da pata com a superfície do vidro resultou em uma imagem da pegada (Figura 12C). A plataforma de vidro foi monitorada por uma câmara de

vídeo colocada sob a plataforma e conectada a um computador equipado com o software Noldus CatWalk XT 9.1 de aquisição de vídeo e análise das pegadas (LEITE et al., 2019, 2023). Foram registradas 3 corridas para cada animal.

Os critérios adotados para que uma corrida seja considerada adequada foram (LEITE et al., 2023):

- Duração mínima da corrida: 0,50 segundos;
- Duração máxima da corrida: 20 segundos;
- Número mínimo de pegadas: 4 pegadas;
- Variação máxima de velocidade: 60%.

Os parâmetros avaliados foram (LEITE et al., 2023; TIMOTIUS et al., 2023):

- Parâmetros de impressão: Área da pegada (cm²); Área máxima de contato (cm²); Comprimento da pegada (cm); Largura da pegada (cm); Índice funcional do Fibular (IFF).

  Para o cálculo do IFF foi utilizada a seguinte fórmula: IFF = 174.9 [(ETS-NTS)/NTS] + 80.3 x [(EPL-NPL)/NPL] - 13.4. Onde E se refere ao lado lesionado e N ao lado não lesionado, a sigla TS se refere a distância entre o primeiro e o quinto dedos (*toe spread*) e a sigla PL a distância entre o terceiro dedo e o calcanhar (*print length*) (BAIN; MACKINNON; HUNTER, 1989).
- Parâmetros temporais: Duração das corridas (s); “Stand” (fase de apoio, duração do contato da pata com o vidro, s); “Swing” (fase de balanço, duração da ausência de contato da pata com o vidro, s); Velocidade média das corridas (cm/s); Número de passos; Cadência (número de passos por segundo).
- Parâmetro de coordenação: Índice de regularidade (IR) (%) (expressa o número de padrões normais de sequência de passos em relação ao número total de colocações de patas, é mostrado com base em todos os padrões de passos categorizados).

  Fórmula para cálculo: IR = [(NSSP*4)/PP]*100%. Onde NSSP representa o número de padrões normais de sequência de passos e PP o número total de colocações de patas (HAMERS et al., 2001; HAMERS; KOOPMANS; JOOSTEN, 2006; CHEN et al., 2014).

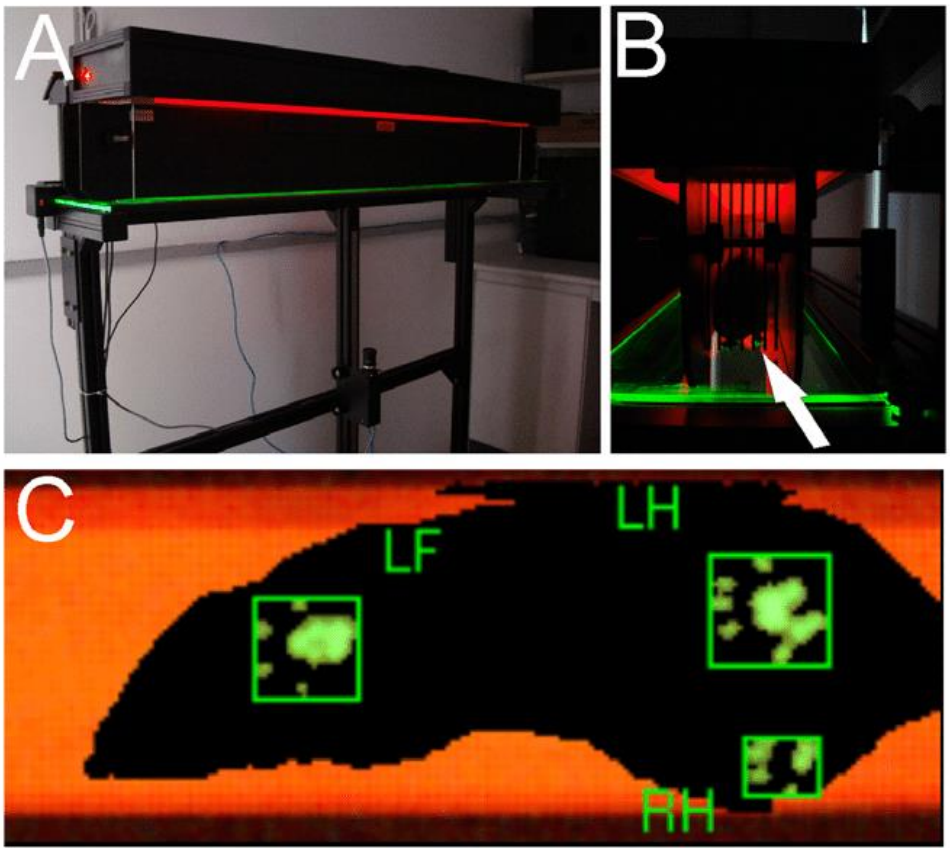


Figura 12. Equipamento para análise funcional da marcha. A: sistema CatWalk XT. B: exemplo de rato na plataforma de vidro iluminada e impressão plantar verde (seta). C: reconhecimento e interpretação das pegadas pelo *software*. Adaptado de Barbizan et al (2013).

EUTANÁSIA DOS ANIMAIS E OBTENÇÃO DAS AMOSTRAS TECIDUAIS

Decorrido o período experimental, 120 dias após a cirurgia, 10 animais de cada grupo foram eutanasiados por meio da sobredosagem de Tiopental sódico (120mg/kg) via intraperitoneal, caso necessário foi aplicado cloreto de potássio via intracardíaca. Os animais foram pesados e 5 animais de cada grupo foram anestesiados através de injeção intraperitoneal de Ketamina (Dopalen, 90 mg/kg) e Xilazina (Anasedan, 10 mg/kg), e submetidos à perfusão transcardíaca. Os nervos isquiáticos e os músculos sóleos direitos foram coletados, pesados, fixados e processados conforme os protocolos de análise a seguir. **OBS.:** O músculo sóleo foi escolhido para este estudo por ser um músculo postural de extrema importância, cuja função está associada à manutenção da estabilidade e locomoção (NEPTUNE; KAUTZ; ZAJAC, 2001). Além disso, oferece maior comodidade para localização e visualização das JNMs, principalmente no terço médio, onde o ponto motor é evidente (TIBÚRCIO et al., 2023b). O nervo isquiático foi utilizado pois a lesão deste nervo já está consolidada como um modelo simples e preciso para investigar muitos aspectos do dano e da recuperação do sistema nervoso periférico (SAVASTANO et al., 2014).

ANÁLISE MORFOLÓGICA E MORFOMÉTRICA DO NERVO ISQUIÁTICO

Os nervos isquiáticos direitos, após fixação em solução de Karnovsky (glutaraldeído 2,5% + paraformaldeído 4% em PBS (tampão fosfato salino 0,1 M, pH 7,4), foram fixados e corados com tetróxido de ósmio (1%, 24h), incluídos em historesina, seccionados transversalmente (2 µm) em ultramicrótomo (Leica RM2265). As lâminas histológicas foram fotografadas através do analisador de imagens Olympus Bx41 (câmera SC30) e foram obtidas imagens de 5 campos aleatórios em objetiva de 40x.

Por meio do *software* ImageJ (v.1.54), as imagens foram analisadas e foram mensurados os valores de: área, perímetro e diâmetro dos axônios e das fibras nervosas, espessura da bainha de mielina (diâmetro da fibra - diâmetro do axônio/2) e cálculo da Razão G (diâmetro axônio/diâmetro fibra) (LEITE et al., 2019, 2023; TIBÚRCIO et al., 2023a).

ANÁLISE MORFOLÓGICA E MORFOMÉTRICA DAS FIBRAS MUSCULARES E QUANTIFICAÇÃO DE COLÁGENO INTRAMUSCULAR

Após a coleta, as extremidades dos músculos foram fixadas em formol tamponado 10% por 24h, lavados em água corrente por 48h, incluídos em Paraplast®, seccionados em micrótomo (4µm).

Duas lâminas histológicas para cada animal de cada grupo experimental foram confeccionadas e submetidas à coloração de Hematoxilina e Eosina (HE) e Picrosirius Red. As lâminas foram fotografadas em objetiva de 20x por meio do microscópio Olympus Bx41 (câmera SC30). Ainda, as lâminas coradas em Picrosirius Red foram fotografadas em Microscópio Confocal de Varredura a Laser (Leica Microsystems, TCS - SP5), onde a autofluorescência da coloração foi captada.

Na lâmina submetida à coloração de HE, foram selecionadas 200 fibras musculares a partir de 3 a 4 campos aleatórios. A quantificação foi realizada através do *software* ImageJ (v.1.54), no qual foram mensurados área, perímetro e diâmetro das fibras musculares (LEITE et al., 2019; TIBÚRCIO et al., 2023a, 2023b).

Na lâmina submetida à coloração de Picrosirius Red, na qual o tecido conjuntivo foi corado em vermelho e as fibras musculares em amarelo, a quantificação foi realizada por meio da porcentagem de colágeno (%) da totalidade do músculo, obtidas através do *software* ImageJ (v.1.54), onde as áreas em vermelho foram detectadas automaticamente, utilizando ferramenta Threshold do *software* (LEITE et al., 2019; TIBÚRCIO et al., 2023b).

ANÁLISE MORFOLÓGICA E MORFOMÉTRICA DAS JUNÇÕES NEUROMUSCULARES

Cinco animais de cada grupo experimental foram anestesiados através de injeção intraperitoneal de Ketamina (Dopalen, 90 mg/kg) e Xilazina (Anasedan, 10 mg/kg), e submetidos à perfusão transcardíaca. Para isso, foi realizada tricotomia da região peitoral,

seguida de toracotomia e exposição das vísceras torácicas, e a perfusão ocorreu por meio do ventrículo esquerdo e canulação da aorta, com bomba dosadora peristáltica Milan®, inicialmente com PBS (tampão fosfato salino) a 0,1 M e posteriormente fixação com paraformaldeído a 4%, ambos em um fluxo de 30 mL/min. A aurícula direita foi seccionada para escoamento do sangue e de líquidos excedentes. Em seguida, os músculos sóleos direitos foram coletados, reduzidos ao terço médio (região contendo o ponto motor) e mantidos em solução fixadora (paraformaldeído a 4%) por 15 min, para pós-fixação. Os músculos foram seccionados longitudinalmente e os fragmentos musculares submetidos a técnica de imunomarcação das JNMs (AChR e terminais nervosos) por imunofluorescência (PINTO et al., 2021; LEITE et al., 2023; TIBÚRCIO et al., 2023b).

Para marcação dos AChR foi utilizado α-bungarotoxina conjugada a rodamina (Rh-BTX, Invitrogen, Thermo Fisher Scientific, T1175, 1:100 em PBS 0,1 M) e para marcação dos terminais nervosos, anticorpo primário anti-neurofilamento 200 (Sigma-Aldrich N5389, 1:100 em solução de PBS 0,1 M + Triton® X-100 a 1%) associado ao anticorpo secundário conjugado a Alexa Fluor® 488 (Abacam, ab150077, 1:400). Os cortes foram montados em lâmina sob lamínula em meio de montagem para fluorescência VECTASHIELD® (Vector Laboratories, Burlingame, CA, EUA).

Foram obtidas imagens de 50 JNMs para cada animal de cada grupo experimental utilizando Microscópio Confocal de Varredura a Laser (Leica Microsystems, TCS - SP5). Os parâmetros básicos utilizados para a captura das imagens foram aumento de 63x, zoom de 2, com 1 µm de intervalo entre as imagens para construção da imagem final, com a finalidade de captura das JNMs da forma mais individualizada possível, facilitando assim sua posterior análise (Leite *et al.*, 2022). As imagens foram analisadas no *software* Fiji/ImageJ (v.1.54) por meio do *plugin* NMJ-morph (JONES et al., 2016; MINTY et al., 2020).

Análise morfométrica da JNM e dos AChR utilizando o plugin NMJ-morph

As análises foram realizadas usando o software Fiji/ImageJ (v.1.54), seguindo a sequência específica e as ferramentas do plugin NMJ-morph, para uma análise robusta e confiável das JNMs (JONES et al., 2016). Foram analisadas em torno de 50 imagens de cada animal, 250 por grupo experimental, totalizando o valor aproximado de 1000 imagens. Os parâmetros avaliados foram: área e perímetro dos AChR; área, perímetro e diâmetro da placa motora; índices de compactação e fragmentação; número e área média dos *clusters* de AChR; e área não ocupada pelos AChR (LEITE et al., 2023).

Inicialmente, as imagens que estavam em máxima projeção (Figura 13A) foram convertidas para formato binário (Figura 13B), em seguida, os parâmetros foram analisados na seguinte ordem:

- Área e perímetro dos AChR (Figura 13B).

- Perímetro, área e diâmetro da placa motora: análise que engloba não só os AChR, mas a área toda em que se distribuem, totalizando todo o compartimento pós-sináptico ou placa motora (Figura 13C).
- Número de clusters de AChR: para essa análise o número dos clusters formados pelos AChR foi contabilizado manualmente e com segurança, devido à ferramenta de segmentação de partículas aplicada a imagem, que separa os clusters, facilitando a contagem (Figura 13D).
- Área média dos clusters de AChR: área dos AChR/número de clusters. Essa análise leva em consideração a distribuição dos AChR, cujo valor foi obtido através da razão entre a área dos AChR pelo número de clusters em que se organizam.
- Índice de Compactação: (área dos AChR/área da placa motora) *100.
- Índice de Fragmentação: 1 – (1/número de clusters de AChR). A partir do número de clusters de AChR, foi possível calcular o índice de fragmentação, sendo considerado o valor 0 para um cluster de AChR e quanto maior for o número de clusters formado mais próximo de 1 será o valor.
- Área não ocupada dos AChR: área da placa - área dos AChR. Área da placa motora não ocupada pelos AChR.

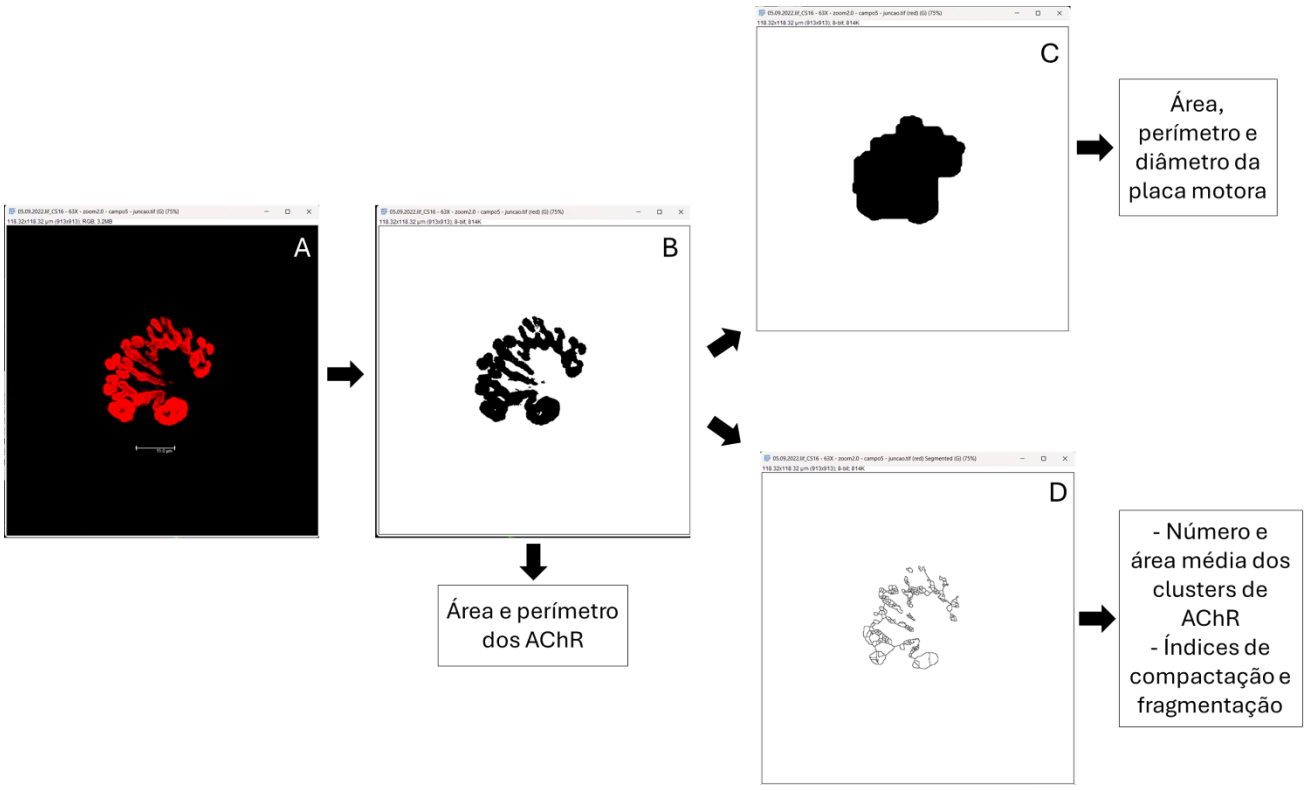


Figura 13. Fluxograma da análise da JNM e dos AChR utilizando o plugin NMJ-morph. A: imagem original dos AChR obtida no confocal (em máxima projeção). B: conversão para formato binário (preto e branco). C: criação do background e obtenção da placa motora. D: segmentação das partículas e obtenção dos clusters. Arquivo pessoal.

ANÁLISE ESTATÍSTICA

Os dados foram analisados pelo *software* GraphPad Prism 9, no qual foi realizado teste de normalidade. Para as variáveis com dados aderentes à distribuição normal foi utilizada a técnica da análise de variância (ANOVA) para um fator, complementada com o teste de comparações múltiplas de Tukey (ZAR, 2009), e os dados foram expressos em média ± erro padrão da média (SEM). Para as variáveis com dados não aderentes à distribuição normal foi utilizada a técnica da análise de variância não paramétrica (Kruskal-Wallis) complementada com o teste de comparações múltiplas de Dunn (ZAR, 2009), e os dados foram expressos em mediana ± *range*. Todos os dados foram considerados utilizando o nível de 5% de significância ($p \leq 0,05$).

RESULTADOS

ANÁLISE FUNCIONAL DA MARCHA (CatWalk XT)

Antes da cirurgia, todos os parâmetros da marcha avaliados não apresentaram diferenças entre os grupos experimentais.

Ao fim do período experimental, 120 dias após cirurgia, os valores de área, comprimento e largura da pegada, área máxima de contato, Stand (fase de apoio) e índice funcional do fibular, foram menores nos grupos lesionados (D, N e NB), com resultados semelhantes entre si e diferentes do grupo Controle (Figura 14 E-I, P).

Em relação ao índice de regularidade, o grupo NB foi o único que apresentou resultados semelhantes ao grupo C, e ainda maiores que o grupo D, mas semelhantes também ao grupo N. Os grupos D e N apresentaram os menores valores, iguais entre si e diferentes do grupo C (Figura 14J).

O número de passos demonstrou um padrão similar ao índice de regularidade, sendo também o grupo NB único com resultados semelhantes ao grupo C e menores que o grupo D, mas ainda semelhantes também ao grupo N. Já os grupos D e N demonstraram os maiores valores, iguais entre si e diferentes do grupo C (Figura 14K).

Em relação a Cadência, houve apenas um aumento no grupo D, sendo o único grupo diferente do grupo Controle (Figura 14L).

Os parâmetros de duração média das corridas, Swing (fase de balanço) e velocidade média das corridas, não apresentaram diferença entre os grupos experimentais (Figura 14 M-O)

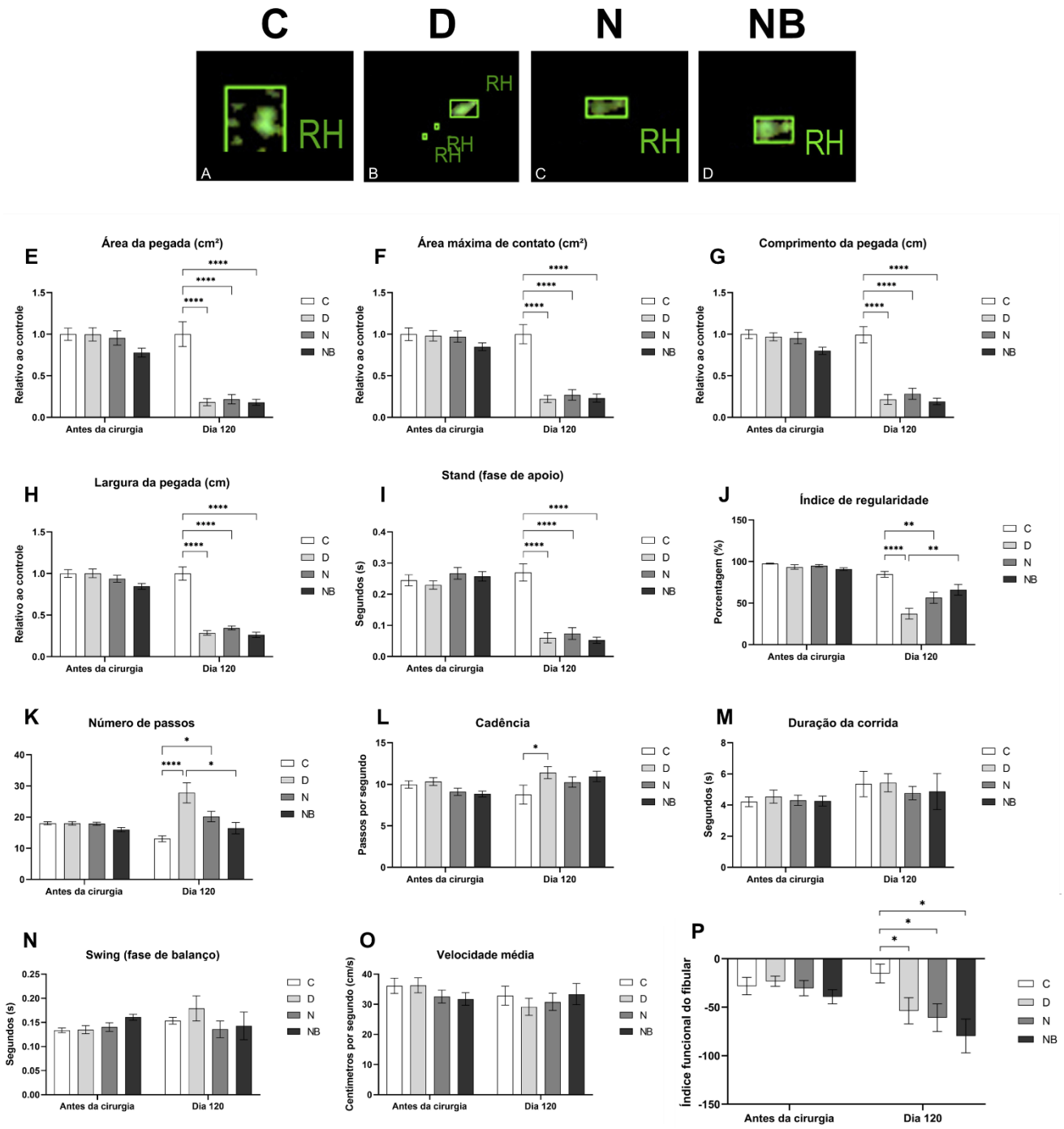


Figura 14. Ilustrações e gráficos da análise funcional da marcha (CatWalk XT) para os grupos experimentais nos diferentes momentos de avaliação. A-D: Imagens das pegadas obtidas pela análise no CatWalk XT de acordo com o grupo experimental. A: Grupo controle (C). B: Grupo desnervado (D). C: Grupo neurorrafia (N). D: Grupo neurorrafia + biopolímero de fibrina (NB). E-P: gráficos das análises de área da pegada (E), área máxima de contato (F), comprimento (G) e largura da pegada (H), Stand - fase de apoio (I), índice de regularidade (J), número de passos (K), cadência (L), duração média das corridas (M), Swing - fase de balanço (N), velocidade média das corridas (O), e índice funcional do fibular (P) de acordo com grupos experimentais. E-J, M-P: Valores expressos em média ± SEM, avaliados pelo teste ANOVA complementado com o teste de comparações múltiplas de Tukey. K, L: Valores expressos em mediana e range, e avaliados pelo teste Kruskal-Wallis, complementado com o teste de comparações múltiplas de Dunn. *p < 0,05; **p < 0,01; ****p < 0,0001. E-H: normalizado pela média do grupo controle.

PESO CORPÓREO E PESO DO MÚSCULO SÓLEO

Não houve diferença no peso corpóreo dos animais entre os grupos experimentais (Figura 15A).

Em relação ao peso do músculo sóleo, os grupos N e NB apresentaram valores intermediários, maiores que o grupo D e menores que o grupo C, mas iguais entre si. O grupo D apresentou os menores valores, diferente de todos os outros grupos. (Figura 15B).

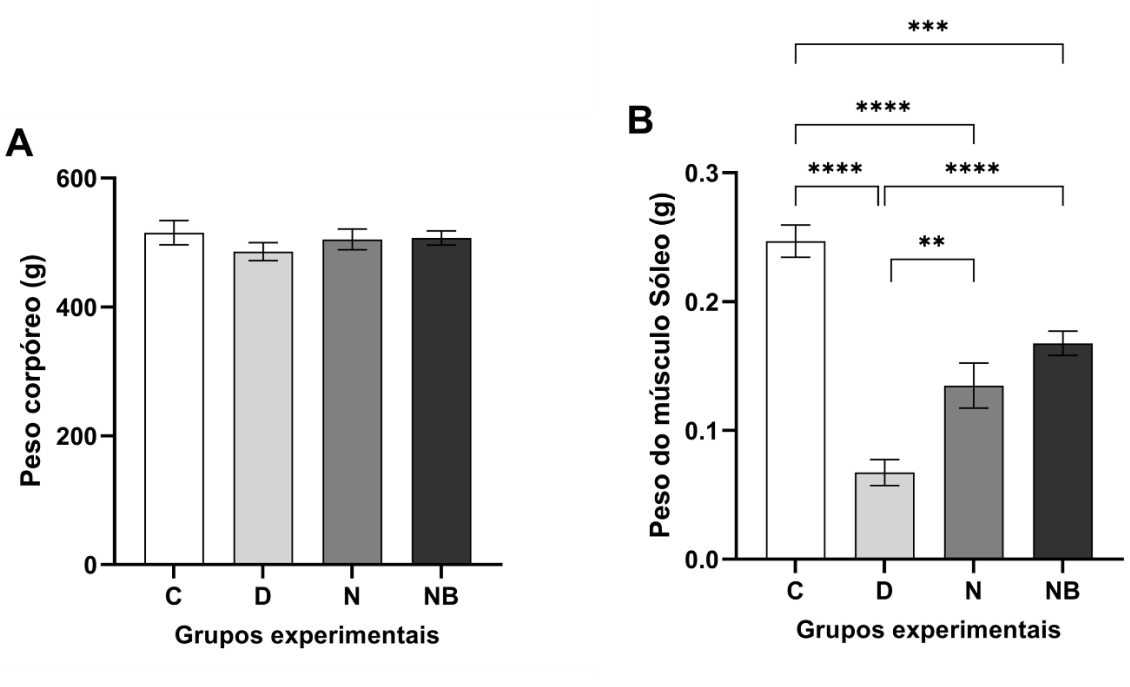


Figura 15. Gráficos de peso corpóreo (A) e peso do músculo sóleo (B), de acordo com os grupos experimentais: Grupo controle (C), Grupo desnervado (D), Grupo neurorrafia (N) e Grupo neurorrafia + biopolímero de fibrina (NB). Valores expressos em média ± SEM, e avaliados pelo teste ANOVA, complementado com o teste de comparações múltiplas de Tukey (**p < 0,01; ***p < 0,001; ****p < 0,0001).

ANÁLISE MORFOLÓGICA E MORFOMÉTRICA DO NERVO ISQUIÁTICO

O grupo C apresentou axônios intactos e bainhas de mielina preservadas e com formatos regulares, demonstrando uma morfologia dentro dos padrões normais de um nervo saudável (Figura 16A).

No grupo D, foram observadas apenas fibras nervosas degeneradas, com estruturas amorfas e sem bainha de mielina, com grande quantidade de núcleos inespecíficos e matriz extracelular (Figura 16B).

Nos grupos N e NB, foi possível observar fibras nervosas íntegras e regeneradas, mas com heterogeneidade do tamanho e aspecto estrutural menor e irregular, quando comparados ao grupo C (Figura 16C, D). Também foi observado aumento da matriz extracelular, mas com uma aparente quantidade aparentemente menor que no grupo D.

Em relação a análise morfométrica, todos os parâmetros avaliados demonstraram valores menores nos grupos reconstruídos (N e NB), com resultados semelhantes entre si e diferentes do grupo Controle (Figura 16 E-L).

No grupo D, devido a intensa degeneração e ausência de fibras nervosas íntegras, não foi possível realizar a morfometria.

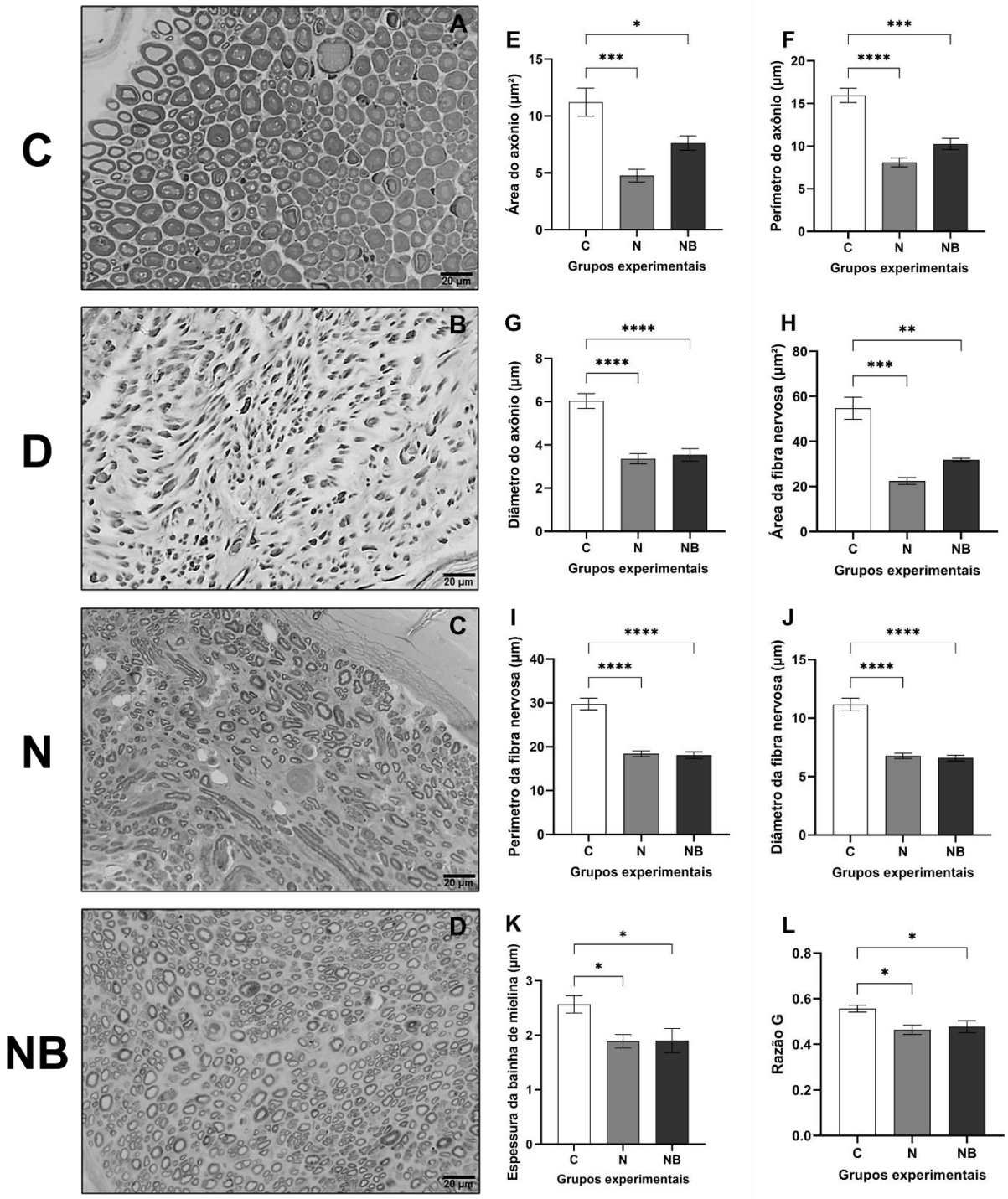


Figura 16. A-D: Fotomicrografias de secções transversais do nervo isquiático de acordo com os grupos experimentais, coradas com tetróxido de ósmio, sob microscopia de luz convencional, aumento de 40x. A: Grupo controle (C). B: Grupo desnervado (D). C: Grupo neurorrafia (N). D: Grupo neurorrafia + biopolímero de fibrina (NB). E-L: gráficos das análises de área (E), perímetro (F) e diâmetro (G) do axônio, área (H), perímetro (I) e diâmetro (J) da fibra nervosa, espessura da bainha de mielina (K) e razão G (L). Valores expressos em média ± SEM, avaliados pelo teste ANOVA complementado com o teste de comparações múltiplas de Tukey (*p < 0,05; **p < 0,01; ***p < 0,001; ****p < 0,0001).

ANÁLISE MORFOLÓGICA E MORFOMÉTRICA DAS FIBRAS MUSCULARES E QUANTIFICAÇÃO DE COLÁGENO INTRAMUSCULAR

A análise morfológica realizada após a coloração de HE demonstrou, no grupo C, fibras musculares em formato poligonal, com núcleos periféricos e pouca quantidade de matriz extracelular, ou seja, características compatíveis com a normalidade (Figura 17A).

No grupo D, estavam presentes aglomerado de pequenas fibras musculares, algumas delas com formato arredondado e outras com núcleo central, além de grande quantidade de matriz extracelular e núcleos inespecíficos (Figura 17B), características típicas de degeneração e atrofia muscular.

Uma morfologia intermediária foi observada nos grupos N e NB, com algumas fibras de formato poligonal e outras arredondado, algumas com núcleos centrais e outras periféricos, moderada quantidade de tecido conjuntivo (Figura 17C, D). Ainda, o grupo NB apresentou fibras musculares com tamanho heterogêneo, sendo sua maioria com aspecto estrutural maior que o grupo N (Figura 17D).

A morfometria das fibras musculares evidenciou que a área, perímetro e diâmetro do grupo NB apresentou valores intermediários, maiores que os grupos N e D, mas ainda menores que o grupo C. O grupo D apresentou os menores valores, diferente de todos os outros grupos. O grupo N, valores maiores que o D, mas menores que o NB e C (Figura 17E-G).

Em relação a porcentagem de colágeno intramuscular, o grupo NB foi o único que apresentou resultados semelhantes ao grupo C, e ainda diferentes dos grupos N e D. O grupo D apresentou os maiores valores, diferente de todos os outros grupos. O grupo N demonstrou valores intermediários, menores que o grupo D, mas maiores que os grupos NB e C (Figura 17H).

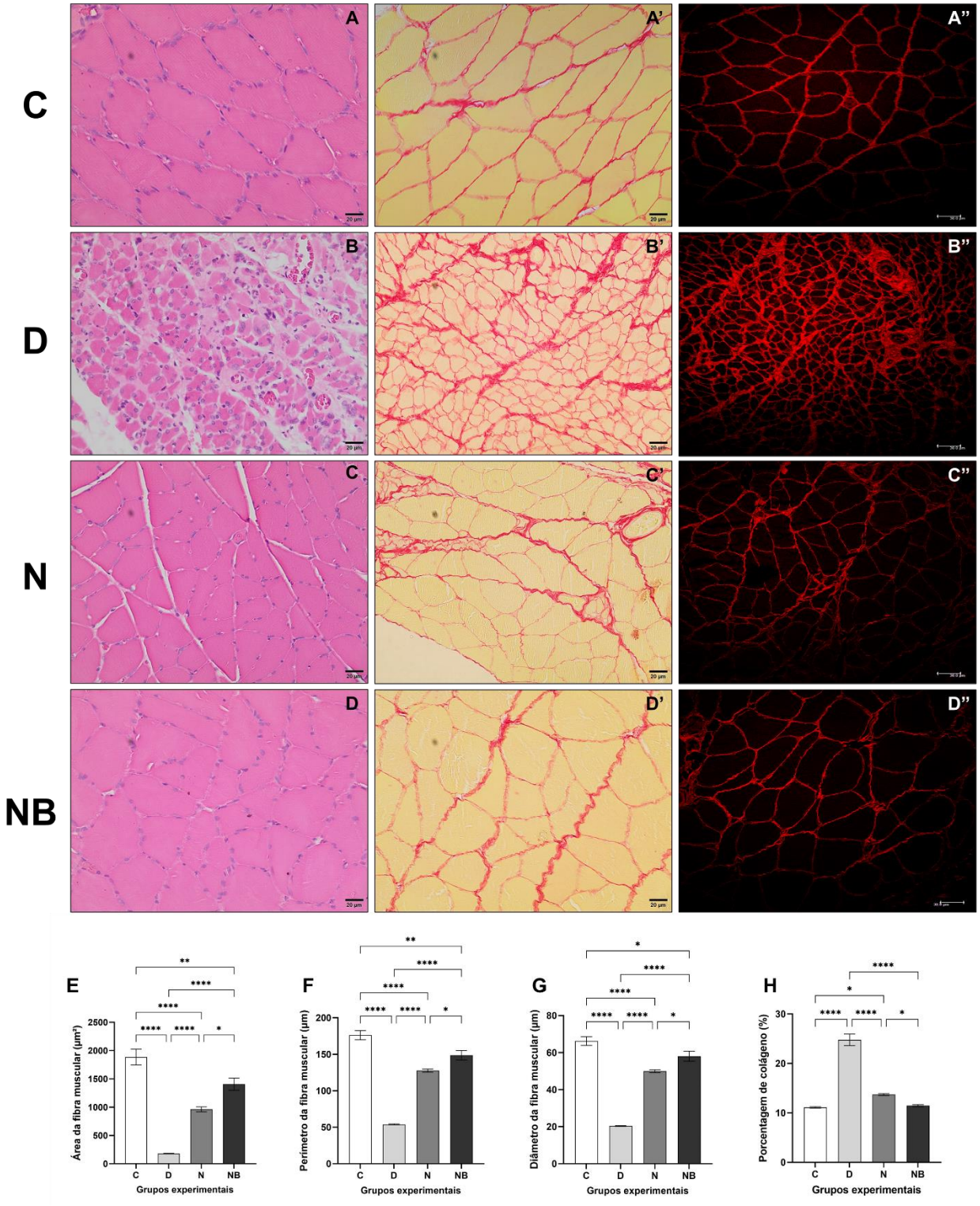


Figura 17. A-D: Fotomicrografias de cortes transversais do músculo sóleo de acordo com os grupos experimentais, corados com Hematoxilina e Eosina (A-D) e Picrosirius Red (A'A"-D'D"), sob microscopia de luz convencional (AA'-DD' e microscopia confocal (A"-D"), aumento de 40x. A: Grupo controle (C). B: Grupo desnervado (D). C: Grupo neurorrafia (N). D: Grupo neurorrafia + biopolímero de fibrina (NB). E-H: gráficos das análises de área (E), perímetro (F), diâmetro (G) da fibra muscular, e porcentagem de colágeno intramuscular (E), de todos os grupos experimentais. Valores expressos em média ± SEM, avaliados pelo teste ANOVA complementado com o teste de comparações múltiplas de Tukey (*p < 0,05; **p < 0,01; ****p < 0,0001).

ANÁLISE MORFOLÓGICA E MORFOMÉTRICA DAS JUNÇÕES NEUROMUSCULARES

Foi possível observar que houve respostas homogêneas dos fluoróforos com os AChR em autofluorescência em todos os grupos. No grupo C, os AChR apresentaram distribuição compatível com a normalidade, caracterizando-se a presença de ramos/braços contínuos ou em forma de “pretzel”, correndo em várias orientações ao longo da fibra muscular (Figura 18A). Uma morfologia semelhante foi observada no grupo NB (Figura 18D). No grupo D, observou-se achatamento e fragmentação dos AChR, e a maior parte distribuiu-se em padrão de “ilha”, indicando uma distribuição mais esparsa (Figura 18B), com aproximação morfológica ao grupo N (Figura 18C). Embora o achatamento tenha sido observado em algumas placas motoras, uma morfologia intermediária foi observada nos grupos de reparo (N e NB) (Figura 18C, D) em comparação aos grupos C e D (Figura 18A, B), embora a morfologia do NB estar mais próxima de C (Figura 18A, D).

Em relação aos terminais nervosos, o grupo C apresentou distribuição compatível com a normalidade, com terminais íntegros, preservados e sem descontinuidade (Figura 18a). No grupo D, os axônios estavam entrelaçados, sem visualização clara dos terminais nervosos, indicando ausência de preservação e integridade (Figura 18b). Nos grupos N e NB, uma morfologia intermediária foi observada (Figura 18c, d), sendo que as ramificações dos terminais nervosos estavam mais finas quando comparadas aos grupos C (Figura 18a).

A análise morfométrica corroborou com esses aspectos. Sendo que o grupo NB foi o único que apresentou resultados semelhantes ao grupo C, diferenciando-se dos grupos N e D, em relação aos valores da área dos AChR e da placa motora e ao número de cluster de AChR. O grupo D mostrou resultados distintos de todos os outros grupos, enquanto o grupo N apresentou valores intermediários, entre NB e C, sendo diferente de ambos (Figura 19A, C, F).

Em relação a área média dos clusters, o grupo NB também foi o único semelhante ao grupo C e diferente dos grupos N e D, que foram semelhantes entre si (Figura 19G).

Os índices de compactação e fragmentação demonstraram padrão similar, sendo o grupo NB foi o único semelhante ao grupo C e diferente do grupo D, mas também foi semelhante ao grupo N. Os grupos D e N foram semelhantes entre si e diferentes do grupo C (Figura 19H, I).

A respeito do perímetro dos AChR e da placa motora e área não ocupada dos AChR, o grupo NB foi semelhante aos grupos N e C, que também foram semelhantes entre si. O grupo D obteve os menores valores, diferenciando-se de todos os outros grupos (Figura 19B, D, J).

Em relação ao diâmetro da placa motora, não houve diferenças significativas entre os grupos (Figura 19E).

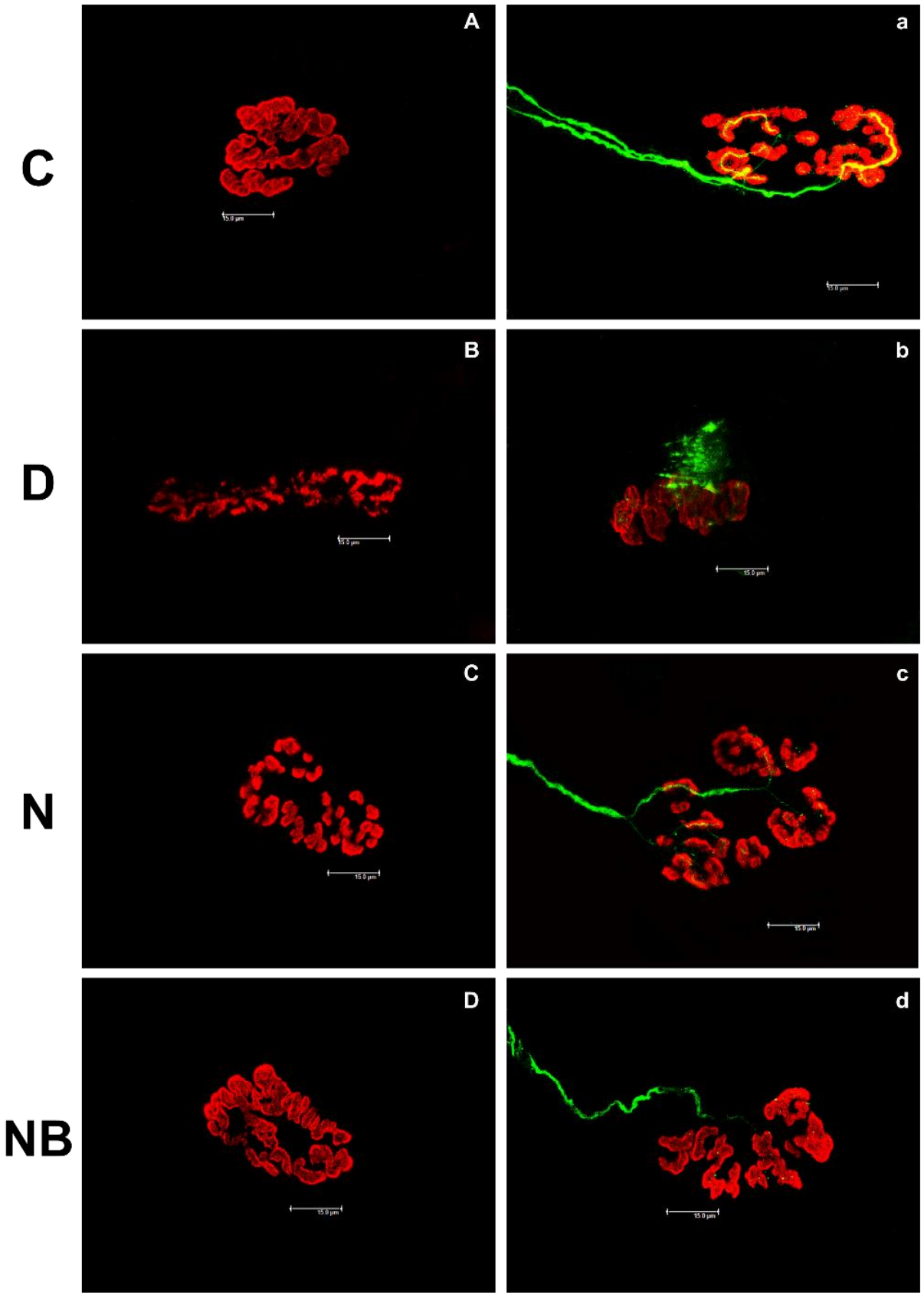


Figura 18. Microscopia confocal dos receptores de acetilcolina (em vermelho, Aa-Dd) e terminais nervosos (em verde, a-d), de acordo com os grupos experimentais, aumento de 63x, zoom 2. A, a: Grupo controle (C). B, b: Grupo desnervado (D). C, c: Grupo neurorrafia (N). D, d: Grupo neurorrafia + biopolímero de fibrina (NB).

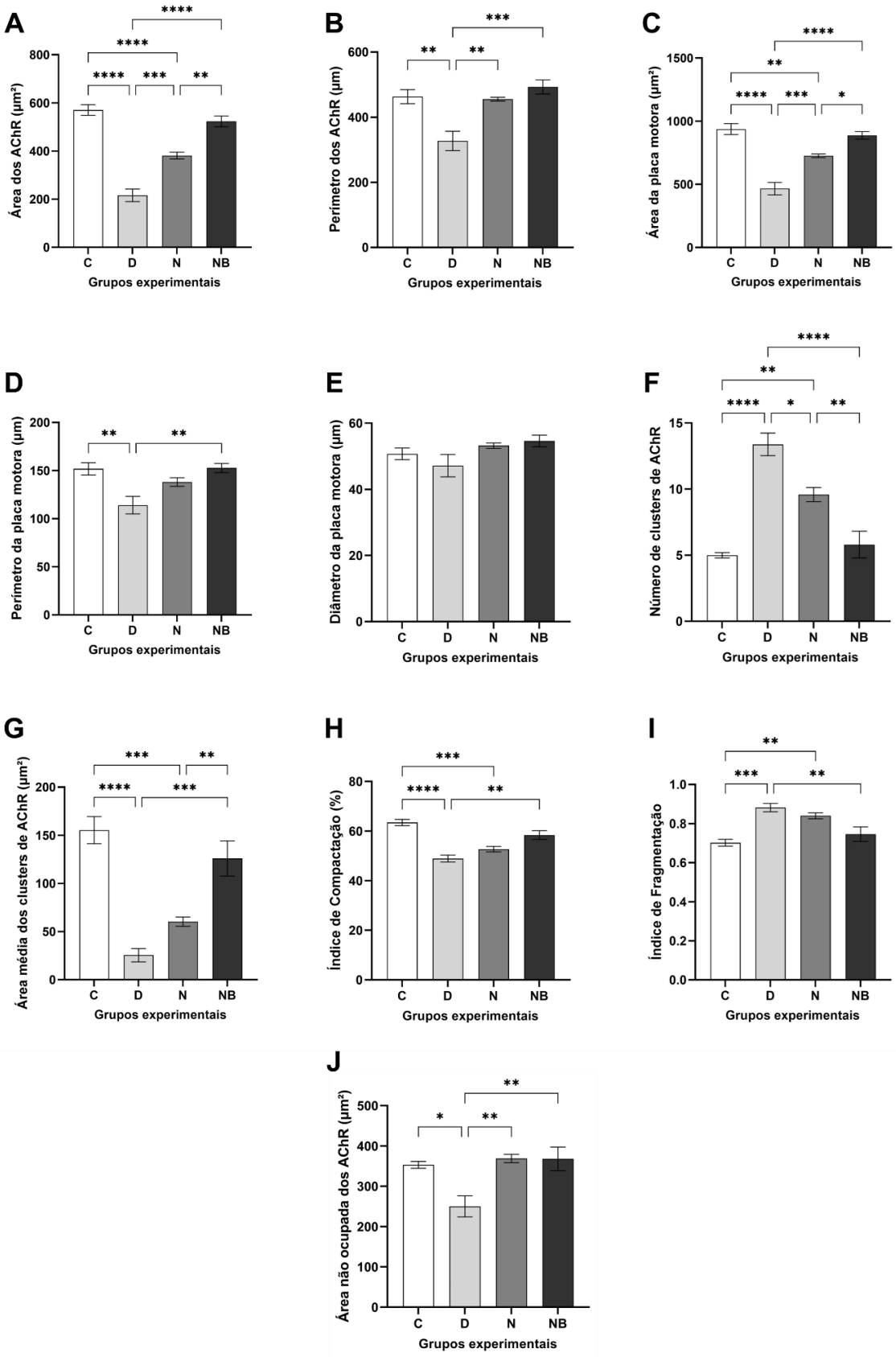


Figura 19. Gráficos das análises da JNM por meio do NMJ-morph. Área (A) e perímetro (B) dos AChR, área (C), perímetro (D) e diâmetro (E) da placa motora, número (F) e área média (G) de *clusters* de AChR, índices de compactação (H) e fragmentação (I), e área não ocupada pelos AChR (J). Valores expressos em média ± SEM, avaliados pelo teste ANOVA complementado com o teste de comparações múltiplas de Tukey (*p < 0,05; **p < 0,01; ***p < 0,001; ****p < 0,0001).

DISCUSSÃO

O reparo de nervos periféricos continua sendo um desafio para a saúde pública, pois mesmo após intervenções cirúrgicas a recuperação da função motora é na maioria dos casos insatisfatória. Mesmo com a vasta disponibilidade de informações relacionadas a fisiopatologia das lesões nervosas, ainda não há um tratamento que assegure uma recuperação funcional completa em casos graves (PALISPIS; GUPTA, 2017; PAN; MACKINNON; WOOD, 2020; WILCOX et al., 2020). Desse modo, o modelo de lesão nervosa utilizado foi a secção completa do nervo isquiático, correspondendo a neurotmese de Seddon (1942) ou lesão de grau 5 de Sunderland (1951), seguida de reconstrução imediata via neurorrafia término-terminal associada ou não ao BHF.

Este biopolímero possui a singularidade de ser livre de sangue humano, sendo constituído apenas de derivados animais, o que o torna um produto distinto dos demais e único no mundo. Trata-se de uma tecnologia brasileira, comercialmente viável, possuindo a vantagem de não ser transmissor de doenças infecciosas e não gerar reações adversas (BUCHAIM et al., 2019).

Considerando que o SNP possui uma notável capacidade de regeneração após lesão, no grupo Desnervado foi realizado a remoção de um fragmento do nervo e a fixação dos cotos nervosos na tela subcutânea a fim de evitar a regeneração espontânea.(GAUDET; POPOVICH; RAMER, 2011).

O período experimental de 120 dias após a cirurgia foi escolhido visando uma investigação cronológica da ação do BHF na regeneração neuromuscular, considerando estudos anteriores de nosso grupo de pesquisa. Onde aos 7 e 30 dias (TIBÚRCIO et al., 2023a), aos 60 dias (LEITE et al., 2019; PINTO et al., 2021) e aos 90 dias (LEITE et al., 2023) o BHF proporcionou uma melhora na morfologia do nervo, do músculo e das JNMs desnervados após períodos mais curtos de recuperação. Somente a partir de 90 dias após neurorrafia isolada em ratos, é que as placas motoras estão completamente reinervadas, no entanto, esses mesmos animais, 120 dias após reparo, ainda não apresentam recuperação funcional (SAKUMA et al., 2016).

Neste estudo, após 120 dias de reconstrução, foi evidenciado um efeito significativo da associação do BHF com a neurorrafia. Esse efeito foi particularmente notável nas fibras musculares e matriz extracelular do músculo sóleo e nas JNMs associadas. A combinação com o BHF teve um impacto positivo, com vários parâmetros morfométricos se aproximando dos valores observados no grupo Controle, com redução da fibrose, da atrofia muscular e havendo reinervação das JNMs, em comparação com o grupo Neurorrafia isolada.

Em relação aos resultados funcionais da marcha, os parâmetros de índice de regularidade e número de passos demonstraram resultados positivos no grupo NB, sendo o único grupo que alcançou resultados semelhantes ao grupo Controle. O Índice de Regularidade é uma medida fracionária de coordenação entre patas, que indica o estado da coordenação motora global do animal analisado. Em animais saudáveis e totalmente coordenados o seu valor é de 100% (HAMERS et al., 2001; CHEN et al., 2014). A perda de coordenação entre membros leva a uma diminuição deste parâmetro (HAMERS et al., 2001). Os grupos D e N apresentaram os menores valores de Índice de Regularidade, iguais entre si e diferentes do grupo C, indicando perda significativa de coordenação entre as patas (CHIANG et al., 2014).

Hamers e colaboradores (2001), estudando lesão da medula espinal de ratos, observaram que uma semana após os ratos terem sido submetidos a lesão por transecção o Índice de Regularidade diminuiu de 100% (pré-tratamento) para aproximadamente 80%, sendo que após 4 semanas houve aumento para 90%.

Resultados semelhantes, com o mesmo período experimental, foi observado por Chiang e colaboradores (2014) estudando lesão constritiva crônica do nervo isquiático de ratos. Segundo esses autores, alterações no índice de regularidade e na sequência de passos estavam correlacionadas com alterações histopatológicas do nervo, as quais podem estar associadas a expressão de citocinas inflamatórias como o TNF-a e marcadores de plasticidade como sinaptofisina. Com base nessas alterações histopatológicas do nervo, o índice de regularidade e a sequência de passos foram altamente correlacionados com a alteração na remodelação neuronal, que ocorre durante a lesão nervosa constritiva crônica, indicando que o aumento da plasticidade neuronal refletiu no aumento do índice de regularidade e a consequente melhora da recuperação funcional.

Su e colaboradores (2018) descrevem resultados semelhantes estudando lesão por esmagamento do nervo seguida de estimulação elétrica de alta frequência. Onde a análise da marcha mostrou que a estimulação elétrica imediata levou a um índice de regularidade significativamente alto, sendo um indicativo de melhora da função motora.

Outros resultados encontrados nesta pesquisa também apontam para uma recuperação. Nos grupos reconstruídos (N e NB), foram observados axônios com bainhas de mielina íntegras e que também estavam em processo de remielinização, indicando um processo regenerativo (RĂDUCAN et al., 2013). Já está descrito que o BHF pode potencializar a regeneração do nervo em períodos iniciais após lesão. Os mesmos achados foram observados em trabalhos anteriores do nosso grupo (LEITE et al., 2019, 2023; TIBÚRCIO et al., 2023a), bem como em outros trabalhos na literatura utilizando BHF em reparo de nervos de roedores (RODRÍGUEZ-SÁNCHEZ et al., 2021; BUENO et al., 2023, 2024), mas com períodos de recuperação menores.

A análise morfométrica do nervo demonstrou similaridade entre os grupos reconstruídos (NB e N). Especificamente no grupo NB, todos parâmetros relacionados ao tamanho das fibras musculares (área, perímetro e diâmetro) demonstraram valores intermediários, maiores que os grupos N e D, mas ainda não semelhante ao grupo Controle. Em relação ao peso do músculo sóleo, os grupos reconstruídos (NB e N) apresentaram resultados semelhantes e intermediários, maiores que o grupo D, mas ainda menores que o grupo C, indicando que que a regeneração está em curso e com maior grau que o grupo desnervado, corroborando com esses resultados morfométricos. Esses resultados indicam uma regeneração muscular acentuada no grupo NB induzida pelo BHF, mas o músculo ainda não retornou ao seu estado anterior à lesão, evidenciando que a regeneração está em curso, mas ainda insuficiente (GAUDET; POPOVICH; RAMER, 2011; RĂDUCAN et al., 2013).

O grupo NB apresentou ainda diversas fibras musculares muito grandes ao lado de fibras muito pequenas, indicando possível hipertrofia compensatória, comum em lesões nervosas periféricas (MARTINELLI et al., 2021). Já está descrito que os mecanismos fisiopatológicos das LNPs incluem hipertrofia compensatória, alongamento anormal e atividade elétrica espontânea de fibras musculares desnervadas (TEN HOLTER; VAN NIEUWSTADT, 1993). A hipertrofia compensatória nas fibras musculares pode ser causada traumas musculares e nervosos ou doenças que promovam a perda da condução nervosa, ou ainda ser um indicativo de remodelação tecidual acentuada (MARTINELLI et al., 2021).

Ainda, no grupo NB, uma significativa redução de colágeno intramuscular foi evidenciada, com valores menores que o grupo N e iguais ao grupo Controle, o que sugere maior grau de regeneração muscular, quando comparado aos demais grupos lesionados, acompanhado de menor grau de fibrose e atrofia, bem como menor grau de inflamação. Esses achados podem ter sido causados pela melhora da regeneração axonal, e consequente potencialização da reinervação das fibras musculares, induzidas pelo BHF, que foi eficaz na recuperação muscular após lesão, auxiliando assim na recuperação funcional parcial. Após desnervação, ocorre degeneração das fibras musculares, com diminuição da área e volume das fibras, as quais são substituídas por gordura e tecido conjuntivo rico em colágeno, ocorrendo aumento da matriz extracelular colagênica, um tecido excedente que prejudica a capacidade de contração muscular, configurando um quadro de fibrose e atrofia, que leva à perda gradual de massa muscular (MULLER et al., 2007; MOIMAS et al., 2013; CARRARO et al., 2015; TUFFAHA et al., 2016; HUANG et al., 2019). Carraro e colaboradores (2015) evidenciaram que fibras musculares degeneradas e músculos atróficos e fibróticos podem ser observados até 7 meses após desnervação em roedores.

Em relação às JNMs, no grupo NB, os AChR estavam organizados em ramos contínuos (forma de “pretzel”), correndo em várias orientações ao longo da fibra muscular, características presentes também no grupo controle, indicando distribuição compatível com a

normalidade (RODRÍGUEZ CRUZ et al., 2020). Em relação aos terminais nervosos, uma morfologia intermediária foi observada nos grupos reconstruídos (N e NB), com espessura mais delgada quando comparadas aos grupos C, mas em estado íntegro, diferentemente do grupo D. A análise morfométrica corroborou com os esses resultados.

Junções saudáveis apresentam um padrão contínuo, enquanto junções desnervadas exibem fragmentação, com aumento no número de clusters de AChR, o que compromete a continuidade e reduz a área e o perímetro dos AChR, assim como da placa motora como um todo (LEITE et al., 2023). Com a falha na transmissão do sinal elétrico e, consequentemente, na contração muscular, ocorrem alterações na agregação dos clusters de AChR. Essas mudanças são principalmente atribuídas a alterações na via de sinalização Agrina/LRP4/Musk/Rapsina, principal via responsável pela ancoragem dos AChR e estabilização global da JNM, o que leva a um aumento na fragmentação da placa motora (WALKER et al., 2021).

Os resultados encontrados, especialmente em relação à área dos AChR e da placa motora, e ao número e área média dos clusters de AChR, onde o grupo NB apresentou maior área e menor número de clusters, e consequente menor grau fragmentação em relação ao grupo N, evidenciando uma aproximação do estado saudável, com maior continuidade dos AChR.

Esses achados indicam que, no grupo NB, houve um retorno dos AChR e da morfologia das JNMs aos seus padrões normais, sugerindo que o BHF possui potencial para restabelecer a estrutura da JNM, promovendo seu retorno a um estado saudável, anterior à lesão. Já foi evidenciado que o BHF pode melhorar a recuperação morfológica e molecular das JNMs e de seus AChR após desnervação, quando associado a neurorrafia (PINTO et al., 2021) ou a tubulização (LEITE et al., 2023), atuando principalmente no retorno da via molecular da Agrina e a consequente melhora na estabilização dos AChR e da JNM como um todo.

Em estudo anterior, aos 7 e 30 dias após reconstrução, o BHF proporcionou um efeito pró-regenerativo no local da lesão, devido a potencialização da resposta imune com aumento no número de macrófagos M2 (anti-inflamatórios) e outras células inflamatórias (TIBÚRCIO et al., 2023a). Estas células, juntamente com as células de Schwann, atuam acelerando os processos de degeneração e regeneração, que são sequenciais e interdependentes, favorecendo o crescimento axonal e melhorando o processo regenerativo (NOCERA; JACOB, 2020). Esses macrófagos M2 produzem citocinas anti-inflamatórias e fatores de crescimento, além de promover angiogênese, cicatrização e remodelação tecidual, sendo essenciais no microambiente da lesão, logo que fornecem suporte trófico para aumentar o crescimento axonal (ZIGMOND; ECHEVARRIA, 2019; BOMBEIRO; FERNANDES; RIBOT, 2024).

Estudos envolvendo o reparo do sistema nervoso central, após lesão da medula espinal (SPEJO et al., 2018) e avulsão da raiz ventral do plexo braquial (KEMPE et al., 2020) de roedores utilizando BHF demonstraram resultados semelhantes. Nos quais o BHF estimulou resposta anti-inflamatória, com aumento de citocinas e macrófagos M2, sugerindo que a fibrina heteróloga pode estimular o recrutamento e a migração dessas células para o local da lesão. A presença de fibrina heteróloga e outros fatores de coagulação, além da fibronectina, na composição do BHF contribuem para estimular a resposta imune, levando a um efeito imunomodulador e potencial imunogênico, induzindo mecanismos anti-inflamatórios (SPEJO et al., 2018).

A fibrina heteróloga, além de manter um microambiente que acelera a regeneração, também estimula a resposta imune por várias semanas. Como o BHF não possui componentes do sangue humano não sofre rápida fibrinólise, formando uma rede de fibrina densa e estável, que pode durar por um longo tempo (PINTO et al., 2021; ABBADE et al., 2021). É importante notar que o BHF difere dos selantes de fibrina comerciais, que são produzidos a partir de sangue humano, pois possuem uma rápida fibrinólise, que se inicia antes de 24horas após aplicação (PINTO et al., 2021; TIBÚRCIO et al., 2023a). Assim, o retardo na quebra da fibrina heteróloga pode garantir a manutenção da imunomodulação e a consequente regeneração acentuada.

Os achados neste estudo, como a melhora da morfologia do músculo e das JNMs no grupo NB, corroboram com os resultados funcionais relativos ao índice de regularidade e com os estudos anteriores, sugerindo que o BHF pode potencializar a regeneração nervosa e neuromuscular em períodos tardios de recuperação após lesão severa. Devido a lenta fibrinólise, o BHF pode ter se mantido estável por um longo período no local da lesão, e assim mantido a modulação da resposta imune e a consequente favorecimento do crescimento axonal.

É bastante conhecido que o aumento da inflamação se correlaciona com o agravamento da atrofia muscular e da fibrose. A inflamação é uma resposta biológica à lesão com o recrutamento e ativação de vários fatores anti- e pró-inflamatórios (MUKUND; SUBRAMANIAM, 2020). A proteína mTORC1 (Mammalian Target of Rapamycin Complex 1) é uma das proteínas envolvida na regulamentação de autofagia e síntese de outras proteínas e, recentemente, foi demonstrado que a via de sinalização mTORC desempenha um papel crucial na regeneração muscular (WANG et al., 2021). A via de sinalização mTORC nas fibras musculares esqueléticas é fundamental para manter a inervação adequada das fibras, preservando a estrutura da JNM tanto na fibra muscular quanto no neurônio motor (BARALDO et al., 2020).

Nosso grupo de pesquisa tem se dedicado a estudos cronológicos utilizando BHF em LNPs, com ênfase na recuperação neuromuscular, e tem encontrado resultados promissores.

Aos 7 e 30 dias após reparo, o BHF demostrou efeitos imunomodulatório, angiogênico e pró-regenerativos, além de auxiliar na recuperação morfológica parcial das JNMs e previnir degeneração severa do músculo (TIBÚRCIO et al., 2023a). Aos 60 dias, após reparo tardio, o BHF potencializou a regeneração axonal e ainda permitiu a redução do número de pontos quando comparado a neurorrafia isolada, com a consequente diminuição do tempo de procedimento cirúrgico (LEITE et al., 2019); ainda, potencializou a recuperação morfológica e molecular das JNMs, com retorno ao seu padrão molecular maduro (PINTO et al., 2021). Aos 90 dias, após lesão nervosa grave, o BHF resultou na estabilização dos AChR, que apresentaram distribuição normal após reparo, o que potencializa a regeneração neuromuscular, além de uma recuperação parcial da função motora (marcha) (LEITE et al., 2023); agora aos 120 dias evidenciamos que o BHF mesmo em períodos prolongados contribui para recuperação funcional parcial (melhora da coordenação evidenciada pelo IR), para a reinervação das JNMs e retorno de seus AChR aos seus padrões normais/saudáveis (maior área e menor grau de fragmentação), e para a regeneração das fibras musculares (diminuição de atrofia e fibrose).

A ausência de testes eletrofisiológicos e medidas de velocidade de regeneração são consideradas limitações deste estudo. Pretendemos explorá-los em estudos futuros, pois podem trazer resultados mais aprofundados sobre o papel do BHF em LNPs.

CONCLUSÕES

Este estudo demonstrou que o biopolímero heterólogo de fibrina, em estágios prolongados de recuperação, contribui para a recuperação funcional parcial, par a restauração morfológica das junções neuromusculares e dos receptores de acetilcolina aos padrões normais, além de promover a reinervação das placas motoras e a regeneração das fibras musculares. Esses efeitos contribuem para uma melhora global na regeneração neuromuscular. Além disso, o BHF, sendo um produto biológico não humano, oferece vantagens como a retardo da fibrinólise, ausência de risco de transmissão de doenças infecciosas e a não ocorrência de efeitos adversos. A combinação de neurorrafia com o BHF surge como uma abordagem médica emergente e economicamente viável, que merece investigação mais aprofundada. Ensaios clínicos futuros são necessários para otimizar a dose e estabelecer um protocolo padronizado para o reparo de nervos periféricos.

REFERÊNCIAS

ABBADE, L. P. F. et al. Treatment of Chronic Venous Ulcers With Heterologous Fibrin Sealant: A Phase I/II Clinical Trial. **Frontiers in Immunology**, v. 12, 2021.

ALVITES, R. D. et al. Biomaterials and Cellular Systems at the Forefront of Peripheral Nerve Regeneration. Em: **Peripheral Nerve Disorders and Treatment**. [s.l.] IntechOpen, 2020.

ARAÚJO, M. R. et al. Transgenic human embryonic stem cells overexpressing FGF2 stimulate neuroprotection following spinal cord ventral root avulsion. **Experimental Neurology**, v. 294, p. 45–57, ago. 2017.

ARNOLD, W. D.; CLARK, B. C. Neuromuscular junction transmission failure in aging and sarcopenia: The nexus of the neurological and muscular systems. **Ageing Research Reviews**, v. 89, p. 101966, 1 ago. 2023.

ARSLANTUNALI, D. et al. Peripheral nerve conduits: technology update. **Medical Devices (Auckland, N.Z.)**, v. 7, p. 405–424, 2014.

BAIN, J. R.; MACKINNON, S. E.; HUNTER, D. A. Functional evaluation of complete sciatic, peroneal, and posterior tibial nerve lesions in the rat. **Plastic and Reconstructive Surgery**, v. 83, n. 1, p. 129–138, jan. 1989.

BARALDO, M. et al. Skeletal muscle mTORC1 regulates neuromuscular junction stability. **Journal of Cachexia, Sarcopenia and Muscle**, v. 11, n. 1, p. 208–225, fev. 2020.

BARBIZAN, R. et al. Motor recovery and synaptic preservation after ventral root avulsion and repair with a fibrin sealant derived from snake venom. **PloS One**, v. 8, n. 5, p. e63260, 2013.

BARIK, A. et al. Schwann Cells in Neuromuscular Junction Formation and Maintenance. **The Journal of Neuroscience: The Official Journal of the Society for Neuroscience**, v. 36, n. 38, p. 9770–9781, 21 set. 2016.

BARROS, L. C. et al. A new fibrin sealant from Crotalus durissus terrificus venom: applications in medicine. **Journal of Toxicology and Environmental Health. Part B, Critical Reviews**, v. 12, n. 8, p. 553–571, out. 2009.

BEAR, M.; CONNORS, B.; PARADISO, M. A. **Neuroscience: Exploring the Brain, Enhanced Edition: Exploring the Brain, Enhanced Edition**. [s.l.] Jones & Bartlett Learning, 2020.

BHATNAGAR, D. et al. Fibrin glue as a stabilization strategy in peripheral nerve repair when using porous nerve guidance conduits. **Journal of Materials Science. Materials in Medicine**, v. 28, n. 5, p. 79, maio 2017.

BISCOLA, N. P. et al. Multiple uses of fibrin sealant for nervous system treatment following injury and disease. **The Journal of Venomous Animals and Toxins Including Tropical Diseases**, v. 23, p. 13, 14 mar. 2017.

BOEHM, I. et al. Comparative anatomy of the mammalian neuromuscular junction. **Journal of Anatomy**, v. 237, n. 5, p. 827–836, nov. 2020.

BOMBEIRO, A. L.; FERNANDES, R. G. Q.; RIBOT, J. C. New immune regulators of sciatic nerve regeneration? Lessons from the neighborhood. **Neural Regeneration Research**, v. 19, n. 4, p. 705–706, abr. 2024.

BRAGA SILVA, J. et al. End-to-side neurorrhaphy in peripheral nerves: Does it work? **Hand Surgery & Rehabilitation**, v. 41, n. 1, p. 2–6, fev. 2022.

BUCHAIM, D. V. et al. Unique heterologous fibrin biopolymer with hemostatic, adhesive, sealant, scaffold and drug delivery properties: a systematic review. **The Journal of Venomous Animals and Toxins Including Tropical Diseases**, v. 25, p. e20190038, 2019.

BUCHAIM, D. V. et al. A biocomplex to repair experimental critical size defects associated with photobiomodulation therapy. **The Journal of Venomous Animals and Toxins Including Tropical Diseases**, v. 28, p. e20210056, 2022.

BUCHAIM, R. L. et al. Effect of low-level laser therapy (LLLT) on peripheral nerve regeneration using fibrin glue derived from snake venom. **Injury**, v. 46, n. 4, p. 655–660, abr. 2015.

BUENO, C. R. DE S. et al. Morphofunctional Improvement of the Facial Nerve and Muscles with Repair Using Heterologous Fibrin Biopolymer and Photobiomodulation. **Pharmaceuticals (Basel, Switzerland)**, v. 16, n. 5, p. 653, 27 abr. 2023.

BUENO, C. R. DE S. et al. Delayed repair of the facial nerve and its negative impacts on nerve and muscle regeneration. **The Journal of Venomous Animals and Toxins Including Tropical Diseases**, v. 30, p. e20230093, 2024.

CARRARO, U. et al. Persistent Muscle Fiber Regeneration in Long Term Denervation. Past, Present, Future. **European Journal of Translational Myology**, v. 25, n. 2, p. 4832, 11 mar. 2015.

CARTAROZZI, L. P. et al. Mesenchymal stem cells engrafted in a fibrin scaffold stimulate Schwann cell reactivity and axonal regeneration following sciatic nerve tubulization. **Brain Research Bulletin**, v. 112, p. 14–24, mar. 2015.

CHEN, M. et al. P2Y2 promotes fibroblasts activation and skeletal muscle fibrosis through AKT, ERK, and PKC. **BMC Musculoskeletal Disorders**, v. 22, p. 680, 11 ago. 2021.

CHEN, Y.-J. et al. Detection of subtle neurological alterations by the Catwalk XT gait analysis system. **Journal of NeuroEngineering and Rehabilitation**, v. 11, n. 1, p. 62, 16 abr. 2014.

CHHABRA, A. et al. Peripheral nerve injury grading simplified on MR neurography: As referenced to Seddon and Sunderland classifications. **The Indian Journal of Radiology & Imaging**, v. 24, n. 3, p. 217–224, 2014.

CHIANG, C.-Y. et al. Comprehensive analysis of neurobehavior associated with histomorphological alterations in a chronic constrictive nerve injury model through use of the CatWalk XT system. **Journal of Neurosurgery**, v. 120, n. 1, p. 250–262, jan. 2014.

CONTI-FINE, B. M.; MILANI, M.; KAMINSKI, H. J. Myasthenia gravis: past, present, and future. **The Journal of Clinical Investigation**, v. 116, n. 11, p. 2843–2854, nov. 2006.

CRESTE, C. F. Z. et al. Highly Effective Fibrin Biopolymer Scaffold for Stem Cells Upgrading Bone Regeneration. **Materials**, v. 13, n. 12, p. 2747, 17 jun. 2020.

DESCHENES, M. R. et al. Adaptive Remodeling of the Neuromuscular Junction with Aging. **Cells**, v. 11, n. 7, p. 1150, 29 mar. 2022.

DIVAC, N. et al. Pharmacology of repair after peripheral nerve injury. **International Journal of Clinical Pharmacology and Therapeutics**, v. 59, n. 6, p. 447–462, jun. 2021.

ENGEL, A. G. The neuromuscular junction. **Handbook of Clinical Neurology**, v. 91, p. 103–148, 2008.

FERREIRA JR, R. S. et al. Heterologous fibrin sealant derived from snake venom: from bench to bedside – an overview. **Journal of Venomous Animals and Toxins including Tropical Diseases**, v. 23, p. 21, 6 jul. 2017.

GAUDET, A. D.; POPOVICH, P. G.; RAMER, M. S. Wallerian degeneration: gaining perspective on inflammatory events after peripheral nerve injury. **Journal of Neuroinflammation**, v. 8, n. 1, p. 110, 30 ago. 2011.

GEUNA, S. et al. Chapter 3: Histology of the peripheral nerve and changes occurring during nerve regeneration. **International Review of Neurobiology**, v. 87, p. 27–46, 2009.

GORDON, T. Peripheral Nerve Regeneration and Muscle Reinnervation. **International Journal of Molecular Sciences**, v. 21, n. 22, p. 8652, 17 nov. 2020.

GUIDI PINTO, C. et al. Cholecalciferol in ethanol-preferring rats muscle fibers increases the number and area of type II fibers. **Acta Histochemica**, v. 120, n. 8, p. 789–796, nov. 2018.

HAMERS, F. P. et al. Automated quantitative gait analysis during overground locomotion in the rat: its application to spinal cord contusion and transection injuries. **Journal of Neurotrauma**, v. 18, n. 2, p. 187–201, fev. 2001.

HAMERS, F. P. T.; KOOPMANS, G. C.; JOOSTEN, E. A. J. CatWalk-assisted gait analysis in the assessment of spinal cord injury. **Journal of Neurotrauma**, v. 23, n. 3–4, p. 537–548, 2006.

HEINZEL, J. et al. Use of the CatWalk gait analysis system to assess functional recovery in rodent models of peripheral nerve injury - a systematic review. **Journal of Neuroscience Methods**, v. 345, p. 108889, 1 nov. 2020.

HUANG, Z. et al. Skeletal Muscle Atrophy Was Alleviated by Salidroside Through Suppressing Oxidative Stress and Inflammation During Denervation. **Frontiers in Pharmacology**, v. 10, p. 997, 10 set. 2019.

HUGHES, B. W.; KUSNER, L. L.; KAMINSKI, H. J. Molecular architecture of the neuromuscular junction. **Muscle & Nerve**, v. 33, n. 4, p. 445–461, abr. 2006.

HUSSAIN, G. et al. Current Status of Therapeutic Approaches against Peripheral Nerve Injuries: A Detailed Story from Injury to Recovery. **International Journal of Biological Sciences**, v. 16, n. 1, p. 116–134, 1 jan. 2020.

ISAACS, J. E. et al. Comparative analysis of biomechanical performance of available “nerve glues”. **The Journal of Hand Surgery**, v. 33, n. 6, p. 893–899, 2008.

JONES, R. A. et al. NMJ-morph reveals principal components of synaptic morphology influencing structure-function relationships at the neuromuscular junction. **Open Biology**, v. 6, n. 12, p. 160240, dez. 2016.

JONES, R. A. et al. Cellular and Molecular Anatomy of the Human Neuromuscular Junction. **Cell Reports**, v. 21, n. 9, p. 2348–2356, 28 nov. 2017.

JONES, S.; EISENBERG, H. M.; JIA, X. Advances and Future Applications of Augmented Peripheral Nerve Regeneration. **International Journal of Molecular Sciences**, v. 17, n. 9, p. 1494, 7 set. 2016.

KANG, J. R.; ZAMORANO, D. P.; GUPTA, R. Limb salvage with major nerve injury: current management and future directions. **The Journal of the American Academy of Orthopaedic Surgeons**, v. 19 Suppl 1, p. S28-34, 2011.

KEMPE, P. R. G. et al. Neuroprotection and immunomodulation by dimethyl fumarate and a heterologous fibrin biopolymer after ventral root avulsion and reimplantation. **The Journal of Venomous Animals and Toxins Including Tropical Diseases**, v. 26, p. e20190093, 20 maio 2020.

KEMPE, P. R. G. et al. Ultrastructural Evidence of Synapse Preservation and Axonal Regeneration Following Spinal Root Repair with Fibrin Biopolymer and Therapy with Dimethyl Fumarate. **Polymers**, v. 15, n. 15, p. 3171, 26 jul. 2023.

KERNS, J. M. The microstructure of peripheral nerves. **Techniques in Regional Anesthesia and Pain Management**, Anatomy in Regional Anesthesia. v. 12, n. 3, p. 127–133, 1 jul. 2008.

KO, C.-P.; ROBITAILLE, R. Perisynaptic Schwann Cells at the Neuromuscular Synapse: Adaptable, Multitasking Glial Cells. **Cold Spring Harbor Perspectives in Biology**, v. 7, n. 10, p. a020503, out. 2015.

LEITE, A. P. S. et al. Heterologous fibrin sealant potentiates axonal regeneration after peripheral nerve injury with reduction in the number of suture points. **Injury**, v. 50, n. 4, p. 834–847, abr. 2019.

LEITE, A. P. S. et al. Acetylcholine receptors of the neuromuscular junctions present normal distribution after peripheral nerve injury and repair through nerve guidance associated with fibrin biopolymer. **Injury**, v. 54, n. 2, p. 345–361, fev. 2023.

LEMOS, R. S. et al. End-to-side neurorrhaphy in the reconstruction of peripheral segmental neural loss: an experimental study. **Acta Cirurgica Brasileira**, v. 39, p. e394024, 2024.

LEPORE, E. et al. Neuromuscular Junction as an Entity of Nerve-Muscle Communication. **Cells**, v. 8, n. 8, p. 906, 16 ago. 2019.

LOPES, B. et al. Peripheral Nerve Injury Treatments and Advances: One Health Perspective. **International Journal of Molecular Sciences**, v. 23, n. 2, p. 918, 14 jan. 2022.

MA, J. et al. Gene expression of myogenic regulatory factors, nicotinic acetylcholine receptor subunits, and GAP-43 in skeletal muscle following denervation in a rat model. **Journal of Orthopaedic Research: Official Publication of the Orthopaedic Research Society**, v. 25, n. 11, p. 1498–1505, nov. 2007.

MARIEB, E. N.; WILHELM, P. B.; MALLATT, J. **Anatomia Humana**. [s.l.] Pearson Education do Brasil, 2014.

MARTINELLI, A. et al. Photobiomodulation modulates the expression of inflammatory cytokines during the compensatory hypertrophy process in skeletal muscle. **Lasers in Medical Science**, v. 36, n. 4, p. 791–802, jun. 2021.

MINTY, G. et al. aNMJ-morph: a simple macro for rapid analysis of neuromuscular junction morphology. **Royal Society Open Science**, v. 7, n. 4, p. 200128, 15 abr. 2020.

MOIMAS, S. et al. Effect of vascular endothelial growth factor gene therapy on post-traumatic peripheral nerve regeneration and denervation-related muscle atrophy. **Gene Therapy**, v. 20, n. 10, p. 1014–1021, out. 2013.

MOZAFARI, R. et al. Combination of heterologous fibrin sealant and bioengineered human embryonic stem cells to improve regeneration following autogenous sciatic nerve grafting repair. **The Journal of Venomous Animals and Toxins Including Tropical Diseases**, v. 24, p. 11, 12 abr. 2018.

MUKUND, K.; SUBRAMANIAM, S. Skeletal muscle: A review of molecular structure and function, in health and disease. **Wiley Interdisciplinary Reviews. Systems Biology and Medicine**, v. 12, n. 1, p. e1462, jan. 2020.

MULLER, F. L. et al. Denervation-induced skeletal muscle atrophy is associated with increased mitochondrial ROS production. **American Journal of Physiology. Regulatory, Integrative and Comparative Physiology**, v. 293, n. 3, p. R1159-1168, set. 2007.

MURTAZINA, A.; ADAMEYKO, I. The peripheral nervous system. **Development (Cambridge, England)**, v. 150, n. 9, p. dev201164, 1 maio 2023.

NEPTUNE, R. R.; KAUTZ, S. A.; ZAJAC, F. E. Contributions of the individual ankle plantar flexors to support, forward progression and swing initiation during walking. **Journal of Biomechanics**, v. 34, n. 11, p. 1387–1398, nov. 2001.

NOCERA, G.; JACOB, C. Mechanisms of Schwann cell plasticity involved in peripheral nerve repair after injury. **Cellular and molecular life sciences: CMLS**, v. 77, n. 20, p. 3977–3989, out. 2020.

ORSI, P. R. et al. A unique heterologous fibrin sealant (HFS) as a candidate biological scaffold for mesenchymal stem cells in osteoporotic rats. **Stem Cell Research & Therapy**, v. 8, n. 1, p. 205, 29 set. 2017.

PAIVA, G. R. et al. Stem cells in end-to-side neurorrhaphy. Experimental study in rats. **Acta Cirurgica Brasileira**, v. 35, n. 12, p. e351207, 2021.

PALISPIS, W. A.; GUPTA, R. Surgical repair in humans after traumatic nerve injury provides limited functional neural regeneration in adults. **Experimental Neurology**, v. 290, p. 106–114, abr. 2017.

PAN, D.; MACKINNON, S. E.; WOOD, M. D. Advances in the repair of segmental nerve injuries and trends in reconstruction. **Muscle & Nerve**, v. 61, n. 6, p. 726–739, jun. 2020.

PATTON, B. L. Basal lamina and the organization of neuromuscular synapses. **Journal of Neurocytology**, v. 32, n. 5–8, p. 883–903, 2003.

PERRIN, F. E. et al. Involvement of monocyte chemoattractant protein-1, macrophage inflammatory protein-1alpha and interleukin-1beta in Wallerian degeneration. **Brain: A Journal of Neurology**, v. 128, n. Pt 4, p. 854–866, abr. 2005.

PINTO, C. G. et al. Heterologous fibrin biopolymer associated to a single suture stitch enables the return of neuromuscular junction to its mature pattern after peripheral nerve injury. **Injury**, v. 52, n. 4, p. 731–737, abr. 2021.

POMINI, K. T. et al. Tissue Bioengineering with Fibrin Scaffolds and Deproteinized Bone Matrix Associated or Not with the Transoperative Laser Photobiomodulation Protocol. **Molecules (Basel, Switzerland)**, v. 28, n. 1, p. 407, 3 jan. 2023.

RĂDUCAN, A. et al. Morphological and functional aspects of sciatic nerve regeneration after crush injury. **Romanian Journal of Morphology and Embryology = Revue Roumaine De Morphologie Et Embryologie**, v. 54, n. 3 Suppl, p. 735–739, 2013.

RAY, W. Z.; MACKINNON, S. E. Management of nerve gaps: autografts, allografts, nerve transfers, and end-to-side neurorrhaphy. **Experimental Neurology**, v. 223, n. 1, p. 77–85, maio 2010.

RAZA, C. et al. Repair strategies for injured peripheral nerve: Review. **Life Sciences**, v. 243, p. 117308, 15 fev. 2020.

REIS, C. H. B. et al. Effects of a Biocomplex Formed by Two Scaffold Biomaterials, Hydroxyapatite/Tricalcium Phosphate Ceramic and Fibrin Biopolymer, with Photobiomodulation, on Bone Repair. **Polymers**, v. 14, n. 10, p. 2075, 19 maio 2022.

ROBINSON, L. R. Traumatic injury to peripheral nerves. **Muscle & Nerve**, v. 23, n. 6, p. 863–873, jun. 2000.

RODRÍGUEZ CRUZ, P. M. et al. The Neuromuscular Junction in Health and Disease: Molecular Mechanisms Governing Synaptic Formation and Homeostasis. **Frontiers in Molecular Neuroscience**, v. 13, p. 610964, 2020.

RODRÍGUEZ-SÁNCHEZ, D. N. et al. 3D-printed nerve guidance conduits multi-functionalized with canine multipotent mesenchymal stromal cells promote neuroregeneration after sciatic nerve injury in rats. **Stem Cell Research & Therapy**, v. 12, n. 1, p. 303, 29 maio 2021.

RUFF, R. L. Neurophysiology of the neuromuscular junction: overview. **Annals of the New York Academy of Sciences**, v. 998, p. 1–10, set. 2003.

SAKUMA, M. et al. Lack of motor recovery after prolonged denervation of the neuromuscular junction is not due to regenerative failure. **The European Journal of Neuroscience**, v. 43, n. 3, p. 451–462, fev. 2016.

SANES, J. R. The basement membrane/basal lamina of skeletal muscle. **The Journal of Biological Chemistry**, v. 278, n. 15, p. 12601–12604, 11 abr. 2003.

SANES, J. R.; LICHTMAN, J. W. Development of the vertebrate neuromuscular junction. **Annual Review of Neuroscience**, v. 22, p. 389–442, 1999.

SAVASTANO, L. E. et al. Sciatic nerve injury: a simple and subtle model for investigating many aspects of nervous system damage and recovery. **Journal of Neuroscience Methods**, v. 227, p. 166–180, 30 abr. 2014.

SEDDON, H. J. A Classification of Nerve Injuries. **British Medical Journal**, v. 2, n. 4260, p. 237–239, 29 ago. 1942.

SHEN, J. et al. How muscles recover from paresis and atrophy after intramuscular injection of botulinum toxin A: Study in juvenile rats. **Journal of Orthopaedic Research: Official Publication of the Orthopaedic Research Society**, v. 24, n. 5, p. 1128–1135, maio 2006.

SPEJO, A. B. et al. Neuroprotection and immunomodulation following intraspinal axotomy of motoneurons by treatment with adult mesenchymal stem cells. **Journal of Neuroinflammation**, v. 15, n. 1, p. 230, 14 ago. 2018.

STOLL, G.; JANDER, S.; MYERS, R. R. Degeneration and regeneration of the peripheral nervous system: from Augustus Waller's observations to neuroinflammation. **Journal of the peripheral nervous system: JPNS**, v. 7, n. 1, p. 13–27, mar. 2002.

SU, H.-L. et al. Late administration of high-frequency electrical stimulation increases nerve regeneration without aggravating neuropathic pain in a nerve crush injury. **BMC neuroscience**, v. 19, n. 1, p. 37, 25 jun. 2018.

SUGIURA, Y.; LIN, W. Neuron–glia interactions: the roles of Schwann cells in neuromuscular synapse formation and function. **Bioscience reports**, v. 31, n. 5, p. 295–302, out. 2011.

SULLIVAN, R. et al. Peripheral Nerve Injury: Stem Cell Therapy and Peripheral Nerve Transfer. **International Journal of Molecular Sciences**, v. 17, n. 12, p. 2101, 14 dez. 2016.

SUNDERLAND, S. A classification of peripheral nerve injuries producing loss of function. **Brain: A Journal of Neurology**, v. 74, n. 4, p. 491–516, dez. 1951.

TEN HOLTER, J. B.; VAN NIEUWSTADT, M. A. [Neurogenic muscle hypertrophy]. **Nederlands Tijdschrift Voor Geneeskunde**, v. 137, n. 51, p. 2655–2658, 18 dez. 1993.

TERESHENKO, V. et al. Peripheral neural interfaces: Skeletal muscles are hyper-reinnervated according to the axonal capacity of the surgically rewired nerves. **Science Advances**, v. 10, n. 9, p. eadj3872, mar. 2024.

TIBÚRCIO, F. C. et al. Neuroregeneration and immune response after neurorrhaphy are improved with the use of heterologous fibrin biopolymer in addition to suture repair alone. **Muscle & Nerve**, v. 67, n. 6, p. 522–536, jun. 2023a.

TIBÚRCIO, F. C. et al. Effects of Nandrolone Decanoate on Skeletal Muscle and Neuromuscular Junction of Sedentary and Exercised Rats. **Medicina**, v. 59, n. 11, p. 1940, 1 nov. 2023b.

TIMOTIUS, I. K. et al. CatWalk XT gait parameters: a review of reported parameters in pre-clinical studies of multiple central nervous system and peripheral nervous system disease models. **Frontiers in Behavioral Neuroscience**, v. 17, p. 1147784, 2023.

TUFFAHA, S. H. et al. Growth Hormone Therapy Accelerates Axonal Regeneration, Promotes Motor Reinnervation, and Reduces Muscle Atrophy following Peripheral Nerve Injury. **Plastic and Reconstructive Surgery**, v. 137, n. 6, p. 1771–1780, jun. 2016.

VIGLIAR, M. F. R. et al. Photobiomodulation Therapy Improves Repair of Bone Defects Filled by Inorganic Bone Matrix and Fibrin Heterologous Biopolymer. **Bioengineering (Basel, Switzerland)**, v. 11, n. 1, p. 78, 13 jan. 2024.

VITERBO, F. et al. End-to-side versus end-to-end neurorrhaphy at the peroneal nerve in rats. **Acta Cirurgica Brasileira**, v. 32, n. 9, p. 697–705, set. 2017.

VITERBO, F.; MAGNANI, L. V.; NUNES, H. C. Zygomatic Muscle Neurotization with Nerve Grafts and End-to-Side Neurorrhaphies: A New Technique for Facial Palsy. **Plastic and Reconstructive Surgery. Global Open**, v. 10, n. 7, p. e4288, jul. 2022.

WALDRAM, M. Peripheral nerve injuries. **Trauma**, v. 5, n. 2, p. 79–96, 1 abr. 2003.

WALKER, L. J. et al. Agrin/Lrp4 signal constrains MuSK-dependent neuromuscular synapse development in appendicular muscle. **Development (Cambridge, England)**, v. 148, n. 21, p. dev199790, 1 nov. 2021.

WANG, Y. et al. Simvastatin Enhances Muscle Regeneration Through Autophagic Defect-Mediated Inflammation and mTOR Activation in G93ASOD1 Mice. **Molecular Neurobiology**, v. 58, n. 4, p. 1593–1606, abr. 2021.

WILCOX, M. et al. Strategies for Peripheral Nerve Repair. **Current Tissue Microenvironment Reports**, v. 1, n. 2, p. 49–59, 1 jun. 2020.

WU, P. et al. Key changes in denervated muscles and their impact on regeneration and reinnervation. **Neural Regeneration Research**, v. 9, n. 20, p. 1796–1809, 15 out. 2014.

ZAR, J. H. **Biostatistical Analysis**. 5ª edição ed. Upper Saddle River, N.J: Prentice Hall, 2009.

ZHANG, K.; JIANG, M.; FANG, Y. The Drama of Wallerian Degeneration: The Cast, Crew, and Script. **Annual Review of Genetics**, v. 55, p. 93–113, 23 nov. 2021.

ZIGMOND, R. E.; ECHEVARRIA, F. D. Macrophage biology in the peripheral nervous system after injury. **Progress in Neurobiology**, v. 173, p. 102–121, fev. 2019.

ARTIGO (Manuscrito em Inglês)

Neuromuscular junction and skeletal muscle recovery are improved in the long-term with heterologous fibrin biopolymer following rat sciatic nerve repair

Felipe Cantore Tiburcio[1,2]; Kevin Silva Muller[1,2]; Manuela Almeida e Silva[2]; Stephanye Caroline Moreira Rodrigues[2]; Benedito Barraviera[1,3,4]; Rui Seabra Ferreira Junior[3,4]; Cintia Yuri Matsumura[1,2]; Selma Maria Michelin Matheus[1,2*]

1 Botucatu Medical School, São Paulo State University (Unesp), Botucatu, SP, Brazil.

2 Department of Structural and Functional Biology, Institute of Biosciences, São Paulo State University (Unesp), Botucatu, SP, Brazil.

3 Center for the Study of Venoms and Venomous Animals (Cevap), São Paulo State University (Unesp), Botucatu, SP, Brazil.

4 Center for Translational Sciences and Biopharmaceuticals Development, São Paulo State University (Unesp), Botucatu, SP, Brazil.

***Corresponding author:** Selma Maria Michelin Matheus, PhD, Division of Anatomy, Department of Structural and Functional Biology, Institute of Biosciences, São Paulo State University (Unesp). Rua Professor Doutor Antonio Celso Wagner Zanin, 250, Unesp Campus de Botucatu, Botucatu, SP, Brazil. Zip code: 18618689. Telephone: +55 (14) 3880-0025. Email: selma.matheus@unesp.br

Funding: This study was financed in part by the Coordination for the Improvement of Higher Education Personnel (CAPES, Brazil) - Finance Code 001. It was partly supported by São Paulo Research Foundation (FAPESP, Brazil) - grant 23/16239-4, 22/07551-1, 21/11936-37, 17/06472-2. National Council for Scientific and Technological Development (CNPq, Brazil) No. 306339/2020-0, 303224/2018-5. The funding sources were not involved in the conduct of the research, preparation, and decision to submit the manuscript.

Conflict of interest: All the authors declare that they have no conflict of interest.

Ethics approval: All procedures were approved by the Ethics Committee on Animal Use of the São Paulo State University (CEUA/FMB/Unesp/SP/Brazil, protocol 1402/2021) and following the ethical principles regulated by the National Council of Animal Experimentation (CONCEA, Brazil).

Consent for publication: Not applicable.

Authors' contributions: FCT, and SMMM conceived the study. FCT and KSM conducted the surgeries. FCT, KSM, MAS, SCMR, CYM, and SMMM conducted the experiments, interpretation of the data, formal analysis, and writing of the original draft. KSM, MAS, SCMR, BB, RSFJr, CYM, and SMMM contributed to data analysis, writing, and revision of the submitted manuscript. All authors read and approved the final manuscript.

Acknowledgments: The authors are grateful to the Graduate Program in Surgery and Translational Medicine and Experimental Research Unit (Unipex) of Botucatu Medical School of Unesp, Carlos Roberto Padovani for the statistical expertise and consultation, and to the Electron Microscopy Center of IBB/Unesp for the equipment used.

Availability of data and materials: The datasets generated or analyzed during the current study are available from the corresponding author upon reasonable request.

Statement: We confirm that we have read the Journal's position on issues involved in ethical publication and affirm that this report is consistent with those guidelines.

Abstract: 265 words.

Manuscript: 4418 words.

Abstract

Peripheral nerve injuries (PNIs) affect skeletal muscle and its neuromuscular junctions (NMJs), leading to several morphofunctional and molecular alterations. Despite advances in surgical techniques, neurorrhaphy (suture) is the “gold standard”, but functional recovery is rarely complete. Adjuvant methods have been used to accelerate regeneration and improve neuromuscular recovery, such as heterologous fibrin biopolymer (HFB). This study aimed to evaluate the long-term effects of sciatic nerve repair using neurorrhaphy with HFB on the morphofunctional aspects of neuromuscular interactions after 120 days. Sixty adult male Wistar rats were divided into four groups (n=15/group): Control (C), only nerve location. Denervated (D), neurotmesis with 6mm gap. Neurorrhaphy (N), neurotmesis followed neurorrhaphy. Neurorrhaphy+HFB (NB): neurotmesis followed by neurorrhaphy plus HFB. One day before and 120 days after surgeries, functional gait analysis (CatWalk XT) was performed. At day 120, the animals were euthanized, and the sciatic nerves and soleus muscles were collected for morphological and morphometric analyses. The NB was the only one that presented similarity or greater proximity to C in the coordination parameters of the functional analysis (regularity index and number of steps), the morphology of NMJs and AChR (area of AChR and motor endplate, number of AChR clusters, compactness and fragmentation), and muscle fibers (area, perimeter, and diameter), and intramuscular collagen, with lower atrophy and fibrosis. The HFB contributes to partial functional recovery, and morphological restoration of NMJs and AChR to normal patterns, in addition to promoting reinnervation of motor endplates and regeneration of muscle fibers. In conclusion, the combination of neurorrhaphy and HFB emerges as a promising and economically viable medical approach advantageous in peripheral nerve repair.

Keywords: heterologous fibrin biopolymer, neuromuscular junction, peripheral nerve injury, neurorrhaphy, nerve regeneration, skeletal muscle.

Introduction

Among the factors that affect neuromuscular interactions, peripheral nerve injuries (PNIs) are particularly notable. PNIs are common and often disabling, affecting motor function and sensation either transiently or permanently (1–3). These injuries cause damage to the skeletal muscle and its neuromuscular junctions (NMJs), leading to several morphological and functional alterations (4–8).

Skeletal muscle exhibits significant plasticity and attempts to remodel following denervation (9,10). However, when these attempts are unsuccessful, they can lead to chronic fibrosis and atrophy, resulting in a diminished capacity for contraction and impaired motor function (11,12).

After denervation, fragmentation of NMJs and alterations in the levels of proteins associated with signaling pathways occur. Specifically, changes in the agrin protein pathway lead to the disaggregation and fragmentation of acetylcholine receptors (AChR), resulting in their redistribution throughout the muscle fiber (6,13–15).

The 'gold standard' technique for peripheral nerve repair is end-to-end neurorrhaphy (epineural suture) (6,7,16–18). However, this surgical approach alone often does not achieve optimal regeneration and leads to limited functional recovery (19–22). Approximately one-third of all nerve repairs result in incomplete recovery of motor function (7,19).

New approaches have been developed to complement neurorrhaphy and enhance nerve regeneration, including the use of biopharmaceuticals such as heterologous fibrin biopolymer (HFB) (23,24). HFB is a natural, biodegradable, bioabsorbable, and non-toxic biopolymer with excellent adhesive properties (25). It is composed of a thrombin-like enzyme derived from *Crotalus durissus terrificus* venom and a cryoprecipitate rich in fibrinogen from buffalo (*Bubalus bubalis*) blood (25). This unique heterologous fibrin does not use human blood, does not carry the risk of transmitting infectious diseases, and is suitable for various surgical procedures, particularly in peripheral nerve repair (3,5–7,15,17,18,24,26).

Our research group is conducting a chronological study using HFB in PNIs, focusing on neuromuscular recovery. We have found promising results at 7 and 30 days (7), and even at 60 days post-delayed repair (5,6). At 90 days, we observed further improvements when combined with nerve guidance conduit (15). In this study, we aim to deepen and solidify our findings in a long-term recovery period of 120 days.

This study aimed to evaluate the long-term effects of experimental nerve repair using neurorrhaphy combined with heterologous fibrin biopolymer, focusing on nerve regeneration, and the morphological and functional aspects of neuromuscular interactions after 120 days.

Methods

Experimental design

Sixty adult male Wistar rats, 60 days old and with an average body weight between 300 and 350 g, were used. This study was approved by the Ethics Committee on Animal Use of the São Paulo State University (CEUA/FMB/Unesp/SP/Brazil), under protocol 1402/2021. The animals were randomly distributed into 4 experimental groups (n=15/group): Control (C); Denervated (D); Neurorrhaphy (N), Neurorrhaphy + HFB (NB).

Surgical procedure

The animals were anesthetized by intraperitoneal injection of ketamine (90mg/kg) and xylazine (10mg/kg), followed by an incision into the caudal part of the right pelvic limb and exposure of the sciatic nerve (27). In the C group, the visualization and dissection of the nerve were performed. In the D, N, and NB groups, nerve injury was performed by transection (neurotmesis) about 3mm proximal to the trifurcation. In D, a 6mm fragment was removed, and the nerve stumps were inverted at 180° and fixed to the subcutaneous tissue, to avoid spontaneous regeneration (28,29). In N and NB, after neurotmesis, the nerve stumps were immediately reconnected. In N, only the suture (end-to-end epineural neurorrhaphy, 2 stitches, nylon 10-0), and in NB the suture was followed by 250µL of HFB application (7,25,30).

The components of the HFB were supplied separately in three microtubes stored at -20°C: a thrombin-like enzyme (gyroxin) extracted from snake venom, a fibrinogen-rich cryoprecipitate extracted from buffalo blood, and the diluent calcium chloride. Initially, the thrombin-like enzyme was mixed with the diluent; these components and the cryoprecipitate were then deposited on the nerve repair area at room temperature. After mixing, polymerization occurred, forming a complex consisting of a dense and stable fibrin network, similar to a gelatinous substance (7,26,30).

Functional gait analysis

One day before and 120 days after the surgeries, a functional gait analysis of all animals was performed, using the CatWalk XT (Noldus 9.1) software (31,32). Three runs were recorded for each animal.

The parameters evaluated were (32):

- Print parameters: Print area (cm²); Maximum contact area (cm²); Print length (cm); Print width (cm); Fibular Functional Index (FFI). Manually calculated by the formula: FFI = 174.9 [(ETS-NTS)/NTS] + 80.3 x [(EPL-NPL)/NPL] - 13.4. Where E refers to the

injured side, N to the uninjured side, TS to the toe spread, and PL to print length (15,33,34).

- Temporal parameters: Run duration (s); Stand (duration of paw contact with the glass, s); Swing (duration of absence of paw contact with the glass, s); Average speed of runs (cm/s); Number of steps; Cadence (number of steps per second).

- Coordination parameter: Regularity Index (RI) (%). Automatically calculated by the formula: RI = [(NSSP*4)/PP]*100%. Where NSSP represents the number of normal step sequence patterns and PP the total number of paw placements (35–37).

Euthanasia of animals and obtaining tissue samples

After 120 days after surgery, 10 animals from each group were weighed and euthanized by an overdose of sodium thiopental (120 mg/kg) intraperitoneally; if necessary, potassium chloride was administered intracardially. Five animals from each group were anesthetized by intraperitoneal injection of ketamine (Dopalen, 90 mg/kg) and xylazine (Anasedan, 10 mg/kg) and subjected to transcardiac perfusion. The sciatic nerves and soleus muscles were collected, weighed, fixed, and processed according to the analysis protocols below.

The soleus muscle was chosen for this study because it is an extremely important postural muscle, whose function is associated with maintaining stability and locomotion (38). Furthermore, it offers greater convenience for locating and viewing the NMJs, especially in the middle third, where the motor point is evident (39). The sciatic nerve was used because the injury to this nerve is already consolidated as a simple and accurate model for investigating many aspects of damage and recovery of the peripheral nervous system (27).

Morphological and morphometric analysis of the sciatic nerve

The right sciatic nerves, after fixation in Karnovsky's solution (2.5% glutaraldehyde + 4% paraformaldehyde in PBS (0.1 M phosphate-buffered saline, pH 7.4), were fixed and stained with osmium tetroxide (1%, 24h), embedded in historesin, and sectioned transversally (2 µm) in an ultramicrotome (Leica RM2265). The histological slides were photographed using an Olympus Bx41 image analyzer (SC30 camera) and images of 5 random fields were obtained using a 40x objective.

Using ImageJ software (v.1.54), the images were analyzed and the following values were measured: area, perimeter, and diameter of axons and nerve fibers, myelin sheath thickness (fiber diameter - axon diameter/2), and calculation of the G Ratio (axon diameter/fiber diameter) (15).

Morphological and morphometric analysis of muscle fibers and quantification of intramuscular collagen

After collection, the ends of the muscles were fixed in 10% buffered formalin for 24h, washed in water for 48h, embedded in Paraplast®, and sectioned in a microtome (4µm).

Two histological slides for each animal in each experimental group were prepared and stained with Hematoxylin and Eosin (HE) and Picrosirius Red. The slides were photographed using a 20x objective using an Olympus Bx41 microscope (SC30 camera). Furthermore, the slides stained with Picrosirius Red were photographed using a Confocal Laser Scanning Microscope (Leica Microsystems, TCS - SP5), where the autofluorescence of the staining was captured.

In the slide subjected to HE staining, 200 muscle fibers were selected from 3 to 4 random fields. Quantification was performed using ImageJ software (v.1.54), in which the area, perimeter, and diameter (Feret) of the muscle fibers were measured (5,7,39,40).

In the slide subjected to Picrosirius Red staining, in which the collagen was stained red and the muscle fibers yellow, quantification was performed using the percentage of collagen (%) of the entire muscle, obtained through the ImageJ software (v.1.54), where the red areas were automatically detected, using the software's Threshold tool (5,39,41).

Morphological and morphometric analysis of neuromuscular junctions

Five animals from each experimental group were anesthetized through intraperitoneal injection of Ketamine (90 mg/kg) and Xylazine (10 mg/kg), and subjected to transcardiac perfusion through the left ventricle and cannulation of the Aorta, with a Milan® peristaltic dosing pump, initially with saline solution (0,9% NaCl in distilled water + heparin 1mL/L) and subsequently fixation with 4% tamponed paraformaldehyde, both at a flow rate of 30 mL/min. The right auricle was sectioned to drain blood and excess fluids. Then, the right soleus muscles were collected, reduced to the middle third (region containing the motor point), and kept in 4% paraformaldehyde for 15 min, for post-fixation. The muscles were sectioned longitudinally, and the muscle fragments were subjected to the immunostaining technique of the NMJs (AChR and nerve terminals) by immunofluorescence (6).

To label the AChR, α-bungarotoxin conjugated to rhodamine (Rh-BTX, Invitrogen, Thermo Fisher Scientific, T1175, 1:100 in 0.1M PBS) was used, and to label the nerve terminals, the primary antibody anti-neurofilament 200 (anti-NF200, Sigma-Aldrich N5389, 1:100 in 0.1M PBS + 1% Triton® X-100 solution) associated with the

secondary antibody conjugated to Alexa Fluor® 488 (Abcam, ab150077, 1:400) was used. The sections were mounted on a slide with VECTASHIELD® fluorescence mounting medium (Vector Laboratories, Burlingame, CA, USA). Images of 50 NMJs were obtained for each animal in each experimental group using a Confocal Laser Scanning Microscope (Leica Microsystems, TCS - SP5). The basic parameters used to capture the images were 63x magnification, 2x zoom, with a 1 µm interval between images to construct the final image, to capture the NMJs in the most individualized way possible, thus facilitating their subsequent analysis (15).

Morphometric analysis of NMJ and AChR using the "NMJ-morph" plugin

The analyses were performed using the Fiji/ImageJ software (v.1.54), following the specific sequence and tools of the "NMJ-morph" plugin, for a robust and reliable analysis of NMJs (42,43). Around 50 images of each animal were analyzed. The parameters evaluated were: the AChR area and perimeter; motor endplate area, perimeter, and diameter (Feret); number and average area of AChR clusters (AChR area/number of clusters); unoccupied AChR area (endplate area–AChR area); compactness (AChR area/endplate area*100) and fragmentation (1–1/number of clusters) (15).

Statistical analysis

The data were analyzed using GraphPad Prism 9 software, which performed a normality test. For variables with data that adhered to a normal distribution, the one-way analysis of variance (ANOVA) test was used, complemented with Tukey's multiple comparisons test (44), and the data were expressed as mean ± standard error of the mean (SEM). For variables with data that did not adhere to a normal distribution, the Kruskal-Wallis test was used, complemented with Dunn's multiple comparisons test (44), and the data were expressed as median ± range. All data were considered using the 5% significance level ($p \leq 0.05$).

Results

Functional gait results

Before surgery, none of the gait parameters evaluated showed differences between the experimental groups.

After 120 days, the values of print area, length and width, maximum contact area, stand, and fibular functional index were lower in the injured groups (D, N, and NB), with similar results among themselves and different from the Control group (Figure 1 E - J).

Regarding the regularity index, the NB group was the only one that presented results similar to group C, and even higher than group D, but also similar to group N. Groups D and N presented the lowest values, equal to each other and different from group C (Figure 1P).

The number of steps showed a pattern similar to the regularity index, with the NB group also being the only one with results similar to group C and lower than group D, but still similar to group N. Groups D and N showed the highest values, equal to each other and different from group C (Figure 1N).

Regarding Cadence, there was only an increase in group D, being the only group different from the Control group (Figure 1O).

The parameters of the average duration of the runs, swing, and average speed of the runs showed no difference between the experimental groups (Figure 1 K-M).

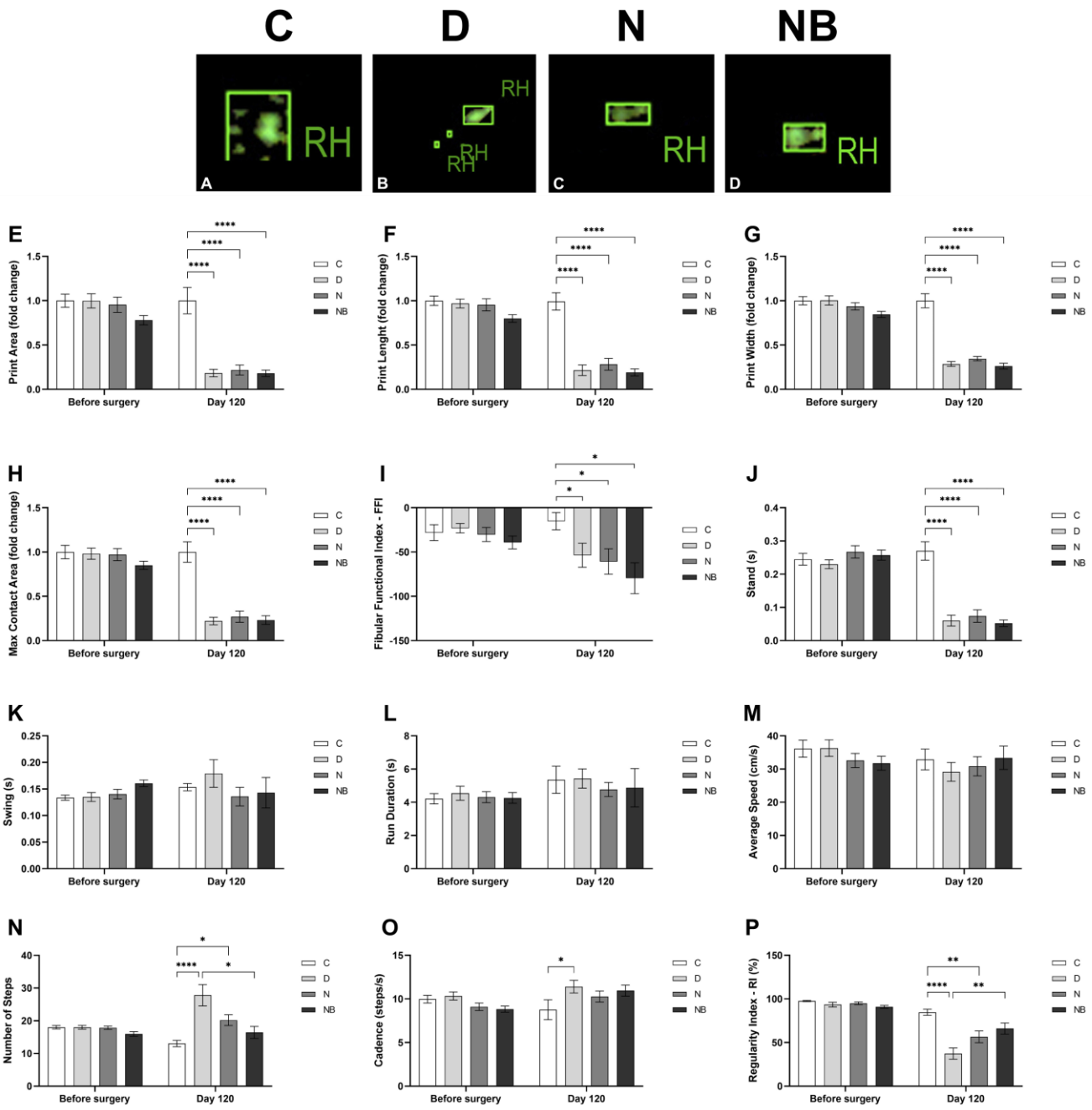


Figure 1. Illustrations and graphs of functional gait analysis (CatWalk XT) for the experimental groups at different evaluation times. A-D: Images of footprints obtained by analysis in the CatWalk XT according to the experimental group. A: Control group (C). B: Denervated group (D). C: Neurorrhaphy group (N). D: Neurorrhaphy + fibrin biopolymer group (NB). E-P: graphs of the analyses of footprint area (E), maximum contact area (F), footprint length (G) and width (H), Stand - support phase (I), regularity index (J), number of steps (K), cadence (L), average running duration (M), Swing - swing phase (N), average running speed (O), and fibular functional index (P) according to experimental groups. E-J, M-P: Values expressed as mean ± SEM, evaluated by ANOVA test complemented with Tukey's multiple comparisons test. K, L: Values expressed as median and range, and evaluated by the Kruskal-Wallis test, complemented with Dunn's multiple comparisons test. *p < 0.05; **p < 0.01; ****p < 0.0001. E-H: normalized by the control group mean (fold change).

Body weight and soleus muscle results

There was no difference in the body weight of the animals between the experimental groups (Figure 2A)

Regarding the soleus muscle weight, N and NB groups presented intermediate values, higher than the D group and lower than the C group, but equal to each other. Group D presented the lowest values, different from all other groups (Figure 2B).

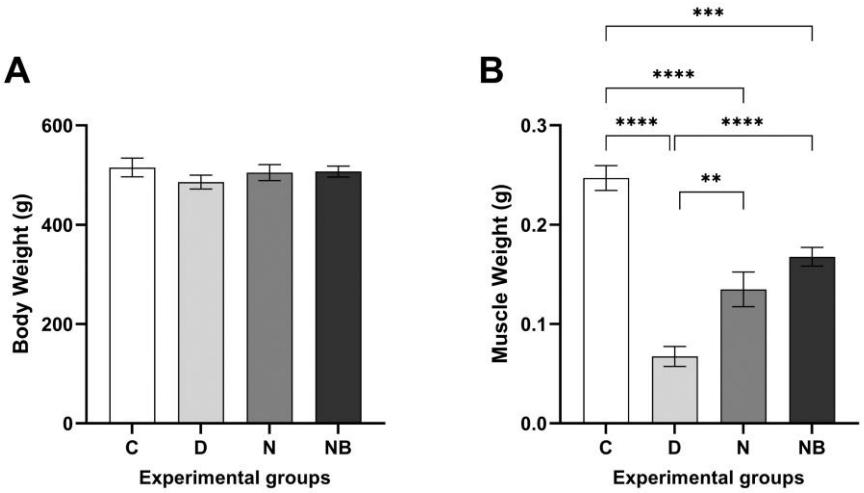


Figure 2. Graphs of body weight (A) and soleus muscle weight (B), according to the experimental groups: Control group (C), Denervated group (D), Neurorrhaphy group (N), and Neurorrhaphy + fibrin biopolymer group (NB). Values expressed as mean ± SEM, and evaluated by the ANOVA test, complemented with the Tukey multiple comparisons test (**p < 0.01; ***p < 0.001; ****p < 0.0001).

Sciatic nerve results

Group C presented intact axons and preserved myelin sheaths with regular shapes, demonstrating a morphology within the normal standards of a healthy nerve (Figure 3A).

In the D group, only degenerated nerve fibers were observed, with amorphous structures and without myelin sheath, with a large amount of nonspecific nuclei and extracellular matrix (Figure 3B).

In the N and NB groups, it was possible to observe intact and regenerated nerve fibers, but with heterogeneity in size and a smaller and irregular structural appearance, when compared to the C group (Figure 3C, D). An increase in the extracellular matrix was also observed but with an apparent smaller quantity than in the D group.

Regarding the morphometric analysis, all the parameters evaluated demonstrated lower values in the reconstructed groups (N and NB), with similar results among themselves and different from the Control group (Figure 16 E-L).

In the D group, due to intense degeneration and the absence of intact nerve fibers, it was not possible to perform morphometry.

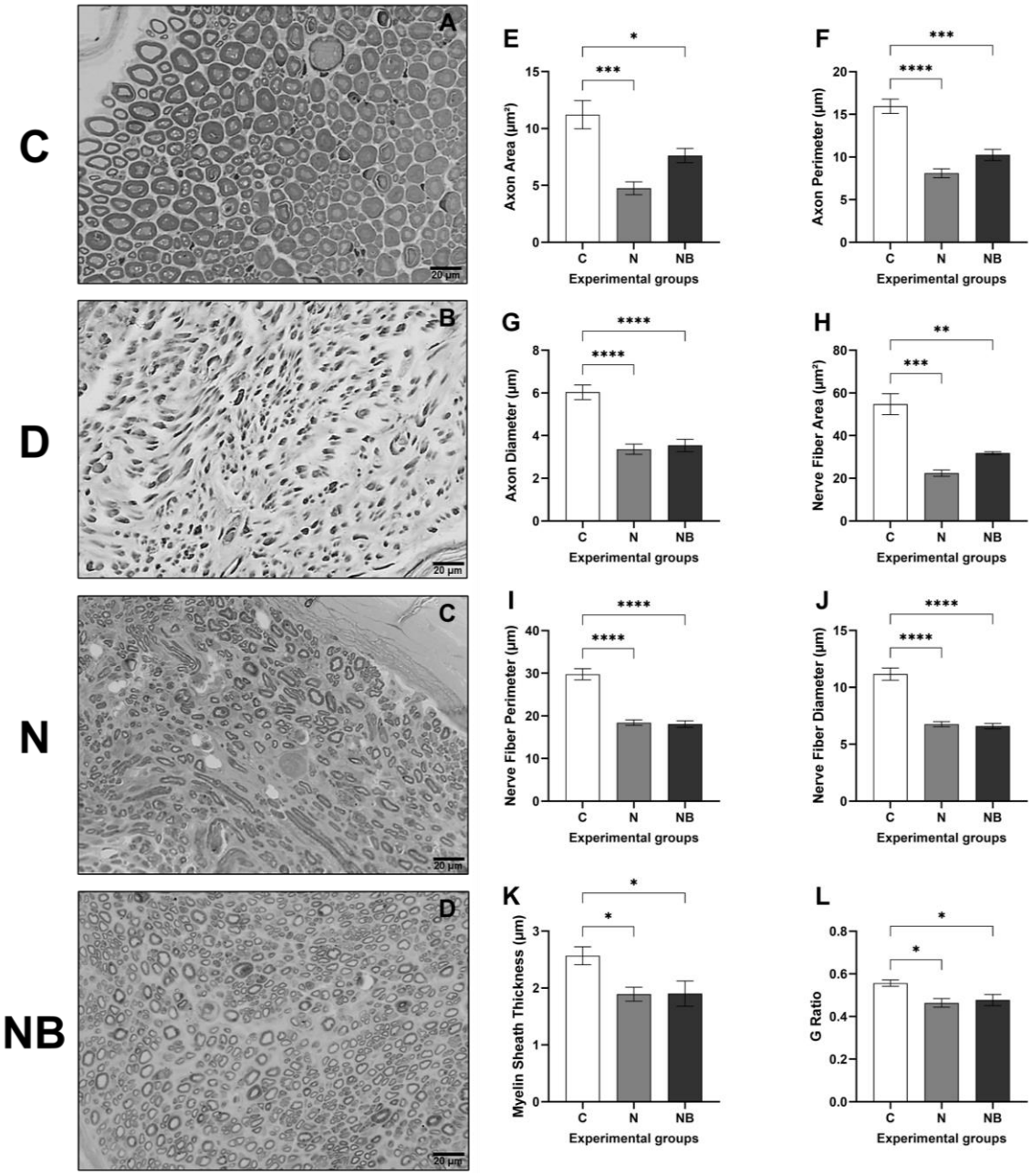


Figure 3. A-D: Photomicrographs of cross sections of the sciatic nerve according to the experimental groups, stained with osmium tetroxide, under conventional light microscopy, 40x magnification. A: Control group (C). B: Denervated group (D). C: Neurorrhaphy group (N). D: Neurorrhaphy + fibrin biopolymer group (NB). E-L: graphs of the analyses of axon area (E), perimeter (F) and diameter (G), nerve fiber area (H), perimeter (I) and diameter (J), myelin sheath thickness (K), and G ratio (L). Values expressed as mean ± SEM, evaluated by ANOVA test complemented with Tukey's multiple comparisons test (*p < 0.05; **p < 0.01; ***p < 0.001; ****p < 0.0001).

Skeletal muscle results

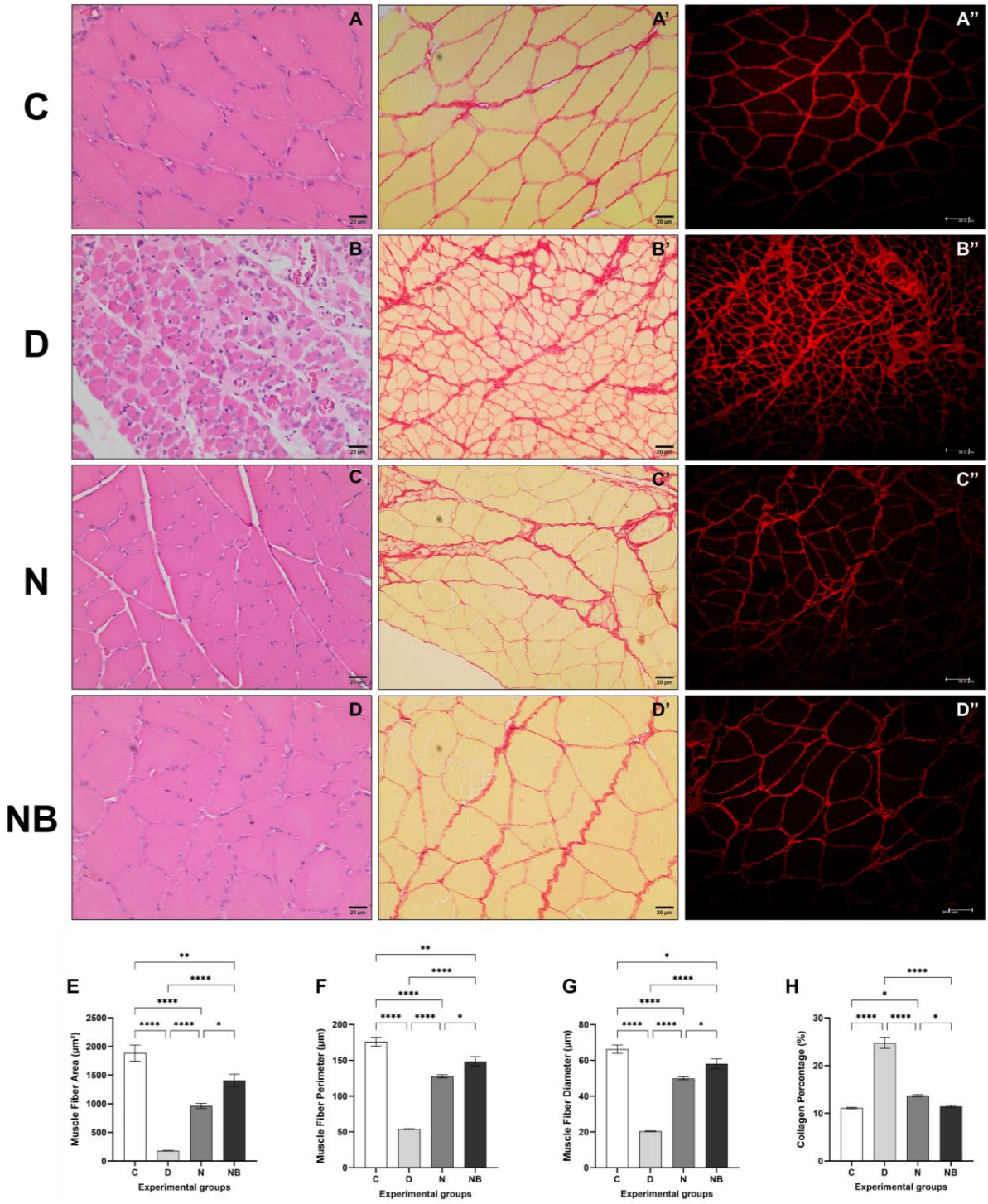
The morphological analysis performed after HE staining demonstrated, in the C group, polygonal-shaped muscle fibers, with peripheral nuclei and a small amount of extracellular matrix, i.e., characteristics compatible with normality (Figure 4A).

In the D group, a cluster of small muscle fibers, some of them with a rounded shape and others with a central nucleus, in addition to a large amount of extracellular matrix and nonspecific nuclei (Figure 4B), are typical characteristics of muscle degeneration and atrophy.

An intermediate morphology was observed in N and NB groups, with some fibers with a polygonal shape and others with a rounded shape, some with central and others with peripheral nuclei, and a moderate amount of connective tissue (Figure 4C, D). Furthermore, the NB group presented muscle fibers with heterogeneous sizes, with most of them having a larger structural aspect than the N group (Figure 4D).

The morphometry of the muscle fibers showed that the area, perimeter, and diameter of the NB group presented intermediate values, larger than the N and D groups, but still smaller than the C group. The D group presented the lowest values, different from all the other groups. The N group values are larger than the D group but smaller than the NB and C groups (Figure 4E-G).

Regarding the percentage of intramuscular collagen, the NB group was the only one that presented results similar to the C group, and still different from the N and D groups. The D group presented the highest values, different from all the other groups. The N group demonstrated intermediate values, smaller than the D group, but larger than the NB and C groups (Figure 4H).



306

307

308 **Figure 4**. A-D: Photomicrographs of cross sections of the soleus muscle according to the experimental
309 groups, stained with Hematoxylin and Eosin (A-D) and Picrosirius Red (A'A"-D'D"), under conventional light
310 microscopy (AA'-DD') and confocal microscopy (A"-D"), 40x magnification. A: Control group (C). B:
311 Denervated group (D). C: Neurorrhaphy group (N). D: Neurorrhaphy + fibrin biopolymer group (NB). E-H:
312 graphs of the analyses of area (E), perimeter (F), diameter (G) of the muscle fiber, and percentage of
313 intramuscular collagen (E), of all experimental groups. Values expressed as mean ± SEM, evaluated by
314 the ANOVA test complemented with Tukey's multiple comparisons test (*p < 0.05; **p < 0.01; ****p <
315 0.0001).

Neuromuscular junction results

It was possible to observe that there were homogeneous responses of the fluorophores with the AChR in autofluorescence in all groups.

In the C group, the AChR presented a distribution compatible with normality, characterized by the presence of continuous or “pretzel-shaped” branches/arms, running in various orientations along the muscle fiber (Figure 5A). The nerve terminals were colored green and presented a distribution compatible with normality, with intact, preserved terminals without discontinuity. It was possible to observe the branches form a terminal arbor close to AChR (colored in yellow) (Figure 5a). A similar morphology of AChR was observed in the NB group (Figure 5D).

In group D, flattening and fragmentation of the AChR were observed, and most of them were distributed in an “island” pattern (clusters), indicating a sparser distribution (Figure 5B). The nerve terminals were discontinuous with no clear visualization of the terminal axons, indicating an absence of integrity (Figure 5b).

Although flattening was observed in some motor endplates, an intermediate morphology was observed in the repair groups (N and NB) (Figure 5C, D) compared to C and D groups (Figure 5A, B), although the morphology of NB was closer to C (Figure 5A, D). An intermediate morphology was observed in the nerve terminals (Figure 5c, d), with the ramifications of the nerve terminals being thinner when compared to group C (Figure 5A).

The morphometric analysis corroborated these aspects, where the values related to the area of AChR and motor endplate and number of AChR clusters, the NB group was the only one that presented results similar to C group, differentiating itself from groups N and D. Group D showed results distinct from all other groups, while group N presented intermediate values, between NB and C, being different from both (Figure 6A, C, F).

Regarding the average area of the clusters, the NB group was also the only one similar to group C and different from groups N and D, which were similar to each other (Figure 6G).

The compaction and fragmentation indices showed a similar pattern, the NB was the only one similar to the C group and different from the D, but it was also similar to the N group. Groups D and N were similar to each other and different from the C group (Figure 6H, I).

Regarding the perimeter of the AChR the motor endplate and the area not occupied by the AChR, the NB group was like the N and C groups, which were also similar to each other. The D group obtained the lowest values, differentiating itself from all the other groups (Figure 6B, D, J).

The diameter of the motor endplate there were no significant differences between the groups (Figure 6E).

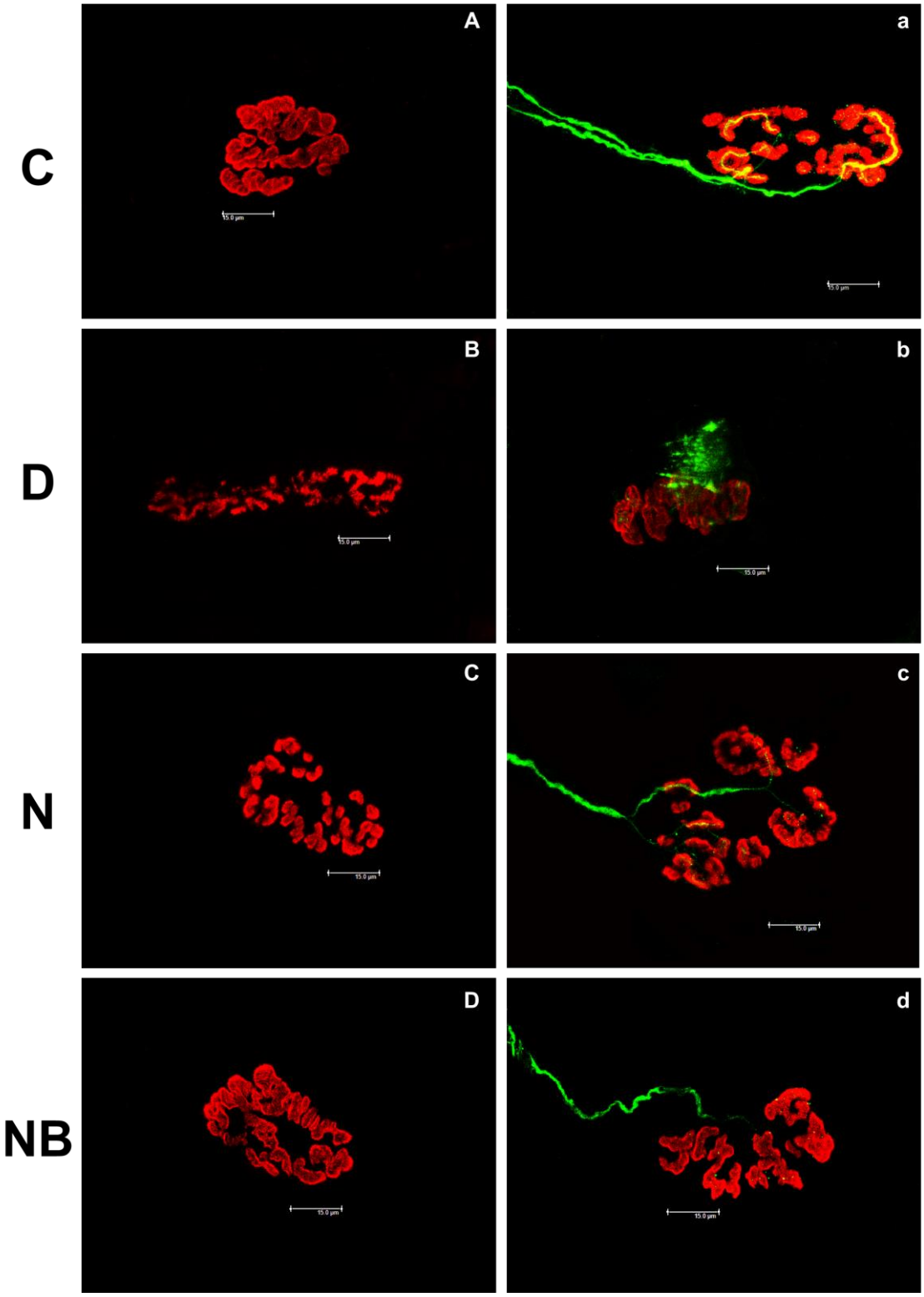


Figure 5. Confocal microscopy of acetylcholine receptors (in red, Aa-Dd) and nerve terminals (in green, a-d), according to experimental groups, 63x magnification, zoom 2. A, a: Control group (C). B, b: Denervated group (D). C, c: Neurorrhaphy group (N). D, d: Neurorrhaphy + fibrin biopolymer group (NB).

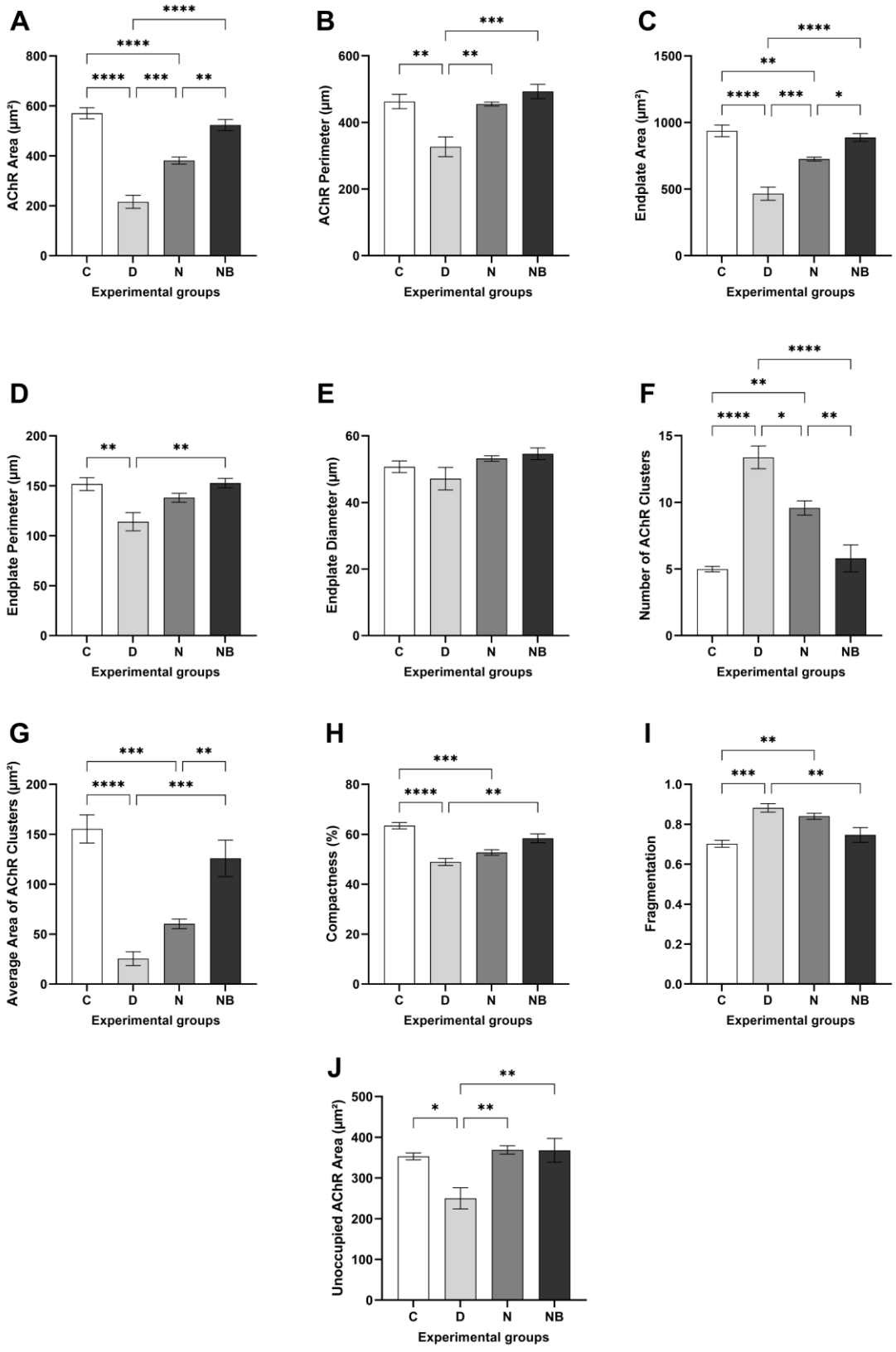


Figure 6. Graphs of NMJ analyses using NMJ-morph. Area (A) and perimeter (B) of AChR, area (C), perimeter (D) and diameter (E) of the motor end plate, number (F) and mean area (G) of AChR clusters, compaction (H) and fragmentation (I) indices, and area not occupied by AChR (J). Values expressed as mean ± SEM, evaluated by ANOVA test complemented with Tukey's multiple comparisons test (*p < 0.05; **p < 0.01; ***p < 0.001; ****p < 0.0001).

Discussion

Peripheral nerve repair remains a challenge for public health, since even after surgical interventions, the recovery of motor function is unsatisfactory in most cases. Even with the vast availability of information related to the pathophysiology of nerve injuries, there is still no treatment that ensures complete functional recovery in severe cases (2,45,46). The nerve injury model used was the complete section of the sciatic nerve, corresponding to Seddon neurotmesis (47) or Sunderland grade 5 injury (48), followed by immediate reconstruction via end-to-end neurorrhaphy associated or not with HFB.

In the Denervated group, a fragment of the nerve was removed and the nerve stumps were fixed to the subcutaneous tissue to prevent spontaneous regeneration, considering that the PNS has a remarkable capacity for regeneration after injury, although tissue retraction and the distance between the stumps resulting from the injury restrict axonal growth, limiting the neuroregeneration process (28).

The experimental period of 120 days after surgery was chosen with a view to a chronological investigation of the action of HFB in neuromuscular regeneration, which is being developed by our research group. Furthermore, previous studies in rats have shown that only 90 days after isolated neurorrhaphy are the motor endplates completely reinnervated; however, these same animals, 120 days after repair, still do not show functional recovery (4). This study was the first to investigate the action of HFB when associated with neurorrhaphy in NMJs and muscle fibers in a late recovery period since our research group has previously demonstrated that HFB provides an improvement in the morphology of the denervated nerve, muscle, and NMJs after shorter recovery periods, at 7 and 30 days (7), at 60 days (5,6) and 90 days (15).

The results of the analyses performed demonstrated an important effect of the association of HFB with neurorrhaphy after 120 days of reconstruction. This effect was particularly notable in the muscle fibers and extracellular matrix of the soleus muscle and associated NMJs. The combination with HFB had a positive impact, with several morphometric parameters approaching the values observed in the Control group. A clear reduction in fibrosis and muscle atrophy was observed, as well as reinnervation of the NMJs, compared to the Neurorrhaphy group alone.

Regarding the functional gait results, although print and temporal parameters demonstrated similarity between the injured groups (D, N, and NB), the coordination parameters of Regularity Index and number of steps showed positive results in the NB group, being the only ones that achieved results similar to the Control. The Regularity Index is a fractional measure of coordination between paws, which indicates the state of global motor coordination of the animal analyzed. In healthy and fully coordinated

animals, its value is 100% (35–37), values also found in our Control group and which were similar to the NB group. The loss of coordination between limbs leads to a decrease in this parameter (35). Groups D and N presented the lowest Regularity Index values, equal to each other and different from Group C, indicating a significant loss of coordination between the paws (49). Hamers and collaborators (35), studying spinal cord injury in rats, observed that one week after the rats had been subjected to transection injury, the Regularity Index decreased from 100% (pre-treatment) to approximately 80%, and it increased again to 90% after 4 weeks. Similar results, with the same experimental period, were observed by Chiang et al. (49) studying chronic constrictive injury of the sciatic nerve in rats, who also described that changes in the regularity index and step sequence were highly correlated with histopathological changes in the nerve, which may be associated with the expression of inflammatory cytokines such as TNF-a and plasticity markers such as synaptophysin. Based on these histopathological changes in the nerve, the regularity index and step sequence were highly correlated with changes in neuronal remodeling during chronic constrictive nerve injury, indicating that increased neuronal plasticity was reflected in an increase in the regularity index and the consequent improvement in functional recovery.

Su et al. (50) described similar results studying nerve crush injury followed by high-frequency electrical stimulation. Gait analysis showed that immediate electrical stimulation led to a significantly high regularity index, indicating improved motor function. Thus, the results of the Regularity Index found in this study, relating to the NB group, suggest a partial improvement in functional recovery caused by HFB.

Although the functional gait analysis showed, for some parameters, that the animal's gait did not completely return to the state before the injury, other results which will be described below, indicate a morphological recovery of the soleus muscle and associated NMJs.

In the repair groups (N and NB), axons with intact myelin sheaths and which were also in the process of remyelination were observed, indicating a regenerative process (51). It has already been described that HFB can enhance nerve regeneration in the initial periods after injury. The same findings were observed in previous studies by our group (5,7,15), as well as in other studies in the literature using HFB in rodent nerve repair (17,18,52), but with shorter recovery periods.

The morphometric analysis of the nerve demonstrated similarity between the reconstructed groups (NB and N), but which still did not reach the results of group C, showing that regeneration is ongoing, but still insufficient (28,51). In a previous study, we showed that, at 7 and 30 days after reconstruction, HFB promotes a pro-regenerative effect at the injury site, due to the enhancement of the immune response

with an increase in the number of M2 macrophages (anti-inflammatory) and other inflammatory cells (7). These cells, together with Schwann cells, act by accelerating the degeneration and regeneration processes, which are sequential and interdependent, favoring axonal growth and improving the regenerative process (53). These M2 macrophages produce anti-inflammatory cytokines and growth factors, in addition to promoting angiogenesis, healing, and tissue remodeling, being essential in the injury microenvironment, as they provide trophic support to increase axonal growth (54,55).

Similar results were observed using HFB in the repair of the central nervous system, after spinal cord injury (56) and avulsion of the ventral root of the brachial plexus (57) in rodents. These studies also showed that HFB can stimulate an anti-inflammatory response, with an increase in cytokines and M2 macrophages. This indicates that heterologous fibrin can stimulate the recruitment and migration of these cells to the injury site. The presence of heterologous fibrin and other coagulation factors, in addition to fibronectin, in the composition of HFB contributes to stimulating the immune response, leading to an immunomodulatory effect and immunogenic potential, inducing anti-inflammatory mechanisms (56).

Heterologous fibrin, in addition to maintaining a microenvironment that accelerates regeneration, also stimulates the immune response for several weeks. Since HFB does not contain components of human blood, it does not undergo rapid fibrinolysis, forming a dense and stable fibrin network that can last for a long time (6,7,30). It is important to note that HFB differs from commercial fibrin sealants, which are produced from human blood, as they have rapid fibrinolysis, which begins within 24 hours of application (6,7). Thus, the delay in the breakdown of heterologous fibrin can ensure the maintenance of immunomodulation and the consequent marked regeneration.

The findings in this study, such as the improvement in muscle morphology and NMJs in the NB group, corroborate the functional results related to the regularity index and with previous studies, suggesting that HFB can improve neuromuscular regeneration, even in long-term periods of recovery after severe injury. Due to slow fibrinolysis, HFB may have remained stable for a long period at the injury site and thus maintained the modulation of the immune response and the consequent favoring of axonal growth.

Analysis of the morphology of muscle fibers in the NB group showed the presence of several very large fibers alongside very small fibers, indicating possible compensatory hypertrophy, common in peripheral nerve injuries (58). It has already been described that the pathophysiological mechanisms of PNLs include compensatory hypertrophy, abnormal stretching, and spontaneous electrical activity of

denervated muscle fibers (59). Compensatory hypertrophy in muscle fibers can be caused by muscle and nerve trauma or diseases that promote loss of nerve conduction, or it can be an indication of marked tissue remodeling (58).

Regarding the morphometry of the soleus muscle, in the NB group, all parameters related to the size of the muscle fibers (area, perimeter, and diameter) demonstrated intermediate values, greater than the N and D groups, but still not equal to the Control group. These results indicate a marked muscle regeneration in the NB group induced by HFB, but the muscle has not yet returned to its pre-injury state. Regarding the weight of the soleus muscle, the reconstructed groups (NB and N) presented similar and intermediate results, greater than the D group, but still smaller than the C group, indicating that regeneration is ongoing and to a greater degree than the denervated group, corroborating these morphometric results. After denervation, degeneration of muscle fibers occurs, with a decrease in the area and volume of the fibers, which are replaced by fat and connective tissue rich in collagen, with an increase in the collagenous extracellular matrix, an excess tissue that impairs the capacity for muscle contraction, configuring a picture of fibrosis and atrophy, which leads to the gradual loss of muscle mass (11,24,60). Carraro and collaborators (9) demonstrated that degenerated muscle fibers and atrophic and fibrotic muscles can be observed up to 7 months after denervation in rodents.

In the NB group, a significant reduction in intramuscular collagen was observed, with values lower than those in the N group and equal to those in the Control group, suggesting a higher degree of muscle regeneration when compared to the other injured groups, accompanied by a lower degree of fibrosis and atrophy, as well as a lower degree of inflammation. These findings may have been caused by the improvement in axonal regeneration and consequent enhancement of muscle fiber reinnervation induced by HFB, which was effective in muscle recovery after injury, thus aiding in partial functional recovery. In this study, the morphology of the neuromuscular junctions of the NB group demonstrated that the AChR presented continuous or “pretzel-shaped” branches, running in various orientations along the muscle fiber, characteristics also present in the control group, indicating a distribution compatible with normality (61). In the N group, a morphology closer to group D was observed, with flattening and fragmentation of the AChR, and most of them were distributed in an “island” pattern, indicating a sparser distribution and close to the denervation pattern (6,15). Regarding the nerve terminals, an intermediate morphology was observed in the reconstructed groups (N and NB), with thinner thickness when compared to groups C, but in an intact state, unlike group D.

Regarding the morphometry of neuromuscular junctions, it was observed that most of the parameters analyzed showed greater proximity to the Control group in the group treated with the biopolymer compared to the group with isolated neurorrhaphy, corroborating the morphological results.

Healthy junctions present a continuous pattern, while denervated junctions exhibit fragmentation, with an increase in the number of AChR clusters, which compromises continuity and reduces the area and perimeter of AChR, as well as the motor endplate (15). With the failure in the transmission of the electrical signal and, consequently, in muscle contraction, changes occur in the aggregation of AChR clusters. These changes are mainly attributed to alterations in the Agrin/LRP4/Musk/Rapsin signaling pathway, the main pathway responsible for AChR anchoring and global stabilization of the NMJ, which leads to an increase in motor endplate fragmentation (6,14,15).

The results obtained, especially concerning the area of AChR and motor endplate, and the number and average area of AChR clusters, in which the NB group presented a larger area and smaller number of clusters, consequently a lower degree of fragmentation, about the N group, evidencing a greater approximation to the healthy state, with greater continuity of AChR, promoted by HFB.

These findings indicate that, in the NB group, there was a return of AChR and NMJ morphology to their normal patterns, suggesting that HFB has the potential to reestablish the NMJ structure, promoting its return to a healthy state, equal to the state before the injury. It has already been shown that HFB can improve the morphological and molecular recovery of NMJs and their AChR after denervation when associated with neurorrhaphy (6) or nerve guidance conduit (15), acting mainly on the return of the Agrin molecular pathway and the consequent improvement in the stabilization of AChR and the NMJ.

These results complement previous research carried out by our research group in shorter recovery periods, confirming that HFB can improve the morphological recovery of the nerve, skeletal muscle, and NMJs also in late recovery periods, as it can enhance axonal and neuromuscular regeneration. Furthermore, HFB can partially aid in functional recovery after peripheral nerve injury. It is important to note that, to date, our research group is the only one investigating the effects of HFB on the neuromuscular junction, with the results associated with these structures as well as with acetylcholine receptors being innovative.

A chronological study by our group using HFB in PNIs, with an emphasis on neuromuscular recovery, has found promising results. At 7 and 30 days after repair, HFB demonstrated immunomodulatory, angiogenic, and pro-regenerative effects, in

addition to aiding in the partial morphological recovery of NMJs and preventing severe muscle degeneration (7). At 60 days, after late repair, HFB enhanced axonal regeneration and allowed a reduction in the number of stitches when compared to isolated neurorrhaphy, with a consequent reduction in surgical procedure time (5); it also enhanced the morphological and molecular recovery of NMJs, with a return to their mature molecular pattern (6). At 90 days, after severe nerve injury, HFB resulted in the stabilization of AChR, which presented normal distribution after repair, which enhances neuromuscular regeneration, in addition to a partial recovery of motor function (gait) (15).

This study shows that the use of HFB in prolonged periods (after 120 days) contributes to partial functional recovery (improvement of coordination evidenced by IR), to the reinnervation of NMJs, and return of their AChR to their normal/healthy patterns (larger area and lower degree of fragmentation), and the regeneration of muscle fibers (reduction of atrophy and fibrosis).

The absence of electrophysiological tests and regeneration speed measurements are considered limitations of this study. We intend to explore them in future studies, as they may provide more in-depth results on the role of HFB in PNI.

Conclusion

This study demonstrated that the HFB, in long-term stages of recovery, significantly contributes to partial functional recovery, and morphological restoration of NMJ and AChR to normal patterns, in addition to promoting motor endplate reinnervation and muscle fiber regeneration. These effects contribute to an overall improvement in neuromuscular regeneration. Furthermore, the HFB, being a non-human biological product, offers advantages such as delayed fibrinolysis, the absence of risk of transmission of infectious diseases, and the absence of adverse effects. The combined use of neurorrhaphy and HFB emerges as a promising and economically viable medical approach, which deserves further investigation for its consolidation in peripheral nerve repair.

References

1. Robinson LR. Traumatic injury to peripheral nerves. Muscle Nerve. 2000 Jun;23(6):863–73.

2. Pan D, Mackinnon SE, Wood MD. Advances in the repair of segmental nerve injuries and trends in reconstruction. Muscle Nerve. 2020 Jun;61(6):726–39.

3. Hussain G, Wang J, Rasul A, Anwar H, Qasim M, Zafar S, et al. Current Status of Therapeutic Approaches against Peripheral Nerve Injuries: A Detailed Story from Injury to Recovery. Int J Biol Sci. 2020 Jan 1;16(1):116–34.

4. Sakuma M, Gorski G, Sheu SH, Lee S, Barrett LB, Singh B, et al. Lack of motor recovery after prolonged denervation of the neuromuscular junction is not due to regenerative failure. Eur J Neurosci. 2016 Feb;43(3):451–62.

5. Leite APS, Pinto CG, Tibúrcio FC, Sartori AA, de Castro Rodrigues A, Barraviera B, et al. Heterologous fibrin sealant potentiates axonal regeneration after peripheral nerve injury with reduction in the number of suture points. Injury. 2019 Apr;50(4):834–47.

6. Pinto CG, Leite APS, Sartori AA, Tibúrcio FC, Barraviera B, Junior RSF, et al. Heterologous fibrin biopolymer associated to a single suture stitch enables the return of neuromuscular junction to its mature pattern after peripheral nerve injury. Injury. 2021 Apr;52(4):731–7.

7. Tibúrcio FC, Muller KS, Leite APS, de Oliveira IRA, Barraviera B, Ferreira RS, et al. Neuroregeneration and immune response after neurorrhaphy are improved with the use of heterologous fibrin biopolymer in addition to suture repair alone. Muscle Nerve. 2023 Jun;67(6):522–36.

8. Alhindi A, Shand M, Smith HL, Leite AS, Huang YT, van der Hoorn D, et al. Neuromuscular junction denervation and terminal Schwann cell loss in the hTDP-43 overexpression mouse model of amyotrophic lateral sclerosis. Neuropathology and Applied Neurobiology. 2023;49(4):e12925.

9. Carraro U, Boncompagni S, Gobbo V, Rossini K, Zampieri S, Mosole S, et al. Persistent Muscle Fiber Regeneration in Long Term Denervation. Past, Present, Future. Eur J Transl Myol. 2015 Mar 11;25(2):4832.

10. Tereshenko V, Dotzauer DC, Schmoll M, Harnoncourt L, Carrero Rojas G, Gfrerer L, et al. Peripheral neural interfaces: Skeletal muscles are hyper-reinnervated according to the axonal capacity of the surgically rewired nerves. Sci Adv. 2024 Mar;10(9):eadj3872.

11. Huang Z, Fang Q, Ma W, Zhang Q, Qiu J, Gu X, et al. Skeletal Muscle Atrophy Was Alleviated by Salidroside Through Suppressing Oxidative Stress and Inflammation During Denervation. Front Pharmacol. 2019 Sep 10;10:997.

12. Yang X, Xue P, Chen H, Yuan M, Kang Y, Duscher D, et al. Denervation drives skeletal muscle atrophy and induces mitochondrial dysfunction, mitophagy and apoptosis via miR-142a-5p/MFN1 axis. Theranostics. 2020 Jan 1;10(3):1415–32.

13. Iyer SR, Shah SB, Lovering RM. The Neuromuscular Junction: Roles in Aging and Neuromuscular Disease. Int J Mol Sci. 2021 Jul 28;22(15):8058.

14. Walker LJ, Roque RA, Navarro MF, Granato M. Agrin/Lrp4 signal constrains MuSK-dependent neuromuscular synapse development in appendicular muscle. Development. 2021 Nov 1;148(21):dev199790.

15. Leite APS, Pinto CG, Tibúrcio FC, Muller KS, Padovani CR, Barraviera B, et al. Acetylcholine receptors of the neuromuscular junctions present normal distribution after

peripheral nerve injury and repair through nerve guidance associated with fibrin biopolymer. Injury. 2023 Feb;54(2):345–61.

16. Spinner RJ, Kline DG. Surgery for peripheral nerve and brachial plexus injuries or other nerve lesions. Muscle Nerve. 2000 May;23(5):680–95.

17. Bueno CR de S, Tonin MCC, Buchaim DV, Barraviera B, Ferreira Junior RS, Santos PS da S, et al. Morphofunctional Improvement of the Facial Nerve and Muscles with Repair Using Heterologous Fibrin Biopolymer and Photobiomodulation. Pharmaceuticals (Basel). 2023 Apr 27;16(5):653.

18. Bueno CR de S, Buchaim DV, Barraviera B, Ferreira RS, Santos PS da S, Reis CHB, et al. Delayed repair of the facial nerve and its negative impacts on nerve and muscle regeneration. J Venom Anim Toxins Incl Trop Dis. 2024;30:e20230093.

19. Wang ML, Rivlin M, Graham JG, Beredjiklian PK. Peripheral nerve injury, scarring, and recovery. Connect Tissue Res. 2019 Jan;60(1):3–9.

20. Kuffler DP, Foy C. Restoration of Neurological Function Following Peripheral Nerve Trauma. Int J Mol Sci. 2020 Mar 6;21(5):1808.

21. Lee JI, Gurjar AA, Talukder MAH, Rodenhouse A, Manto K, O'Brien M, et al. A novel nerve transection and repair method in mice: histomorphometric analysis of nerves, blood vessels, and muscles with functional recovery. Sci Rep. 2020 Dec 10;10(1):21637.

22. Raza C, Riaz HA, Anjum R, Shakeel NUA. Repair strategies for injured peripheral nerve: Review. Life Sci. 2020 Feb 15;243:117308.

23. Buchaim DV, Cassaro CV, Shindo JVTC, Coletta BBD, Pomini KT, Rosso MP de O, et al. Unique heterologous fibrin biopolymer with hemostatic, adhesive, sealant, scaffold and drug delivery properties: a systematic review. J Venom Anim Toxins Incl Trop Dis. 2019;25:e20190038.

24. Muller KS, Tibúrcio FC, Ferreira RS, Barraviera B, Matheus SMM. Heterologous fibrin biopolymer as an emerging approach to peripheral nerve repair: a scoping review. J Venom Anim Toxins Incl Trop Dis. 2024;30:e20230060.

25. Ferreira Jr RS, Barros LC de, Abbade LPF, Barraviera SRCS, Silvares MRC, Pontes LG de, et al. Heterologous fibrin sealant derived from snake venom: from bench to bedside – an overview. J Venom Anim Toxins incl Trop Dis. 2017 Jul 6;23:21.

26. Reis CHB, Buchaim RL, Pomini KT, Hamzé AL, Zattiti IV, Duarte MAH, et al. Effects of a Biocomplex Formed by Two Scaffold Biomaterials, Hydroxyapatite/Tricalcium Phosphate Ceramic and Fibrin Biopolymer, with Photobiomodulation, on Bone Repair. Polymers (Basel). 2022 May 19;14(10):2075.

27. Savastano LE, Laurito SR, Fitt MR, Rasmussen JA, Gonzalez Polo V, Patterson SI. Sciatic nerve injury: a simple and subtle model for investigating many aspects of nervous system damage and recovery. J Neurosci Methods. 2014 Apr 30;227:166–80.

28. Gaudet AD, Popovich PG, Ramer MS. Wallerian degeneration: gaining perspective on inflammatory events after peripheral nerve injury. Journal of Neuroinflammation. 2011 Aug 30;8(1):110.

29. Gordon T. Peripheral Nerve Regeneration and Muscle Reinnervation. Int J Mol Sci. 2020 Nov 17;21(22):8652.

30. Abbade LPF, Barraviera SRCS, Silvares MRC, Lima ABB de CO, Haddad GR, Gatti MAN, et al. Treatment of Chronic Venous Ulcers With Heterologous Fibrin Sealant: A Phase I/II

Clinical Trial. Frontiers in Immunology [Internet]. 2021 [cited 2024 Mar 1];12. Available from: https://www.frontiersin.org/journals/immunology/articles/10.3389/fimmu.2021.627541

31. Heinzel J, Längle G, Oberhauser V, Hausner T, Kolbenschlag J, Prahm C, et al. Use of the CatWalk gait analysis system to assess functional recovery in rodent models of peripheral nerve injury - a systematic review. J Neurosci Methods. 2020 Nov 1;345:108889.

32. Timotius IK, Roelofs RF, Richmond-Hacham B, Noldus LPJJ, von Hörsten S, Bikovski L. CatWalk XT gait parameters: a review of reported parameters in pre-clinical studies of multiple central nervous system and peripheral nervous system disease models. Front Behav Neurosci. 2023;17:1147784.

33. Bain JR, Mackinnon SE, Hunter DA. Functional evaluation of complete sciatic, peroneal, and posterior tibial nerve lesions in the rat. Plast Reconstr Surg. 1989 Jan;83(1):129–38.

34. Paiva GR, Viterbo F, Deffune E, Custódio MAD. Stem cells in end-to-side neurorrhaphy. Experimental study in rats. Acta Cir Bras. 2021;35(12):e351207.

35. Hamers FP, Lankhorst AJ, van Laar TJ, Veldhuis WB, Gispen WH. Automated quantitative gait analysis during overground locomotion in the rat: its application to spinal cord contusion and transection injuries. J Neurotrauma. 2001 Feb;18(2):187–201.

36. Hamers FPT, Koopmans GC, Joosten EAJ. CatWalk-assisted gait analysis in the assessment of spinal cord injury. J Neurotrauma. 2006;23(3–4):537–48.

37. Chen YJ, Cheng FC, Sheu ML, Su HL, Chen CJ, Sheehan J, et al. Detection of subtle neurological alterations by the Catwalk XT gait analysis system. Journal of NeuroEngineering and Rehabilitation. 2014 Apr 16;11(1):62.

38. Neptune RR, Kautz SA, Zajac FE. Contributions of the individual ankle plantar flexors to support, forward progression and swing initiation during walking. J Biomech. 2001 Nov;34(11):1387–98.

39. Tibúrcio FC, Leite APS, Muller KS, Pinto CG, Valentino E, Castro PAT de S, et al. Effects of Nandrolone Decanoate on Skeletal Muscle and Neuromuscular Junction of Sedentary and Exercised Rats. Medicina. 2023 Nov;59(11):1940.

40. Muller KS, Tibúrcio FC, de Barros JWF, Matsumura CY, Matheus SMM. Statin exposure during pregnancy promotes neuromuscular junction alterations in postpartum Wistar rats. Muscle Nerve. 2023 Jun;67(6):537–47.

41. Valentino E, 2, Leite1 APS, 2, Pinto1 CG, 2, et al. Physical Exercises during Youth Regardless of Nandrolone Decanoate Use Prevent Neuromuscular Morphological Alterations Caused by Aging. World Journal of Physical and Rehabilitation Medicine [Internet]. 2021 May 24 [cited 2023 Sep 8];5(1). Available from: https://www.remedypublications.com/world-journal-of-physical-and-rehabilitation-medicine-abstract.php?aid=6900

42. Jones RA, Reich CD, Dissanayake KN, Kristmundsdottir F, Findlater GS, Ribchester RR, et al. NMJ-morph reveals principal components of synaptic morphology influencing structure-function relationships at the neuromuscular junction. Open Biol. 2016 Dec;6(12):160240.

43. Minty G, Hoppen A, Boehm I, Alhindi A, Gibb L, Potter E, et al. aNMJ-morph: a simple macro for rapid analysis of neuromuscular junction morphology. Royal Society Open Science. 2020 Apr 15;7(4):200128.

44. Zar JH. Biostatistical Analysis. 5ª edição. Upper Saddle River, N.J: Prentice Hall; 2009.

45. Palispis WA, Gupta R. Surgical repair in humans after traumatic nerve injury provides limited functional neural regeneration in adults. Exp Neurol. 2017 Apr;290:106–14.

46. Wilcox M, Gregory H, Powell R, Quick TJ, Phillips JB. Strategies for Peripheral Nerve Repair. Curr Tissue Microenviron Rep. 2020 Jun 1;1(2):49–59.

47. Seddon HJ. A Classification of Nerve Injuries. Br Med J. 1942 Aug 29;2(4260):237–9.

48. Sunderland S. A classification of peripheral nerve injuries producing loss of function. Brain. 1951 Dec;74(4):491–516.

49. Chiang CY, Sheu ML, Cheng FC, Chen CJ, Su HL, Sheehan J, et al. Comprehensive analysis of neurobehavior associated with histomorphological alterations in a chronic constrictive nerve injury model through use of the CatWalk XT system. J Neurosurg. 2014 Jan;120(1):250–62.

50. Su HL, Chiang CY, Lu ZH, Cheng FC, Chen CJ, Sheu ML, et al. Late administration of high-frequency electrical stimulation increases nerve regeneration without aggravating neuropathic pain in a nerve crush injury. BMC Neurosci. 2018 Jun 25;19(1):37.

51. Răducan A, Mirică S, Duicu O, Răducan S, Muntean D, Fira-Mlădinescu O, et al. Morphological and functional aspects of sciatic nerve regeneration after crush injury. Rom J Morphol Embryol. 2013;54(3 Suppl):735–9.

52. Rodríguez-Sánchez DN, Pinto GBA, Cartarozzi LP, de Oliveira ALR, Bovolato ALC, de Carvalho M, et al. 3D-printed nerve guidance conduits multi-functionalized with canine multipotent mesenchymal stromal cells promote neuroregeneration after sciatic nerve injury in rats. Stem Cell Res Ther. 2021 May 29;12(1):303.

53. Nocera G, Jacob C. Mechanisms of Schwann cell plasticity involved in peripheral nerve repair after injury. Cell Mol Life Sci. 2020 Oct;77(20):3977–89.

54. Zigmond RE, Echevarria FD. Macrophage biology in the peripheral nervous system after injury. Prog Neurobiol. 2019 Feb;173:102–21.

55. Bombeiro AL, Fernandes RGQ, Ribot JC. New immune regulators of sciatic nerve regeneration? Lessons from the neighborhood. Neural Regen Res. 2024 Apr;19(4):705–6.

56. Spejo AB, Chiarotto GB, Ferreira ADF, Gomes DA, Ferreira RS, Barraviera B, et al. Neuroprotection and immunomodulation following intraspinal axotomy of motoneurons by treatment with adult mesenchymal stem cells. J Neuroinflammation. 2018 Aug 14;15(1):230.

57. Kempe PRG, Chiarotto GB, Barraviera B, Ferreira RS, de Oliveira ALR. Neuroprotection and immunomodulation by dimethyl fumarate and a heterologous fibrin biopolymer after ventral root avulsion and reimplantation. J Venom Anim Toxins Incl Trop Dis. 2020 May 20;26:e20190093.

58. Martinelli A, Andreo L, Alves AN, Terena SML, Santos TC, Bussadori SK, et al. Photobiomodulation modulates the expression of inflammatory cytokines during the compensatory hypertrophy process in skeletal muscle. Lasers Med Sci. 2021 Jun;36(4):791–802.

59. ten Holter JB, van Nieuwstadt MA. [Neurogenic muscle hypertrophy]. Ned Tijdschr Geneeskd. 1993 Dec 18;137(51):2655–8.

60. Campbell WW. Evaluation and management of peripheral nerve injury. Clin Neurophysiol. 2008 Sep;119(9):1951–65.

61. Rodríguez Cruz PM, Cossins J, Beeson D, Vincent A. The Neuromuscular Junction in Health and Disease: Molecular Mechanisms Governing Synaptic Formation and Homeostasis. Front Mol Neurosci. 2020;13:610964.

UNIVERSIDADE ESTADUAL PAULISTA
"JÚLIO DE MESQUITA FILHO"

Comissão de Ética no Uso de Animais

Criada pela da Portaria DFM nº 611 de 13/12/2012

CERTIFICADO Nº 1402/2021 – CEUA

Certificamos que o projeto intitulado: **"Biopolímero heterólogo de fibrina associado à secretoma de células-tronco mesenquimais na reconstrução nervosa experimental: Aspectos morfofuncionais e moleculares da interação neuromuscular"** - conduzido pelo Pesquisador: **Felipe Cantore Tibúrcio** – **Orientador**: Profa. Assoc. Selma Maria Michelin Matheus, coorientador: Profa. Dra. Cintia Yuri Matsumura – Colaboradores: Kevin Silva Muller e Rui Seabra Ferreira Júnior, registrado com o **nº 1402/2021**, que envolve a produção, manutenção ou utilização de animais pertencentes ao filo Chordata, subfilo Vertebrata (exceto humanos), para fins de pesquisa científica, encontra-se de acordo com os preceitos da Lei n. 11.794, de 08 de outubro de 2008, do Decreto n. 6.899, de 15 de julho de 2009, com as normas editadas pelo Conselho Nacional de Controle de Experimentação Animal (CONCEA), e foi APROVADO pela Comissão de Ética no Uso de Animais da Faculdade de Medicina de Botucatu, em reunião ordinária de 22 de fevereiro de 2022.

Finalidade	( ) Ensino (**X**) Pesquisa Científica
Finalidade	01/12/2025
Espécie/Linhagem/Raça	Ratos Wistar
Nº Total de animais	ZERO ANIMAIS - Animais já adquiridos com certificado do IB
Idade/Peso	90 dias – 300 gramas
Sexo	Machos

Profa. Associada Bertha Furlan Polegato
Presidente da Comissão de Ética no Uso de Animais
Faculdade de Medicina de Botucatu/UNESP

Sara Rosa Stanley Sampaio
Secretária da Comissão de Ética no Uso de Animais
Faculdade de Medicina de Botucatu/UNESP

The research project registered by the number 1402/2021 is in agreement with the Ethical Principles for Animal Research established by the National Council for Control of Animal Experimentation (CONCEA) and was approved by the Committee on Ethics in the Use of Animals of Botucatu Medical School - Sao Paulo State University (UNESP) on 22/february/2022.

Distrito Rubião Júnior, s/nº – Botucatu – SP. CEP: 18618-970 Fones: (14) 3880.1880 – Email Secretaria: ceua@fmb.unesp.br

Ofício nº 021/2023 – CEUA – FMB/UNESP Botucatu, 28 de novembro de 2023.

Prezada Senhora,

Em atendimento ao documento enviado em 06 de nvembro de 2023, solicitando a alteração de título e exclusão de um grupo experimental referente ao subprojeto **"Biopolímero heterólogo de fibrina associado a secretoma de células-tronco mesenquimais na reconstrução nervosa experimental: Aspectos morfofuncionais e moleculares da interação neuromuscular" (Protocolo CEUA 1402/2021)**, essa solicitação **APROVADA**. Reiteramos que a aprovação da solicitação pela CEUA não prevê a inclusão de nenhum animal adicional aos já solicitados no projeto de pesquisa **1402/2021.**

Título Anterior: "Biopolímero heterólogo de fibrina associado á secretoma de células-tronco mesenquimais na reconstrução nervosa experimental: Aspectos morfofuncionais e moleculares da interação neuromuscular"

Novo Título: "Aspectos morfológicos, funcionais e moleculares da interação neuromuscular após neurorrafia associada ao biopolímero heterólogo de fibrina".

Respeitosamente,

Profa. Dra. Débora Cristina Damasceno

Presidente da Comissão de Ética no Uso de Animais

Faculdade de Medicina de Botucatu-UNESP

Faculdade de Medicina de Botucatu – Comissão de Ética no Uso de Animais (CEUA)
Av. Prof. Mário Rubens Guimarães Montenegro, s/nº
Unidade de Pesquisa Experimental (UNIPEX) – Bloco V – Botucatu – S/P – CEP:18618-970
Telefone: (14) 3880-1880 – Voip e Whatsaap
E-mail: ceua.fmb@unesp.br ou sara.sampaio@unesp.br / **Site:** www.fmb.unesp.br

UNIVERSIDADE ESTADUAL PAULISTA
"JÚLIO DE MESQUITA FILHO"

Instituto de Biociências da Universidade Estadual Paulista

Comissão de Ética no Uso de Animais

CERTIFICADO

Certificamos que a proposta intitulada "Aspectos morfológicos, funcionais e moleculares da interação neuromuscular após neurorrafia associada ao biopolímero heterólogo de fibrina", protocolada sob o CEUA nº 1964170821 (ID 000306), sob a responsabilidade de **Selma Maria Michelin Matheus** *e equipe; Felipe Cantore Tibúrcio* - que envolve a produção, manutenção e/ou utilização de animais pertencentes ao filo Chordata, subfilo Vertebrata (exceto o homem), para fins de pesquisa científica ou ensino - está de acordo com os preceitos da Lei 11.794 de 8 de outubro de 2008, com o Decreto 6.899 de 15 de julho de 2009, bem como com as normas editadas pelo Conselho Nacional de Controle da Experimentação Animal (CONCEA), e foi **APROVADA** pela Comissão de Ética no Uso de Animais da Instituto de Biociências da Universidade Estadual Paulista (IBB/UNESP) na reunião de 10/12/2021.

We certify that the proposal "Morphological, functional and molecular aspects of neuromuscular interaction after neurorrhaphy associated with heterologous fibrin biopolymer", utilizing 180 Heterogenics rats (180 males), protocol number CEUA 1964170821 (ID 000306), under the responsibility of **Selma Maria Michelin Matheus** *and team; Felipe Cantore Tibúrcio* - which involves the production, maintenance and/or use of animals belonging to the phylum Chordata, subphylum Vertebrata (except human beings), for scientific research purposes or teaching - is in accordance with Law 11.794 of October 8, 2008, Decree 6899 of July 15, 2009, as well as with the rules issued by the National Council for Control of Animal Experimentation (CONCEA), and was **APPROVED** by the Ethic Committee on Animal Use of the São Paulo State University/Biosciences Institute (IBB/UNESP) in the meeting of 12/10/2021.

Finalidade da Proposta: Pesquisa (Acadêmica)

Vigência da Proposta: de 02/2022 a 12/2024 Área: Ciências Biológicas

Origem:	Biotério Central da UNESP			
Espécie:	Ratos heterogênicos	sexo: Machos	idade: 90 a 120 dias	Quantidade: 90
Linhagem:	Wistar		Peso: 300 a 500 g	

Botucatu, 06 de fevereiro de 2024

Profa. Dra. Ana Carolina Inhasz Kiss
Coordenadora da Comissão de Ética no Uso de Animais
Instituto de Biociências da Universidade Estadual Paulista

Prof. Assoc. Luis Fernando Barbisan
Vice-Coordenador da Comissão de Ética no Uso de Animais
Instituto de Biociências da Universidade Estadual Paulista

Rua Prof. Dr. Antônio Celso Wagner Zanin, 250 - Distrito de Rubião Junior - Botucatu/SP - CEP 18618-689 - tel: 55 (14) 3880-0851
Horário de atendimento: 2ª a 6ª das 8h às 11h30 - 14h ás 18h : e-mail: ceua.ibb@unesp.br
CEUA N 1964170821

ANEXO II (Artigo de Revisão)

Artigo de revisão publicado em 15/04/2024 na revista *Journal of Venomous Animals and Toxins including Tropical Diseases (JVATiTD),* ISSN: 1678-9199, Fator de Impacto: 2.4, Qualis CAPES: A2, SJR: Q2.

Heterologous fibrin biopolymer as an emerging approach to peripheral nerve repair: a scoping review

Kevin Silva Muller[1,2] (kevin.muller@unesp.br - orcid.org/0000-0001-9774-1435)
Felipe Cantore Tibúrcio[1,2] (felipe.cantore@unesp.br - orcid.org/0000-0003-2660-6089)
Rui Seabra Ferreira Junior[3,4] (rui.seabra@unesp.br - orcid.org/0000-0001-6952-0512)
Benedito Barraviera[2,3,4] (benedito.barraviera@unesp.br - orcid.org/0000-0002-9855-5594)
Selma Maria Michelin Matheus[1,2*] (selma.matheus@unesp.br - orcid.org/0000-0001-7870-5404)

1 Department of Structural and Functional Biology, Institute of Biosciences, São Paulo State University (Unesp), Botucatu, SP, Brazil.

2 Botucatu Medical School, São Paulo State University (Unesp), Botucatu, SP, Brazil.

3 Center for the Study of Venoms and Venomous Animals - Cevap, Sao Paulo State University (Unesp), Botucatu, SP, Brazil.

4 Center for Translational Sciences and Biopharmaceuticals Development (CTS), Sao Paulo State University (Unesp) Botucatu, SP, Brazil.

***Correspondence to:** selma.matheus@unesp.br

REVIEW OPEN ACCESS

Journal of Venomous Animals and Toxins including Tropical Diseases

ISSN 1678-9199

www.jvat.org

Heterologous fibrin biopolymer as an emerging approach to peripheral nerve repair: a scoping review

Kevin Silva Muller[1,2*], Felipe Cantore Tibúrcio[1,2], Rui Seabra Ferreira Junior[2,3,4], Benedito Barraviera[2,3,4], Selma Maria Michelin Matheus[1,2]

[1]Department of Structural and Functional Biology, São Paulo State University (UNESP), Botucatu Institute of Biosciences, Botucatu, SP, Brazil.
[2]Botucatu Medical School, São Paulo State University (UNESP), Botucatu, SP, Brazil.
[3]Center for the Study of Venoms and Venomous Animals (CEVAP), São Paulo State University (UNESP), Botucatu, SP, Brazil.
[4]Center for Translational Sciences and Biopharmaceuticals Development (CTS), Center for the Study of Venoms and Venomous Animals (CEVAP), Botucatu, SP, Brazil.

Abstract

Nerve injuries present a substantial challenge within the medical domain due to their prevalent occurrence and significant impact. In nerve injuries, a range of physiopathological and metabolic responses come into play to stabilize and repair the resulting damage. A critical concern arises from the disruption of connections at neuromuscular junctions, leading to profound degeneration and substantial loss of muscle function, thereby hampering motor tasks. While end-to-end neurorrhaphy serves as the established technique for treating peripheral nerve injuries, achieving comprehensive morphofunctional recovery remains a formidable challenge. In pursuit of enhancing the repair process, alternative and supportive methods are being explored. A promising candidate is the utilization of heterologous fibrin biopolymer, a sealant devoid of human blood components. Notably, this biopolymer has showcased its prowess in establishing a stable and protective microenvironment at the site of use in multiple scenarios of regenerative medicine. Hence, this scoping review is directed towards assessing the effects of associating heterologous fibrin biopolymer with neurorrhaphy to treat nerve injuries, drawing upon findings from prior studies disseminated through PubMed/MEDLINE, Scopus, and Web of Science databases. Further discourse delves into the intricacies of the biology of neuromuscular junctions, nerve injury pathophysiology, and the broader utilization of fibrin sealants in conjunction with sutures for nerve reconstruction procedures. The association of the heterologous fibrin biopolymer with neurorrhaphy emerges as a potential avenue for surmounting the limitations associated with traditional sealants while also mitigating degeneration in nerves, muscles, and NMJs post-injury, thereby fostering a more conducive environment for subsequent regeneration. Indeed, queries arise regarding the long-term regenerative potential of this approach and its applicability in reconstructive surgeries for human nerve injuries.

Keywords:
Fibrin sealant
Neurorrhaphy
Nervous system
Regenerative medicine

*** Correspondence:** kevin.muller98@gmail.com

https://doi.org/10.1590/1678-9199-JVATITD-2023-0060
Received: 04 September 2023; Accepted: 29 January 2024; Published online: 15 April 2024

On-line ISSN 1678-9199 © The Author(s). 2024 Open Access This article is distributed under the terms of the Creative Commons Attribution 4.0 International License (http://creativecommons.org/licenses/by/4.0/), which permits unrestricted use, distribution, and reproduction in any medium, provided you give appropriate credit to the original author(s) and the source, provide a link to the Creative Commons license, and indicate if changes were made. The Creative Commons Public Domain Dedication waiver (http://creativecommons.org/publicdomain/zero/1.0/) applies to the data made available in this article, unless otherwise stated.

Background

Peripheral nerves are some of the most delicate structures in the human body, prone to easily being damaged by injuries such as compressions, crushes, and traumas [1]. Nerve injuries are a common clinical case with a high global incidence, affecting around 18 individuals per 100,000 each year [2]. Many individuals affected by nerve injuries, both in severe and moderate cases, have incomplete recovery, resulting in transient or permanent losses of motor and sensory functions, as well as chronic pain, muscle atrophy, and weakness. Approximately one-third of all nerve injuries demonstrate incomplete recovery with poor restoration of function [3]. Several factors hinder axonal regeneration, including severity, mechanism of injury, the large distance between the neuron cell body and target tissue, and the loss of regenerative support from Schwann cells (nerve glial cells) after injury, so that effective functional recovery is typically not achieved [4, 5]. The proper reinnervation of neuromuscular junctions (NMJs) by the nerve terminal plays an important role in obtaining a functional NMJ and, thus, a positive outcome.

Upon transection/neurotmesis, all structures of the neuromuscular apparatus are hindered, from the muscle fibers up to the motor neuron cell body in the spinal cord, undermining the quality of life of patients. Despite advances in microsurgical repair techniques, researchers have not yet achieved satisfactory functional recovery of the affected structures. Even with successful reconnection between the nerve stumps, the rates of motor recovery only reach a 50% success rate [6]. Then, the development of new strategies and approaches aimed at better regeneration is necessary. In this way, a new heterologous fibrin biopolymer (HFB) calls out attention as a promising candidate for adjunct therapy, as it has been showing positive results in a range of regenerative treatments, such as bone, tendon, spinal cord, and skin injuries, developing a more permissive environment for regeneration.

The current HFB consists of two major components, namely a thrombin like-enzyme (serine protease) extracted from the *Crotalus durissus terrificus* venom and a cryoprecipitate rich in fibrinogen, obtained from the blood of the buffalo *Bubalus bubalis* [7]. When both components are mixed with the calcium chloride diluent, the product polymerizes, forming a robust fibrin network. HFB has an activity comparable to commercial sealants, as it is biodegradable, bioabsorbable, and has no toxicity or adverse reaction [8]. Because of its unique composition and absence of human blood, it is considered the only heterologous fibrin biopolymer in the world [9].

The use of HFB as an adjunct in peripheral and central nerve reconstruction has been showing promising results through the development of an immunomodulatory and neuroprotective environment at the injury site [10–13] and has also been applied in various other experimental models of reconstructive surgery [7, 14]. The use of HFB has already been experimentally shown to provide a microenvironment of stability and protection at the reconstruction site, leading to positive scenarios of nerve regeneration. Therefore, this scoping review shed light on the association of HFB with sutures for nerve reconstruction following injury, highlighting its immunomodulatory and neuroprotective properties. Notably, integrating HFB with neurorrhaphy presents a promising avenue for surpassing the constraints of conventional sealants, while concurrently curtailing the extent of initial degeneration subsequent to injury.

Methods

This scoping review follows the guidelines outlined in the Preferred Reporting Items for Systematic Reviews and Meta-Analyses (PRISMA) [15]. To achieve this, we conducted searches in PubMed/MEDLINE, Scopus (Elsevier), Web of Science, and SciELO databases, encompassing articles published until August 2023. The search used the keywords: "heterologous fibrin sealant," "heterologous fibrin biopolymer," "fibrin biopolymer," "neurorrhaphy," and "nerve injury" restricted to English-language publications.

To ensure precision, we carefully analyzed titles and abstracts to account for potential keyword overlaps. Articles were subsequently included or excluded based on predetermined eligibility criteria. Two independent authors conducted the selection process by using standardized procedures. When the title and abstract did not provide sufficient clarity, full-article analyses were undertaken. Review articles were scrutinized to identify potential experimental studies, and articles offering no novel insights were excluded following a comprehensive assessment.

Among the initially identified 103 articles, 31 were eliminated due to duplication, and an additional 58 were excluded in line with eligibility criteria (not animal model study; no nerve injury model or nerve degeneration/regeneration involvement; no HFB use; not a research article). Notably, six research articles aligning with the stipulated eligibility criteria were identified through scoping and systematic reviews. A total of 20 articles regarding the use of HFB for nerve injury repair were then chosen for detailed text evaluation, which meets the predefined inclusion criteria, forming the basis for this review's scope (Figure 1). Furthermore, other articles were freely consulted to delve into further aspects of the biology of the neuromuscular junction, the pathophysiology of nerve injury, and the exploration of fibrin sealants for nerve injury repair. Table 1 summarizes experimental articles, which used HFB for neuronal regeneration included in this review.

Neuromuscular interaction

Nerves are formed by bundles of axons or nerve fibers, which are long and slender projections of a neuron that typically conduct electrical impulses, connecting different parts of the body to the central nervous system (CNS). Sensory signals are transmitted to the CNS through sensory nerve fibers (afferents), and the resulting response is carried by motor nerve fibers (efferents) to the target organs. Thus, a mutual communication pathway is established between the CNS and the peripheral areas of the body [1].

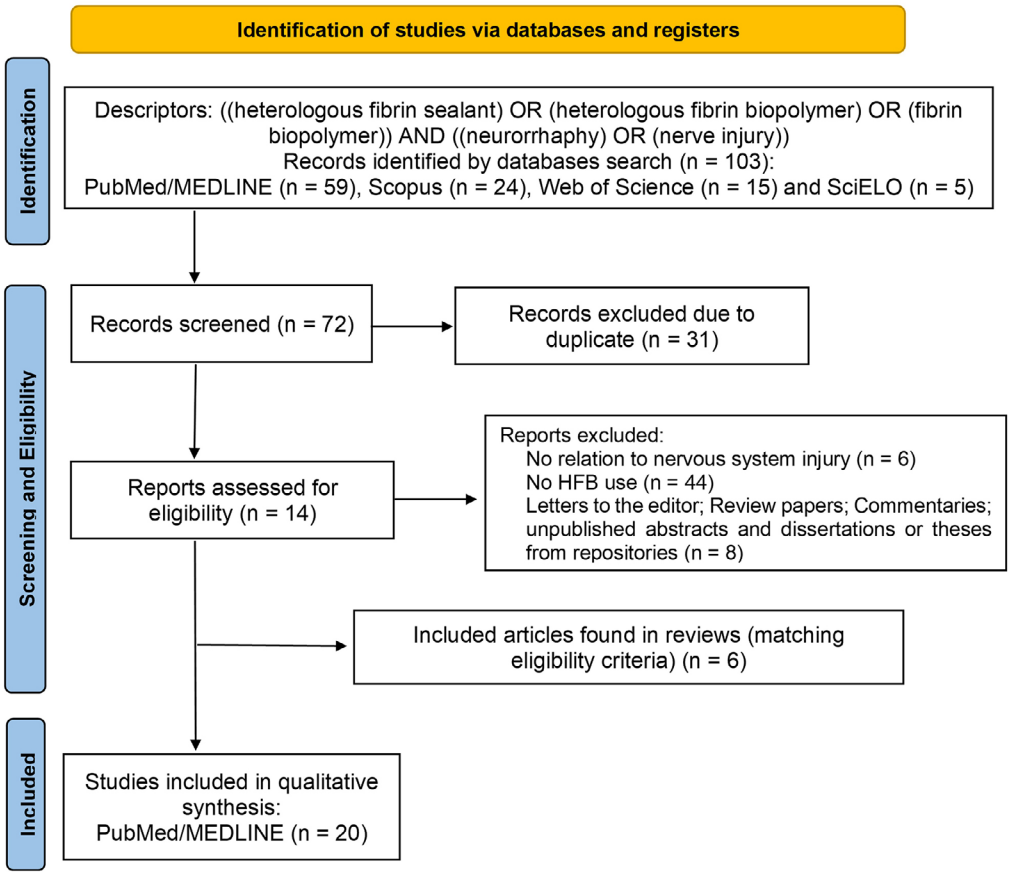


Figure 1. Flow diagram showing the study selection.

Table 1. Summary of experimental articles involving neuronal regeneration (CNS and PNS) included in this scoping review.

Author	Objective	Methods	Results	Conclusion
Barbizan et al. (2014) [16]	To investigate two delivery strategies of mononuclear cells (MC), comparing the local injection to the spinal cord with the possibility of mixing MC with HFB on the interface of the CNS/PNS.	Forty female adult Lewis rats divided into: G1: avulsion only; G2: reimplantation with HFB; G3: root repair with HFB and MC; G4: root repair with HFB and injected MCs.	HFB enhanced cell therapy effects resulting in greater survival of spinal motoneurons up to four weeks post-surgery. MC added to the HFB increased neurotrophic factor gene transcript levels in the spinal cord ventral horn. The motor recovery was similar to cell-treated groups.	The use of HFB as a scaffold for the MC delivery approach gave the best and most long-lasting results. MC therapy was neuroprotective by increasing levels of brain-derived neurotrophic factor (BDNF) and glial-derived neurotrophic factor (GDNF).
Buchaim et al. (2015) [17]	To assess whether HFB permits the collateral repair of axons originating from a vagus nerve to the interior of a sural nerve graft and whether low-level laser therapy (LLLT) assists in the regeneration process.	Thirty-two adult male Wistar rats divided into: G1: intact sural nerve; G2: the ends of the sural nerve graft were coapted to the vagus nerve using HFB; G3: same procedures as G2 + LLLT.	The vagus nerve demonstrated collateral regeneration of axons to the interior of the autologous graft in all groups. G3 was similar to G1 concerning the area and thickness of the myelin sheath.	HFB + LLLT makes axonal regeneration feasible and is an efficient method to recover injured peripheral nerves, as well as improve myelination.
Cartarozzi et al. (2015) [18]	To investigate the effectiveness of mesenchymal stem cells (MSCs) associated with HFB for the peripheral regenerative process after nerve tubulization.	One hundred adult Lewis rats divided into G1: empty tube; G2: tube filled with HFB; G3: tube filled with HFB and grafted with MSCs.	G3 had a greater value for myelinated axon counting, more compact fibers, and a tendency to increase the thickness of the myelin sheath; with better motor function.	MSCs + HFB treatment was effective in improving nerve regeneration, as it positively modulated Schwann Cells reactivity.

Table 1. Cont.

Author	Objective	Methods	Results	Conclusion
Buchaim et al. (2016) [19]	To assess the impact of LLLT on the repair of the buccal branch of the facial nerve using two surgical methods: end-to-end epineural suturing and coaptation with HFB.	Forty adults male Wistar rats divided into: G1: suture; G2: HFB; G3: suture + HFB; G4: suture + LLLT; G5: suture + HFB + LLLT.	Axonal sprouting and morphology were similar among the experimental groups. G5 showed the closest results to the G1, in all measured variables, except in the axon area.	HFB allowed the coaptation of the stumps without trauma to the nerve fibers.
Rosso et al. (2017) [20]	To assess the impact of LLLT on facial nerve injuries repaired with the end-to-side method or coaptation with HFB.	Thirty-two adults male Wistar rats divided into G1: control; G2: suture; G3: HFB; G4: suture + LLLT; G5: suture + HFB + LLLT.	G4 and G5 groups showed higher mean values for histomorphometry and functional recovery variables.	The functional recovery of whisker movement occurred more rapidly in G4 and G5, with results closer to G1. LLLT expedited morphological and functional nerve repair in both techniques.
Spejo et al. (2018) [21]	To evaluate whether the combination of MSCs and HFB enhances the regeneration of the spinal cord following intramedullary axotomy (IA)	Eighty-eight adult female Lewis rats underwent a unilateral ventral funiculus incision at the L4, L5, and L6 spinal levels. The animals were divided into: G1: IA, G2; IA + vehicle; G3: IA + HFB; G4: IA + MSC; G5: IA + HFB + MSC.	MSC therapy: increased neuronal survival and functional recovery, reduced astrogliosis, and preserved spinal circuits. HFB promoted: early macrophage recruitment and expression of proinflammatory cytokines.	MSC therapy provides neuroprotection and, when combined with HFB, shifts the immune response towards the proinflammatory profile.
Mozafari et al. (2018) [22]	To determine whether human embryonic stem cells (hESC), either independently or in conjunction with HFBs, could aid in regeneration in a mouse model of sciatic nerve damage.	Forty-eight C57BL/6 J mice were divided into: G1: suture; G2: suture + HFB; G3: suture + HFB + doxycycline; G4: suture + HFB + wild type hESC; G5: suture + HFB + hESC off; G6: suture + HFB + hESC + doxycycline.	Sensory function was enhanced in G5, resulting in heightened reflexes, upon paw stimulation ipsilateral to the lesion, as evidenced by von-Frey evaluation, which was corroborated by immunohistochemistry.	Transgenic hESC could be used to support regeneration. HFB has the potential to aid nerve repair and is thought to promote superior functional recovery and improved motor neuron reinnervation when combined with this therapy.
Leite et al. (2019) [23]	To assess the effectiveness of HFB in association with suture, with 1 or 3 stitches after ischiatic nerve injury.	Thirty-six Wistar rats were divided into: G1: control; G2: denervated (6 mm gap); G3: 3 stitches suture; G4: 1 stitch suture + HFB.	G3 and G4 muscle analysis indicated an increase in muscle weight, frequency of fast fibers, and a decrease in collagen infiltration, while G4 had better nerve morphometric values compared to G3.	The findings imply a protective effect at the site of the lesion due to the use of HFB. The reduction in sutures lessens the trauma inflicted by the needle and expedites the surgical procedure.
Kempe et al. (2020) [24]	To determine whether the combination of pharmacological treatment with dimethyl fumarate (DF) and root reimplantation using HFB could promote neuroprotection, preservation, and recovery of motor function.	Seventy-nine adult female Lewis rats underwent ventral root avulsion of L4-L6 roots, followed by reimplantation and daily DF treatment for four weeks. HFB was utilized as an adjunct to ventral root reimplantation.	The association between HFB and DF preserved motoneurons and synapses, reduced astrogliosis and microglial reactions, and downregulated the expression of pro-inflammatory gene transcripts.	The association with HFB and DF demonstrated neuroprotective and immunomodulatory properties and 50% of motor function recovery following spinal cord root injury.

Table 1. Cont.

Author	Objective	Methods	Results	Conclusion
Pinto et al. (2021) [25]	To determine whether the combination of HFB with a single stitch has the potential to restore the function of the neuromuscular apparatus following sciatic nerve injury.	Forty Wistar rats divided into G1: Control; G2: Denervated (6 mm gap); G3: 3 stitches suture; G4: 1 stitch suture + HFB.	G1 exhibited normal morphology. In G2 flattening of the NMJ (fragmentation of nAChRs and tangled nerve terminals). G3 and G4: most parameter values were similar to G1 and G2. G3 and G4: planar area.	G3 and G4 showed less fragmentation of nAChRs, and protein expression values suggested a return of nAChRs to a mat The use of HFB in conjunction with a single suture stitch reduced surgical time, minimized suture injuries, did not affect nerve regeneration, and showed potential for restoring the NMJ apparatus.
Rodríguez-Sánchez et al. (2021) [26]	To determine if Polycaprolactone Nerve Guidance Conduits (PCL-NGCs) produced by 3D printing with canine Adipose-derived Mesenchymal Stem Cells (AdMSCs) embedded in HFB could enhance nerve regeneration after sciatic nerve injury.	Twenty-nine adult Wistar rats submitted to sciatic nerve injury were divided into G1: Sham; G2: autograft; G3: PCL (empty NGC); G4: PCL + HFB+ MSCs (NGC multi-functionalized with 10^6 canine AdMSCs embedded in HFB).	G4 showed improved functional motor and electrophysiological recovery compared to the G3 after 12 weeks. G4 also increased the expression of neurotrophins and tended to higher reactivity of Schwann cells and axonal branching.	PCL + HFB+ MSCs promoted neuroregenerative effects and amplified the trophic microenvironment, resulting in a pro-regenerative state. These findings were associated with a shift in the regeneration process towards the formation of myelinated fibers.
Leite et al. (2023) [10]	To assess the impact of combining tubulization and HFB following peripheral nerve injury on the NMJ.	Fifty-two adult male Wistar rats divided into G1: control; G2: denervated; G3: tubulization; and G4: tubulization + HFB.	In G4 the NMJs presented morphological and morphometric similarities to G1 with an increase in S100 and AChRε protein expression and a decrease in MyoD.	The HFB association with tubulization resulted in nAChRs stabilization highlighting the beneficial effect of HFB when used in conjunction with the tubulization technique.
Tibúrcio et al. (2023) [13]	To assess neuroregeneration and the immune response in the context of neuromuscular recovery, using HFB in conjunction with suturing for rat sciatic nerve repair.	Forty male Wistar rats divided into groups of 7 or 30 days after nerve repair: G1: control; G2: denervated; G3: suture; G4: suture + HFB.	G4 had the highest M2 macrophage area in both periods. After seven days, the G4 showed an increase in nerve area, number, and area of blood vessels. In this period, G4 was the only one similar to G1 in terms of the number of axons. After 30 days, the G4 was closer to the G1 concerning blood vessels and central myonuclear numbers, NMJ angle, and connective tissue volume.	HFB enhances the immune response, increases axonal regeneration, induces angiogenesis, prevents severe muscle degeneration, and aids NMJ recovery.
Kempe et al. (2023) [27]	To examine the effects of combining surgical repair of lesioned roots with HFB and pharmacological treatment with dimethyl fumarate (DF).	Forty adult females divided into G1: reimplantation + vehicle; G2: VRA without reimplantation + DF; G3: reimplantation + vehicle + HFB; G4: reimplantation + HFB + DF.	HFB + DF association demonstrated: nerve sprouting, restoration of the 'G' ratio, and that most of the alpha motoneuron synapses were preserved in clusters. These parameters were associated with up to 50% of gait recovery, as the walking track test observed.	Combining root restoration with HFB and DF administration proved to be neuroprotective and can enhance motoneuron survival and regeneration after proximal lesions.
Bueno et al. (2023) [24]	To investigate the application of HFB in the repair of the buccal branch of the facial nerve (BBFN) in conjunction with photobiomodulation (PBM), using a low-level laser (LLLT).	Twenty-one rats divided into: G1: control; G2: LLLT; G3: denervated; G4: denervated + LLLT; G5: suture + HFB; G6: suture + HFB + LLLT.	G5 and G6 presented normal parameters related to functional analysis. G6 showed an increase in nerve fiber diameter and axon diameter compared to G6. In terms of muscle fiber area, G6 was similar to G1.	HFB+LLLT had positive effects on the morphological and functional stimulation of the BBFN, presenting a favorable alternative for the regeneration of severe injuries.

Among the motor nerve fibers, there is the lower motor neuron, a specialized cell with a highly developed dendritic arborization. Its cell body is located in the ventral column of the gray matter of the spinal cord, and its axons extend throughout the body via peripheral nerves until they reach the target organs [28, 29], the skeletal striated muscle, where it forms a morphologically, molecularly, and functionally specialized region called NMJ. At this site, there is transmission and transduction of an electrical signal (nerve impulse) and a chemical signal (neurotransmitters) from the motor neuron to the muscle fiber, promoting muscle contraction. This junction presents a major subclass of synapses in the mammalian nervous system, critical for the transfer of information between the lower motor neuron and the skeletal muscle. It also represents a conveniently accessible "model" synapse within the peripheral nervous system [29].

Neuromuscular junction organization

The NMJs are small structures (30-60 um) when compared to the length of innervated muscle fibers, and each skeletal muscle fiber is recruited by a single NMJ [30]. The classic morphology of the NMJ, first described in rodents, is characterized as a "pretzel" shaped structure, and changes in this structure are closely associated with motor pathologies [28, 30]. The most common classification of NMJs divides them into three closely associated cellular compartments (Figure 2).

I – Presynaptic membrane (nerve terminal)

The terminal branches of lower motor neuron axons form synaptic boutons, hosting synaptic vesicles carrying the neurotransmitter acetylcholine (ACh). This nerve terminal holds various cellular constituents, including mitochondria, endoplasmic reticulum, lysosomes, organic substances, and metal ions [31, 32]. Terminal or perisynaptic Schwann cells (tSCs) are found in this region [33–35], they are non-myelinating glial cells whose extensions cover the nerve terminals, protecting them from chemical and mechanical injuries [36]. Additionally, tSCs are the main cells responsible for the structural plasticity of NMJs by perceiving possible alterations in synaptic transmission [37, 38]. One to three tSCs surround the nerve terminal, and actively participate in the development, maintenance, and repair of synaptic function [30], in addition to producing a basal lamina that maintains the structure of the NMJ [39].

II – Synaptic cleft

The synaptic cleft separates the presynaptic nerve terminal from the postsynaptic membrane by a narrow gap of 50 to 80 nm in width. It is filled with the synaptic basal lamina, composed of molecules secreted by both the nerve terminal and the associated muscle fiber [40]. This region houses crucial proteins for NMJ stability, function, and upkeep, including those responsible for the clustering of nicotinic acetylcholine receptors (nAChRs) on the sarcolemma, such as agrin, laminins-4, 9, and 11, matrix metalloproteinase-3 (MMP3), and collagen IV. Acetylcholinesterase (AChE), essential for degrading ACh post-muscle contraction, is also concentrated here [41, 42], culminating in the termination of neuromuscular transmission [43].

III – Postsynaptic membrane

The postsynaptic membrane compromises the plasma membrane of the muscle fiber with junctional folds, where the nAChRs and the sarcoplasm of the muscle fiber (cytoplasm) are located [34, 35]. These folds exhibit two distinct regions: the crest, enriched with nAChRs and additional proteins like rapsyn, utrophin, and α-dystrobrevin-1 to ensure stability; and the trough, hosting α-dystrobrevin-2, dystrophin, NCAMs for muscle integrity and axonal guidance. Alongside these, voltage-dependent sodium channels responsible for generating action potentials are also present [43–45]. The sarcolemma's invaginations amplify the postsynaptic membrane's surface area and facilitate the juxtaposition of nAChRs with the presynaptic zones, while sodium channels extend within the sarcoplasm. Basal lamina encompassing extracellular matrix components tightly enwraps the muscle fibers, connecting with the basal lamina of the synaptic cleft produced by tSCs at the NMJ's periphery [43].

At the NMJ, nAChRs are the primary receptors in the muscle to establish neuromuscular motor communication [46], thus maintaining and facilitating synaptic transmission. Structurally, they comprise five subunits arranged in a rosette pattern, which collectively form ion channels [47]. These receptors are distributed in two forms: immature extrajunctional, present in embryonic muscle fibers, composed of subunits two alpha (α), beta (β), delta (δ), and gamma (γ); and mature junctional, in which α (2), β, and δ subunits are maintained, and the γ subunit is replaced by epsilon (ε) [31].

Activation of nAChRs is initiated by the simultaneous binding of two ACh molecules or other agonists at the juncture of the αδ and αε subunits, thereby inducing a conformational alteration that opens the ion pore and triggers its active state [48, 49]. This active state's duration is modulated by the interaction between the receptor and ACh molecules, promptly broken down by AChE, returning nAChRs to their quiescent configuration [49]. In instances of injury or pathology, nAChRs often revert to an embryonic pattern, featuring the gamma subunit instead of epsilon [50]. This exchange of γ- for ε-subunits contributes to several changes in stability, kinetic, and transmission properties [28]. There are also positive and negative signals involved in the maintenance of the NMJ, and fundamentally, nAChRs clusters [30]. The main positive signal is the binding that occurs in the Agrin/LRP4/Musk/Rapsyn pathway [25].

Pathophysiology of nerve injury

Following nerve transection, a cascade of physiological and metabolic responses is triggered at the cellular level in the injury site and in the cell body of the affected neurons in an attempt to stabilize the damage resulting from the injury [28].

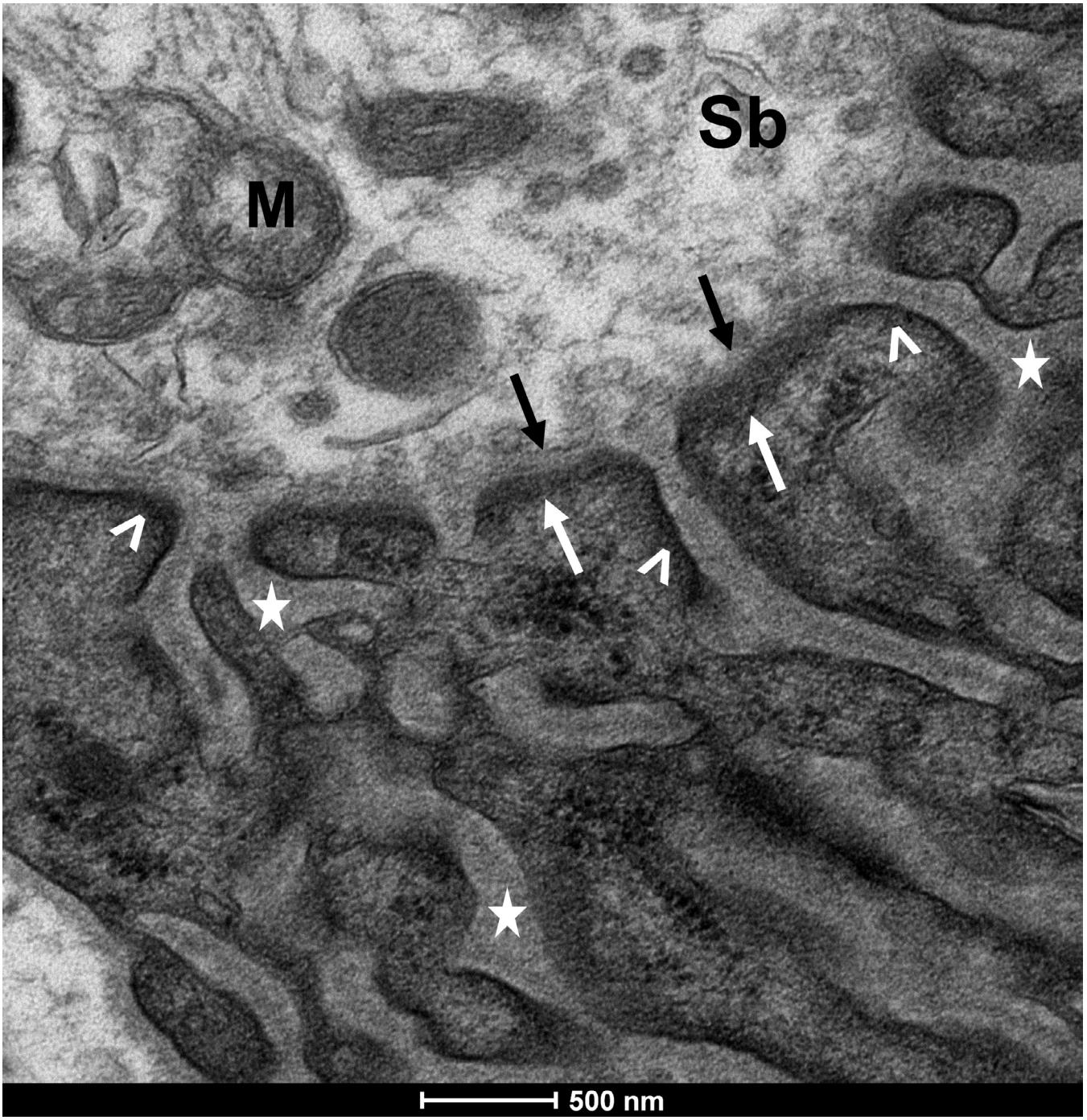


Figure 2. Components of the neuromuscular junction. Transmission electron microscopy image of a Wistar rat soleus muscle NMJ. Sb: synaptic button; M: mitochondria; →: ACh vesicle; *: junctional folds; >: nAChRs cluster. Black arrows: presynaptic membrane; white arrows: postsynaptic membrane.

In neurotmesis, the nerve is divided into two stumps, distal and proximal to the site of injury, which are subject to relatively distinct processes [51]. Shortly after, the process of Wallerian degeneration (WD) begins in the distal stump, while the proximal stump changes its gene expression profile, adopting a repair profile, inducing degenerative changes followed by a regenerative process [30]. Shortly after axotomy, axons from the proximal stump undergo a process of swelling, characterized by a reorganization of the cytoskeletal structure to seal themselves through a fibrotic cascade to contain leakage of the axoplasm [3].

In the distal stump, where axons lose contact with neuronal bodies, Wallerian degeneration takes place, manifesting as myelin breakdown and axonal disintegration. This process initiates with a rapid influx of intracellular calcium, triggering protease activation and granulation within the axoplasm through the proteolysis of microtubules and neurofilaments. This succession

of events further undermines the organizational integrity of the cellular structure [51, 52]. Within this milieu, damage-associated molecular patterns (DAMPs) and pro-inflammatory agents, including tumor necrosis factor (TNF-)α, interleukin (IL-) 1β, and CCL2, activate the initial immune response, mostly attributed to macrophages [53]. One of the primary functions of these macrophages is the clearance of tissue debris, a role reinforced by Schwann cells through myelin autophagy [54]. It is important to note that Schwann cells, fibroblasts, and resident macrophages also contribute to the inflammatory milieu by releasing proinflammatory mediators [55].

Furthermore, additional components of the immune system have been associated with effective Wallerian degeneration, often through their modulation of the macrophage-mediated response. Neutrophils are notably the first subset of cells to infiltrate the injured nerve, driving initial tissue clearance and recruiting monocytes from the peripheral circulation, which subsequently differentiate into macrophages [55]. Complement proteins and antibodies present in the serum enhance macrophage attraction and response by opsonizing cellular debris, thereby facilitating phagocytosis. The last cells to participate in the immune response within the damaged nerve are T lymphocytes [55, 56]. While recognized for their role in the amplification and regulation of the inflammatory response, their specific function in nerve regeneration remains underexplored. It's worth mentioning that nerve regeneration has traditionally been correlated with distinct macrophage subsets: pro-inflammatory type 1 macrophages (M1) driving the degenerative phase, and anti-inflammatory type 2 macrophages (M2) guiding the regenerative phase [57]. These subtypes undergo polarization in response to cues from the degenerative or regenerative environment, yielding unique phenotypes, metabolic traits, and functions [57]. However, classifying macrophages solely into M1 and M2 categories oversimplifies the intricate cell landscape within the nerve, where an array of macrophages expressing various pro- and anti-inflammatory markers coexist.

Within tissue clearance, regeneration slowly begins at the proximal end of the injury site and proceeds toward the distal segment. In this context, Schwann cells close to the damaged region dedifferentiate, proliferate, and migrate to the lesion site. There, they align up within endoneurial tubes, forming longitudinal columns known as bands of Büngner, inside of which they release growth and trophic factors to stimulate axonal elongation up to the target [5]. Importantly, the correct orientation of Büngner's bands depends on a polarized vasculature, induced by macrophage-derived VEGF-A upon hypoxia stimulus. Those newly formed blood vessels are essential for regeneration as they serve as tracks, guiding Schwann cell migration across the wound and subsequent axonal elongation [58].

In the proximal stump, neurotmesis evokes a retrograde response in neuronal cell bodies [59]. Surviving neurons undergo a series of physiological and morphological changes called chromatolysis, which is characterized by swelling and rounding of the cell body, dissolution of Nissl granules, and eccentric displacement of the nucleus and endoplasmic reticulum [1, 60]. These structural modifications are paralleled by a shift in physiological cellular metabolism towards the synthesis of proteins involved in axon regeneration [59], such as those related to the cytoskeleton and growth factors [51]. With the elimination of myelin debris, regeneration slowly begins at the proximal end of the injury site and proceeds toward the distal segment. The severed axons produce a large number of sprouts, closely associated with Schwann cells, forming several growth cones in the distal direction.

On the other hand, the distance of the injury from the cell body implies a worsening of the regenerative condition, as observed in sensory neurons, where the closer proximity to the dorsal root ganglia is directly related to the number of dead nerve cells [61] and a greater effective distance for regeneration. Strikingly, although axons do regenerate, studies have demonstrated that the morphological recovery of the nerve and muscle is not definitive for functional recovery, as there may still be impaired synaptic functionality [62, 63].

Following the injury, nerve endings that formed NMJs are lost, and even with successful axonal sprouting, the failure of reinnervation limits muscle function recovery [64] (Figure 3A). Irregular nerve branching, poly-innervation [65], and collateral reinnervation of muscle fibers commonly occur. Denervated NMJs suffer severe degeneration and subsequent disintegration [66] and disassembly of their nAChRs and anchoring proteins, which are fundamental for their function maintenance [67]. When axons are damaged, they release DAMPs that activate tSCs. In turn, these tSCs release chemokines, which serve as guidance substrates, facilitating the formation of tSCs bridges and thus promoting NMJ reinnervation [28, 39]. The nAChR-ε subunit is replaced by nAChR-γ, altering the transmission of the electrical signal leading to muscle failure and atrophy [68], as ACh is also no longer available at the synapse.

Denervation also leads to significant changes in the Agrin/LRP4/Musk/Ra pathway, prejudicing the maintenance of nAChR clusters [69] and leading to alterations of the area and conformation of the NMJ [10]. Shortly after injury proteins of this pathway have increased synthesis but its complex disorganization leads to failure in proper function, inactivation of MMP3, and accumulation of Agrin in the synaptic cleft [28]. The NMJ microenvironment is also deprived of other retrograde and anterograde signals that maintain its stability [28], in which activated tSC extend their processes synthesizing nAChR in non-synaptic muscle regions.

In the regenerative process, the Agrin protein has a fundamental role in initiating the receptor clustering pathway, remodeling, and returning the NMJs to their conventional shape [30]. The LRP4 protein, dependent on Agrin for activation [69], also has a fundamental role in the regenerative process, contributing to the activation of tSCs after injury, which is responsible for guiding the reinnervation of NMJs in denervated fibers [10]. Notably, active

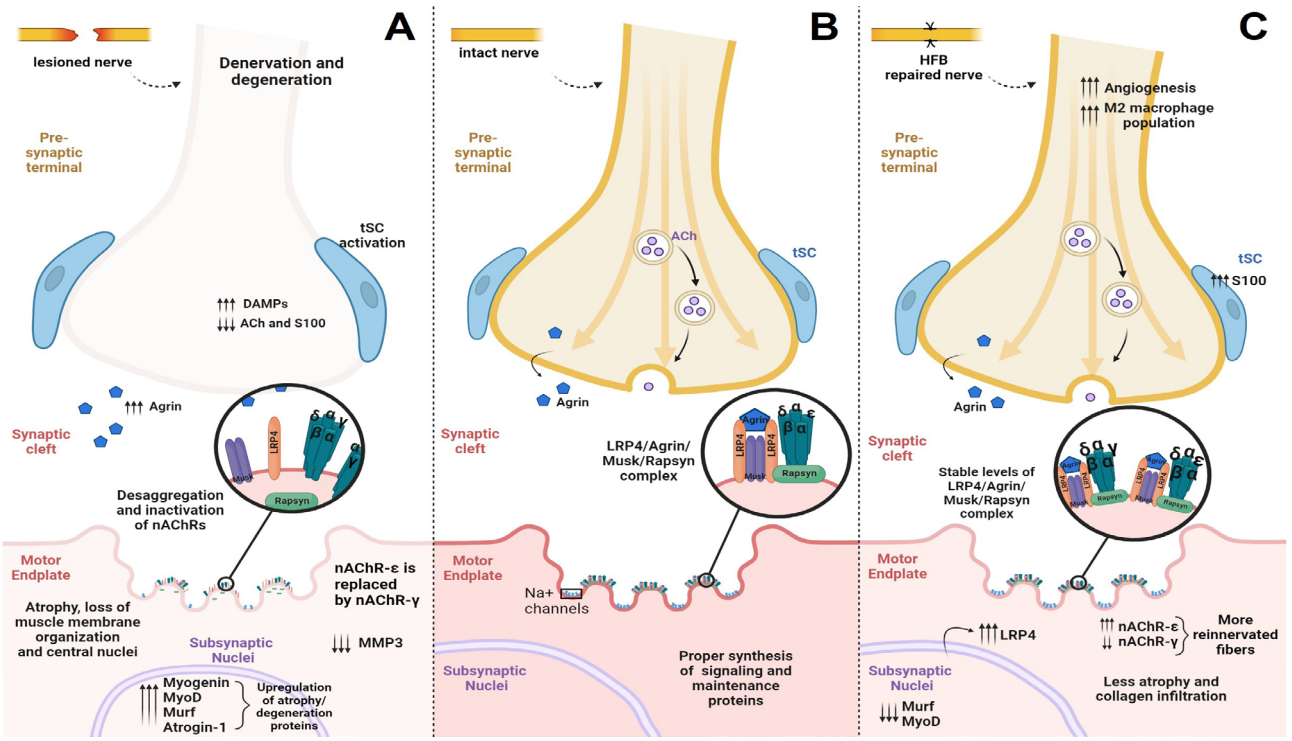


Figure 3. Cellular and molecular events associated with muscle denervation and repair at the neuromuscular junction level. **(A)** Denervated, **(B)** healthy, and **(C)** HFB repaired neuromuscular junction. Following nerve injury, all components of the NMJ are hindered and the Agrin/LRP4/Musk/Rapsyn signaling pathway plays a significant role in the nAChRs cluster formation and NMJ maintenance.

tSCs also maintain NMJ organization by secreting substrates that regulate postsynaptic proteins, such as MMP3, which is involved in basal lamina and endplate integrity [66, 70]. In the maintenance of postsynaptic structures, other muscle-related proteins play a crucial role, as it has been demonstrated that the prevention of denervation is associated with the increased expression of MuSK, Dok7, and those involved in the ubiquitin-proteasome pathway, such as MURF-1 and atrogin-1 [10, 28]. The shift of gamma to the epsilon subunit in the nAChR serves as an indicator of regeneration, as it occurs only after reinnervation and differentiation of the myotube.

Altogether, major cellular and molecular events take place and deprive not only the associated nerve, Schwann cells, and muscle fibers but also the endplate, eliciting a series of retrograde and anterograde signals that, even with morphological regeneration of axons, can result in no definitive association with functional recovery. Understanding the therapeutic niche in the NMJ, as an end-gate player, is essential to provide positive outcomes after reinnervation, which includes not only reinnervation through the arrival of regenerating axons to denervated postsynaptic muscle domains but also its capability of synaptic activation (Figure 3B).

Approaches to peripheral nerve repair

In recent years, several approaches have been tested and used to restore functionality to the injured nerve [71, 72]. Most experimental models use rodents performing surgical lesions of the facial, ulnar, or sciatic nerves [73]. Treatments that result in complete morphologic and functional recovery are still a challenge for medical-surgical practice. The main difficulties are related to nerve reconnection and regeneration itself, in which regenerating axons fail to select their original endoneurial tubes [51], local revascularization, prolonged period of injury without medical intervention, progressive loss of regenerative character in Schwann cells, and atrophy of the innervated organs [51, 74–76].

Among the techniques for correcting nerve transection, end-to-end neurorrhaphy is the gold standard [46]. This type of neurorrhaphy is only possible when the nerve stumps are preserved, visible, and intact, without tissue loss, and there is no tension for re-approximation and reconnection of the stumps [11]. When such favorable characteristics for reconnection are not present, other techniques are used, including end-to-side neurorrhaphy [77], grafts and conduits [10, 22], and the use of tissue repair adjuvants such as fibrin sealants [78] and photobiomodulation [79].

Over the years, suture materials and techniques have presented problems and limitations, which motivated research on adhesive materials that can bond tissues. The first research on hemostatic and adhesive agents began around 1940, during World War II when fibrin glue was proposed. The fibrin glues or sealants, which can connect tissues more quickly, are important as they promote tissue adhesion and hemostasis [7]. At that time, a mixture of

human fibrinogen and thrombin was mainly applied to areas of skin affected by war wounds. The structural characteristics of fibrin(ogen) can be encapsulated by the processes of fibrin polymerization and cross-linking. These processes facilitate a multitude of biological functions, which include, but are not limited to, thrombin binding, fibrinolysis, the control of coagulation protein activity, the binding of growth factors, and interactions with various cells [80].

In the 1970s, the concept of fibrin glue was re-evaluated, leading to the introduction of the first commercial sealant, *Tisseel* (Baxter International, Inc., Deerfield, IL), containing human fibrinogen and bovine thrombin. These sealants have been successfully marketed for years [72, 81, 82]. However, its commercialization was suspended and its use was prohibited in the USA by the Food and Drug Administration (FDA) agency in 1978, due to the risk of transmission of infectious diseases conveyed by human blood-derived products [7, 82]. In the early 1980s, the discovery of the human immunodeficiency virus added credibility to the FDA's position, which feared widespread viral transmission [8]. However, in May 1998, the FDA revoked the suspension and approved the clinical application of fibrin sealants in the USA, when they were once again marketed [8].

Fibrin sealants are adhesive substances that mimic the final stages of blood coagulation. They form a stable, physiological fibrin clot which aids in wound repair. In addition to this, they serve two other primary functions. Firstly, they provide physical support for the extracellular matrix. Secondly, they facilitate the delivery of treatment compounds. This is made possible by their capacity to maintain the biochemical factors and original properties of implants [80, 83–85]. Therefore, they reduce the risk of bleeding, allow for the use of fewer sutures, and protect the injured environment against infections by microorganisms [85, 86]. They also allow for a decrease in inflammatory reactions, a lower incidence of trauma due to sutures [1, 78], and faster surgery and recovery, due to easy and fast applications in emergency conditions, allowing for a non-experienced surgeon to perform the repair. Whitlock et al. [87] investigated experienced and novice surgeons regarding the speed and quality of nerve repair in rodents, and showed a shorter surgery time in both scenarios with sealant repair, instead of sutures, and still, equivalent quality in sealant repairs between surgeons, demonstrating a faster learning curve.

In general lines, fibrin sealants are produced in two ways: from autologous or homologous blood derivatives. Autologous sealants use the patient's blood. Although they are biocompatible and do not present a risk of transmission of infectious diseases, they are not viable in surgeries and emergency applications. As an alternative, homologous fibrin sealants, produced by a pool of human blood, have been used. However, in these cases, there are risks of transmission of infectious diseases such as hepatitis, HIV, and human parvovirus [14]. In addition to having a high cost of raw materials, with a need for blood extraction of bovine or human thrombin and human fibrinogen. Due to their composition with human blood, another common problem is rapid fibrinolysis, which starts less than 24 hours after application and prematurely detaches the nerve stumps [14].

Even with its not-so-recent introduction in human clinics, there is still no consensus on the use and efficacy of fibrin sealants for nerve repair, with a predominance in the literature of studies with rodent models, and few evaluations in humans [9, 78]. The use of sealants is still not approved by regulatory agencies such as the FDA for nerve repair, but the interest in this therapy, not only for nerve reconstruction, is growing. In a study with American surgeons, Owosu et al. [88] showed that a portion of them already use or consider using fibrin sealants in repairs, although there is still a preference for suturing as the main repair technique. The lack of data on the results and knowledge of the treatments were identified as the main barriers to the use of adjuvant therapies. However, most surgeons are open to the possibility.

Regarding efficiency in nerve repair, several studies show beneficial effects associated with the application of sealants, alone or with sutures, at the site of the injury. A systematic review conducted by Sameem and collaborators [78] supports, with the majority of studies in rodents, an equal, if not superior, performance in repair with fibrin sealants compared to micro-sutures only, based on histopathological, biomechanical, and electrophysiological characteristics. However, in treatments with sealant only, cases with difficulties such as complete failure and gaps in neural reconnection were also observed. A recent systematic analysis [9] indicates that nerve regeneration may be similar in fibrin glue repairs and/or suture repairs, but the use of fibrin glue significantly reduced operation times, which may pose both clinical and economic benefits. However, fibrin glue alone was reported to result in lower strength and more dehiscence [9, 89].

Until today, commercially available fibrin sealants are produced from both bovine and human thrombin and fibrinogen (homologous), which present disadvantages and risks, so that in addition to being transmitters of infectious diseases, they can generate fibrosis, toxicity, and necrosis [1]. They can also lead to the development of antibodies against bovine thrombin, and anaphylactic reaction to bovine proteins, among other adverse reactions [7, 82].

HFB in nerve repair

Considering the disadvantages present in commercially available fibrin sealants, a group of researchers from the Center for the Study of Venoms and Venomous Animals (CEVAP) at São Paulo State University, Botucatu, São Paulo, Brazil, began to standardize a new fibrin sealant in the 1990s. The HFB is a unique heterologous fibrin worldwide, as it does not use human blood, and does not transmit infectious diseases. In addition, it is a natural, biodegradable, bioabsorbable, and non-toxic biopharmaceutical with excellent adhesive capacity, and can be used in several surgical procedures.

Compared to other clinically used commercial fibrin sealants, it has a low production cost, high availability of raw materials for its manufacture, and the possibility of adapting its formulation according to the type of procedure [82]. Its formulation allows its use in clinical medicine and various surgical procedures, such as skin grafts and surgical reconstructions, aiding in hemostasis, colostomy, and suture reinforcement [11, 14]. Furthermore, its healing power was tested in 40 patients of a phase I/II clinical trial for the treatment of chronic venous ulcers. Clinical results showed it as a safe, non-immunogenic product with promising efficacy. This is because there was an improvement in the quality of the ulcer bed, a significant reduction in the ulcer area, and healing in several patients [90, 91].

In the last years, HFB has been used in association with sutures (Figure 4) and other therapeutic factors to enhance or face difficulties in the current gold-standard treatment for nerve injury. Generally, in the face of a nerve transection, the application of HFB demonstrated positive results in reducing mechanical trauma to the nerve (points of suture) [23], obtained better or similar morphological and/or molecular performance when adjunct to traditional suture [7, 13, 23, 25], demonstrated easy usability with good adhesive capacity [17], and good biocompatibility with other materials [26, 92] (Figure 3C). Its healing power has been gaining attention and demonstrated valuable potential as an adjunct to enhance regeneration and motor function (Table 2).

Adjunct to suture alone

For short nerve injury gaps (< 1 cm), neurorrhaphy is commonly employed, repairing both proximal and distal ends, but the use of sutures can lead to inflammatory reactions such as granuloma and neuroma formation. In the last years, our group has been

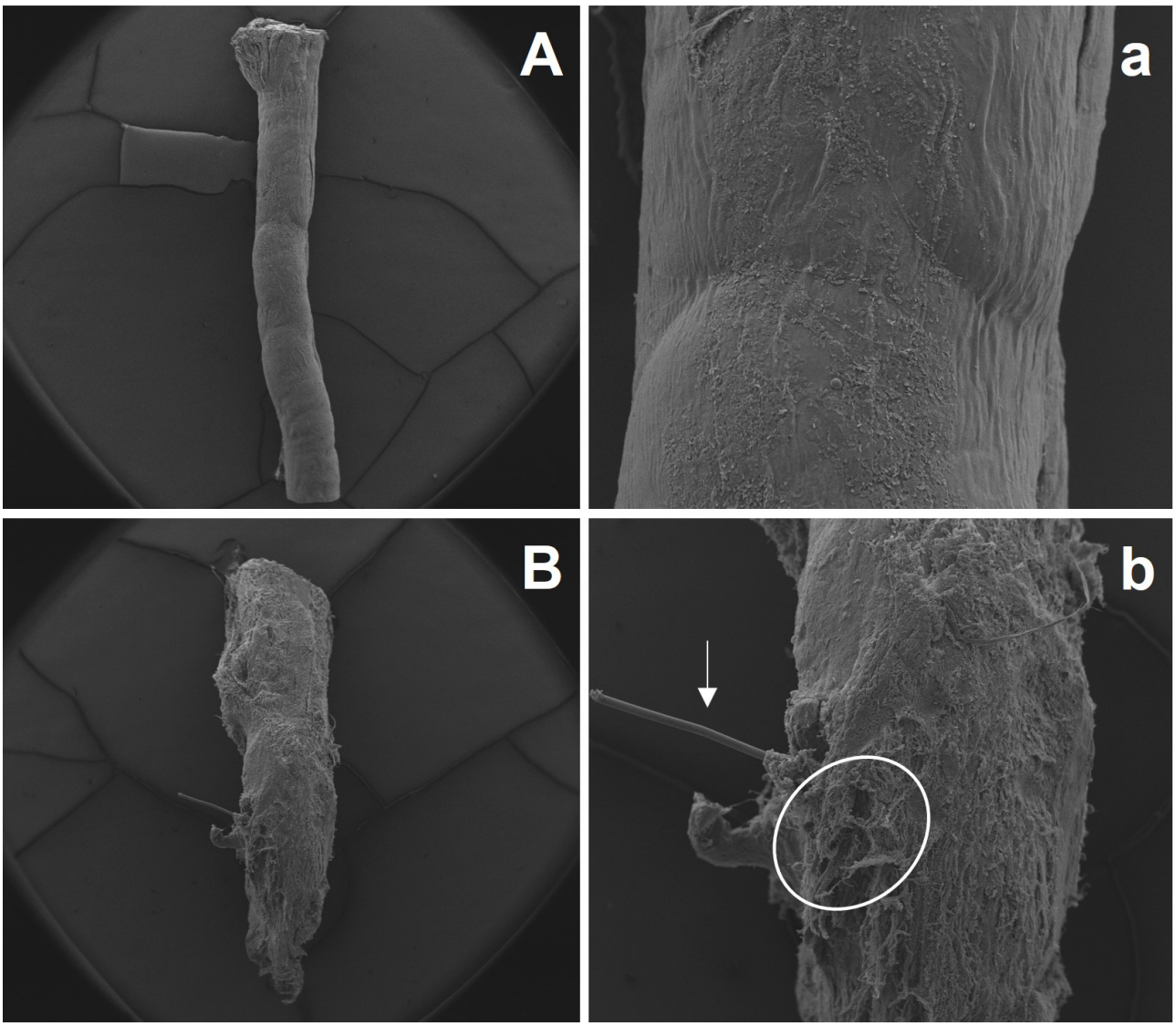


Figure 4. Nerve integrity of healthy and HFB-repaired nerves. Scanning electron microscopy of **(A)** healthy and **(B)** HFB-repaired nerves. Surface detail of epineurium can be seen in **a** and **b**. White arrow: nylon suture thread; white circle: HFB-associated connective tissue.

Table 2. Current strategies and potential therapeutic strategies aligned to HFB use for traumatic peripheral nerve injury.

Strategies (neurorrhaphy)	Intervention	Comments
Alone [13, 17, 19, 20, 23, 25, 93]	HFB as an adjunct to 1 to 3 stitches	HFB demonstrated angiogenic, neuroprotective, and immunomodulatory properties, which can enhance tissue regeneration, motor function, and wound healing, but satisfactory outcomes have not yet been achieved. The use of HFB also reduces trauma and the number of stitches.
Nerve conduit [10, 18, 26]	HFB embedded tubulization with suture	This association suggests a trophic action of the treatment, potentially accelerating regeneration through an increase in regeneration-associated factors, such as those related to Schwann cell reactivity (S100) and Agrin/Rapsyn/LRP4/Musk signaling pathway for the NMJ maintenance. Polycaprolactone has demonstrated good biocompatibility with HFB, surpassing other fibrin sealants.
Cell-based Therapy [16, 18, 22, 26, 94–96]	HFB as a scaffold for Embryonic Stem Cells, Mesenchymal Stem Cells, and Mononuclear Cells	HFB improves the effects of cell therapy by promoting an environment that enhances each particular scenario, such as growth factors release, and increased cell survivability resulting in neuroprotection.
Photobiomodulation [17, 19, 20, 93]	HFB as an adjunct to Low-level laser therapy with and without suture	HFB in association with LLLT has demonstrated a strong capability to accelerate myelination and functional recovery of innervated muscles. HFB allows nerve manipulation without trauma and enhances the nerve regeneration process.

studying the effects of combining HFB with neurorrhaphy, also shading light to the NMJ recovery (Figure 5). HFB plays a crucial role in the healing process as the combination of fibrin with proteins enhances angiogenesis, wound contraction, collagen synthesis, and re-epithelialization. Further, it was able to reduce trauma in reconstruction to minimize the damage and inflammatory responses.

In a recent study, we demonstrated the early beneficial effects of the use of HFB in conjunction with two sutures for the repair of transected sciatic nerves in rats [13]. HFB application in comparison to suture alone improved overall nerve regeneration, with increased axonal growth and tissue vascularization (angiogenesis), proper restoration of neuromuscular junctions, reduced severe muscle degeneration (collagen infiltration), and enhanced relative area of M2 markers, 7 and 30 days after reconstruction. Remarkably, macrophages play a significant role in phagocytosis and cytokines releasement in the denervated NMJ immune response, and its balance between pro- and anti-inflammatory effectors at different phases of NMJ reinnervation appears to be crucial [64].

Sixty days after nerve reconstruction [23], with a 7-day interval between sciatic nerve injury and neurorrhaphy after 60 days of reconstruction, the association of HFB with one suture point showed restoration of nerve impulse and better axonal regeneration than suture alone. Ultra-structurally, the NMJs and associated muscle fibers of the HFB-treated groups showed proper regeneration. In this same study design [25], the use of HFB associated with a single suture point, compared to two suture points, reduced surgical time and showed potential to restore the microstructure of NMJs, as less degeneration was present and nAChRs/proteins associated with the mature pattern were observed to return. In addition, immature receptor values (γ) in the HFB group were lower than those in the suture-only group.

Multimodal approaches (cell-based therapies and nerve conduits)

Another therapeutic option for nerve injury is the use of nerve conduits, which serve as a bridge between the proximal and distal stumps, providing a scaffold for axonal regeneration [1]. This approach prevents intrusion of nearby tissues, guides the regeneration, and makes the repair site less prone to infiltration by fibroblasts and adverse inflammation, which may decrease fibrosis and improve overall nerve mobility [3]. HFB has already been associated with nerve conduit strategies and has demonstrated good biocompatibility with the polycaprolactone (PCL) grafts, which has been a challenge for other commercially available fibrin sealants [26], improving general regeneration (Table 2).

Our group used a PCL graft in addition to one suture point associated with HFB [10], and after 90 days of nerve reconstruction, although not fully regenerated, as indicated by the nAChR cluster area, the compactness and endplate area of NMJs in the treated group were the only similar the Control, suggesting a better morphological approximation between the groups. Notably, it also demonstrated an increase in the expression of LRP-4, S100, and nAChR-ε proteins, and a decrease in MyoD, suggesting a positive influence on the neurodegenerative process, where the LRP-4 activates tSC, thus maintaining higher reinnervation of nAChRs and reducing muscle atrophy. The treatment favored a faster recovery in motor function assessment by improving print area when compared to suture alone. Indeed, the nerve guidance with HFB also enabled an approximation to the control group in terms of protein expression of Agrin, LRP-4, Musk, and Rapsyn.

Another promising augmentation method is cell-based therapy, which is a way of enhancement that can speed up the self-healing process and is currently under extensive research for stimulating regeneration after nerve injury [98]. The therapy

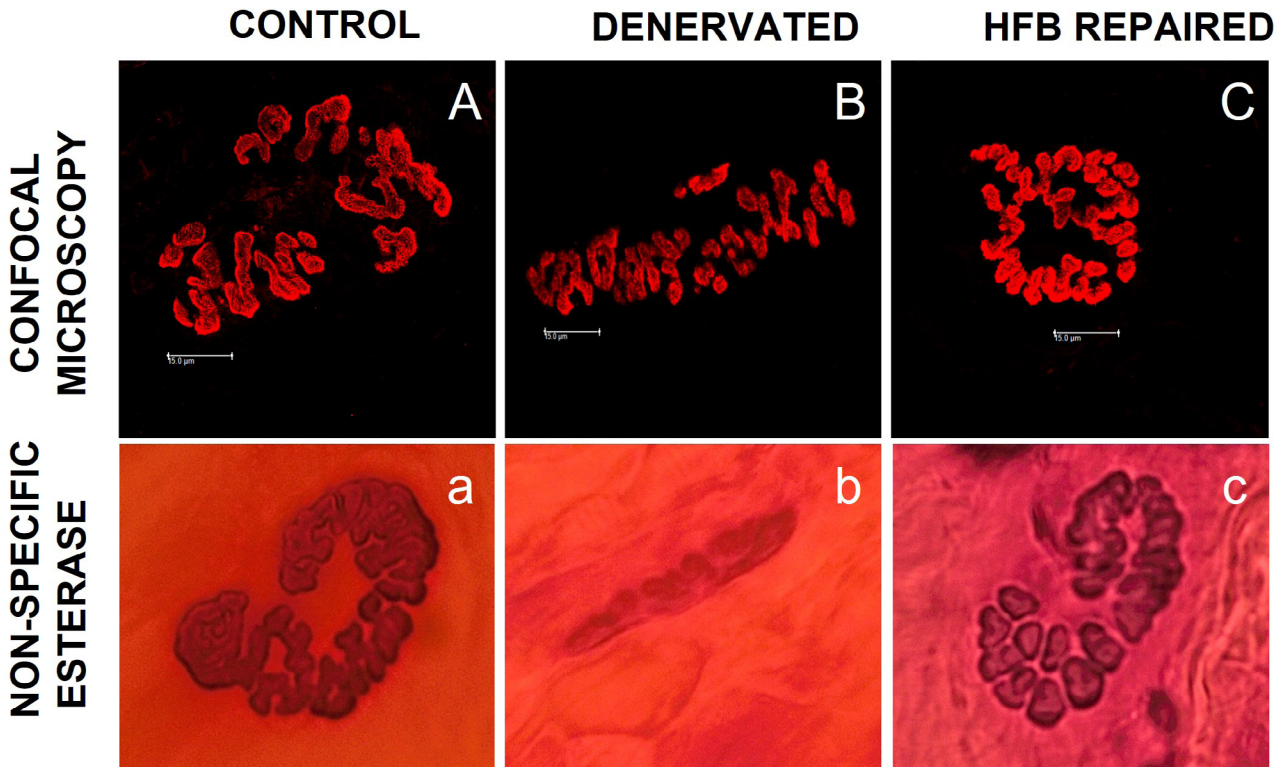


Figure 5. Neuromuscular junction morphology. **(A, a)** Healthy, **(B, b)** denervated, and **(C, c)** HFB repaired states, through nAChRs staining (confocal microscopy) with alpha-bungarotoxin conjugated with rhodamine and by non-specific esterase staining, which is based on the marking of positive esterase sites that contain AChE, leading to visualization of the entire NMJ morphology [97].

employs stem cells due to their inherent ability to self-replicate and differentiate into specific cell types [1], which culminates in the release of neurotrophic growth factors and the myelination of axons. Schwann cells, the primary functional cells of the peripheral nervous system that promote myelination and regeneration, are the preferred initial seed cells, but other cell types have also been used and have achieved remarkable results [99]. For successful cell transplantation and adhesion at the injury site, an appropriate scaffold is necessary. HFB has demonstrated good biocompatibility, while further enhancing the power of regeneration-associated factors of the cell lineage and also improving the survival of the cells (Table 2).

The first study utilizing this association was conducted by Mozafari et al. [22], who observed axonal regeneration and sensory function improved using HFB with embryonic stem cells in a rodent model 60 days after sciatic nerve injury, where the combined effect was successful in supporting Schwann cells at the injury site and HFB facilitated the application and stabilization of the stem cells. In another study, Rodrigues-Sanchez et al. [26] used HFB as a base for PCL graft and canine adipose mesenchymal stem cells, observing that this multimodal approach supports the trophic microenvironment, resulting in a pro-regenerative state after critical sciatic nerve injury in rats. The treatment incorporated in HFB demonstrated enhanced motor function and electrophysiological recovery compared to the PCL group after 12 weeks. These results were linked to a change in the regeneration process favoring the development of myelinated fibers. HFB is demonstrated to be very permissive for use in conjunction with stem cells, allowing for an even more efficient regenerative process [92]. Further, Cartarozzi et al. [18] observed similar results engrafting HFB with mesenchymal stem cells in PCL conduits, where this association resulted in better reactivity of the glial cells leading to better regeneration and compacting of myelinated axons, as well as functional improvement in gait recovery. It was also observed that HFB enabled the survival of the cells seeded in the tubular prosthesis.

Photobiomodulation

Also known as LLLT, photobiomodulation is an emerging therapy that is increasingly being used for rehabilitation and functional restoration following injuries. The therapeutic effects of LLLT are linked to tissue biostimulation. This therapy triggers photoenergetic and photochemical reactions, leading to an increase in DNA and RNA synthesis within the cell nucleus [100]. In turn, this promotes cell proliferation and protein synthesis, including alterations in the action potential of nerve cells. For the treatment of nerve injuries, it has been reported that this therapy stimulates myelination and axon regrowth by promoting Schwann cell proliferation [101]. In recent years, this technique has been studied in association with HFB, which has shown promising results, as HFB minimizes trauma and together exhibits strong regenerative power.

The initial study investigating this association was carried out by Buchaim et al. [17]. This study, which also involved a nerve graft, noted the collateral regeneration of axons from the vagus nerve into the autologous graft in all groups, but HFB+LLLT had enhanced myelination. In a subsequent study, Buchaim et al. [19] reported a comparable improvement in axonal recovery of the facial nerve post-suturing with the HFB-repaired group, which showed the closest results to the control in all nerve measurements. Additionally, the use of HFB facilitated the coaptation of the stumps without causing trauma to the nerve fibers. Further, Rosso et al. [20], also in a facial nerve model, observed better morphofunctional results in sutures or coaptation with HFB associated with LLLT, with an advantage in reducing trauma in the HFB group. In another recent study, this approach improved axonal growth in the stump distal to the lesion and minimized the atrophy on innervated muscles after experimental facial nerve transection [93]. HFB+LLLT had positive effects on the morphological and functional stimulation of the nerve, with the greatest regeneration for axon area and diameter.

Photobiomodulation and HFB were also assessed in other regenerative approaches, such as in bone, tendon, and skin repair [102–104]. All these investigations have revealed positive outcomes, underscoring the potential enhancement achievable through the synergistic use of HFB with other therapies. Unfortunately, no data was obtained regarding the NMJ regeneration process.

HFB in spinal cord injuries

Due to the proximity between the CNS and PNS interface, learnings can be made for the treatment of nerve injuries based on the use of HFB in CNS lesions, which has also been a hot topic approach. Spinal cord injuries result in a significant loss of motor and sensory functions. Ventral root avulsion, an experimental model, involves the detachment of the ventral (motor) roots from the spinal cord's surface. This leads to numerous morphological alterations, including the degeneration of motoneurons and rearrangements in the local spinal cord circuitry. Further, it has several commonly observed pathologies for nerve injury, such as WD.

In a rat ventral root avulsion model, Barbizan et al. [12] demonstrated that the root replantation with HFB enhanced motor recovery preserved the synaptic covering of the motoneurons, and improved neuronal survival. Barbizan et al. [16] further demonstrated that ventral root avulsion repair with HFB as a scaffold for mononuclear cells enhanced motoneuron survival and neurotrophic factor expression levels. In the same model, Spejo et al. [21] reported a potential immunomodulatory effect with increased expression of M2 macrophage marker genes and pro- and anti-inflammatory cytokines, along with greater neuronal survival when combined with HFB reconstruction. Kempe et al. [24] demonstrated a 50% increase in motor function, neuronal and synaptic survival, and immunomodulatory effects with the use of HFB, compared to its absence when combined with dimethyl fumarate after ventral root avulsion. Kempe et al. [27] further demonstrated the preservation of alpha motor neuron synapses and survivability of its associated sciatic nerve with spouting and restoration of proper myelination and axon diameters by the combined treatment through ultrastructural evidence. Paes et al. [105] used HFB as a scaffold for human dental pulp stem cells for reimplantation after ventral root avulsion and also observed higher neuronal survivability and downregulation of glial reactivity, while also enhancing motor function in catwalk analysis.

All those works, for both peripheral and CNS injuries, highlight the HFB potential as an excellent scaffold for adjunct stem cell therapy and drug delivery systems. Indeed, the treatment of motor neuron injuries with HFB demonstrated improvement in tissue regeneration and motor function, although, in a different environment, the axon regeneration process was also enhanced.

Limitations and difficulties

Based on these presented studies and current strategies, which investigate the HFB association with nerve regeneration, further combinations with other therapies, such as regeneration-associated factors (growth factors), may enhance positive benefits. HFB readily allows for the encapsulation of bioactive complexes in its formulation, including growth factors, cytokines, drugs, and nucleic acids, which may further improve the therapy effect. Further, although remarkable results have been achieved with cell therapy, no studies have been conducted using Schwann cells, which are the most studied therapeutic model for nerve injury.

In relation to HFB volume, there is no current consensus on when it is used in nerve repair. The values range from 100 µL (2 drops) to 500 µL (10 drops). Despite this variability, it is believed that the healing effect, or the support provided by the scaffold therapy may not be compromised.

Regarding NMJ regeneration, no data was found on its association with cell therapy and photobiomodulation. Studies of the NMJ are crucial to understanding the sequence that extends from the central stimulus to the nerve-muscle tissue targets; this is particularly important as most therapies, while offering certain morphologic benefits, also present limitations related to motor function. The neuromuscular plasticity observed following nerve injuries and the subsequent reinnervation of muscles is remarkable, however, this may not be sufficient to restore fine movements due to the considerable misdirection of regenerating nerve fibers and failures or insufficiencies in NMJ reinnervation following injuries.

Another challenge lies in the development of pharmaceuticals that adhere to good manufacturing practices and produce consolidated, reproducible batches. To address this, CEVAP

is launching the first Brazilian Contract Development and Manufacturing Organization (CDMO) [106]. This organization will provide services to both the public and private sectors by producing validated samples for clinical trials and offering academic training in translational science research. Furthermore, CEVAP is currently seeking support to conduct a Phase III multicenter clinical trial to validate the HFB findings, register with the Brazilian Health Regulatory Agency, and distribute the product throughout Brazil via the Unified Health System network.

Conclusion

Peripheral nerves inherently possess the ability to heal after an injury. Fibrin sealants have proven to be valuable in regenerative and surgical applications, particularly in cases of nerve injury. However, there's a limited recovery window before tissue degeneration obstructs the regeneration process and reconnection to the target. Despite the high costs and use of human blood associated with commercial sealants, HFB presents as a viable alternative. The use of HFB, in conjunction with conventional sutures, has been shown to enhance this regenerative effect, also reducing the number of suture points and surgical time. Moreover, HFB has an enhancing potential as a scaffold for other adjunct therapies, such as cell-based therapies and drug delivery systems, further improving the regenerative process.

Heterologous fibrin biopolymer provides a more conducive regenerative environment for nerves, muscles, and associated NMJs compared to sutures alone and has several advantages in relation to other fibrin sealants. Indeed, it has demonstrated a good capability of maintaining a less degenerated NMJ microenvironment and promoting early onset regeneration after injury. While clinical trials are necessary to establish definitively the benefits of fibrin sealants in human nerve repair, HFB shows significant promise as a potent bioproduct ready for clinical trials and eventual integration into clinical settings. Further research is warranted to determine if its use over extended periods post-treatment could lead to improved functional outcomes. The CMDO initiative will facilitate the translation of biopharmaceuticals from bench to bedside and pave the way for the international expansion of HFB.

Abbreviations

NMJ: neuromuscular junction; HFB: heterologous fibrin biopolymer; CNS: central nervous system; Sb: synaptic button; ACh: acetylcholine; CEVAP: Center for the Study of Venoms and Venomous Animals; CMDO: contract development and manufacturing organizations; nAChRs: nicotinic acetylcholine receptors; tSC: terminal Schwann cell; AChE: acetylcholinesterase; MMP3: matrix metalloproteinase 3; NCAMS: neural cell adhesion molecules; WD: Wallerian degeneration; DAMPs: damage-associated molecular patterns; TNF: tumor necrosis factor; IL-: interleukin; M1: pro-inflammatory type 1 macrophages; M2: anti-inflammatory type 2 macrophages; VEGF-A: vascular endothelial growth factor; MuSK: muscle-specific kinase; Dok7: docking protein 7; FDA: Food and Drug Administration; HIV: human immunodeficiency virus; LLLT: low-level laser therapy; PCL: polycaprolactone; PNS: peripheral nerve system; MC: mononuclear cells; MSCs: mesenchymal stem cells; IA: intramedullary axotomy; hESCs: human embryonic stem cells; DF: dimethyl fumarate; BBFN: buccal branch of the facial nerve; PBM: photobiomodulation.

Acknowledgments

The authors are grateful to Dr. André Bombeiro (Instituto de Medicina Molecular João Lobo Antunes, Lisbon, Portugal) for the critical reading of the manuscript.

Availability of data and materials

Not applicable

Funding

This study was supported by the São Paulo Research Foundation (FAPESP), which conceived a scholarship to KSM (2022/0755-1) and supported the Center for Translational Sciences and Biopharmaceuticals Development, Botucatu, SP, Brazil (2021/11936-3). BB is a National Council for Scientific and Technological Development (CNPq, Brazil) PQ2 research fellow No. 306339/2020-0, and RSFJr is a CNPq PQ1C research fellow No. 303224/2018-5. The funding sources were not involved in the research conduction, preparation, and decision to submit the manuscript.

Competing interests

RSFJr and BB are, respectively, editor-in-chief and emeritus editor of the Journal of Venomous Animals and Toxins including Tropical Diseases. They did not get involved in the peer review process of this manuscript.

Authors' contributions

KSM conceived the study and conducted the selection interpretation of the data, design, and writing. FCT, BB, RSFJr, and SMMM contributed to the writing, revision, and selection of studies. All authors read and approved the final manuscript.

Ethics approval

Not applicable.

Consent for publication

Not applicable.

Reference

1. Hussain G, Wang J, Rasul A, Anwar H, Qasim M, Zafar S, Aziz N, Razzaq A, Hussain R, de Aguilar JLG, Sun, T. Current Status of Therapeutic Approaches against Peripheral Nerve Injuries: A Detailed Story from Injury to Recovery. Int J Biol Sci. 2020 Jan 1;16(1):116-34.
2. Jones S, Eisenberg HM, Jia X. Advances and Future Applications of Augmented Peripheral Nerve Regeneration. Int J Mol Sci. 2016 Sep 7;17(9):1494.
3. Wang ML, Rivlin M, Graham JG, Beredjiklian PK. Peripheral nerve injury, scarring, and recovery. Connect Tissue Res. 2019;60(1):3-9.
4. Fu SY, Gordon T. Contributing factors to poor functional recovery after delayed nerve repair: prolonged axotomy. J Neurosci. 1995;15(5 Pt 2):3876-85.
5. Chan KM, Gordon T, Zochodne DW, Power HA. Improving peripheral nerve regeneration: from molecular mechanisms to potential therapeutic targets. Exp Neurol. 2014 Nov;261:826-35.
6. Robinson PP, Loescher AR, Smith KG. A prospective, quantitative study on the clinical outcome of lingual nerve repair. Br J Oral Maxillofac Surg. 2000;38(4):255-63.
7. Barros LC, Ferreira RS, Barraviera SR, Stolf HO, Thomazini-Santos IA, Mendes-Giannini MJ, Toscano E, Barraviera B. A new fibrin sealant from *Crotalus durissus terrificus* venom: applications in medicine. J Toxicol Environ Health B Crit Rev. 2009;12(8):553-71.
8. Fattahi T, Mohan M, Caldwell GT. Clinical applications of fibrin sealants. J Oral Maxillofac Surg. 2004;62(2):218-24.
9. Koopman JE, Duraku LS, de Jong T, de Vries RBM, Michiel Zuidam J, Hundepool CA. A systematic review and meta-analysis on the use of fibrin glue in peripheral nerve repair: Can we just glue it? J Plast Reconstr Aesthet Surg. 2022;75(3):1018-33.
10. Leite APS, Pinto CG, Tibúrcio FC, Muller KS, Padovani CR, Barraviera B, Ferreira Jr RS, Leal CV, Matsumura CY, Matheus SMM. Acetylcholine receptors of the neuromuscular junctions present normal distribution after peripheral nerve injury and repair through nerve guidance associated with fibrin biopolymer. Injury. 2023 Feb;54(2):345-61.
11. Biscola NP, Cartarozzi LP, Ulian-Benitez S, Barbizan R, Castro MV, Spejo AB, Ferreira Jr RS, Barraviera B, Oliveira ALR. Multiple uses of fibrin sealant for nervous system treatment following injury and disease. J Venom Anim Toxins incl Trop Dis. 2017;23:13. Epub 20170314. doi: 10.1186/s40409–017–0103–1.
12. Barbizan R, Castro MV, Rodrigues AC, Barraviera B, Ferreira RS, Oliveira AL. Motor recovery and synaptic preservation after ventral root avulsion and repair with a fibrin sealant derived from snake venom. PLoS One. 2013;8(5):e63260.
13. Tibúrcio FC, Muller KS, Leite APS, de Oliveira IRA, Barraviera B, Ferreira Jr RS, Padovani CR, Pinto CG, Matheus SMM. Neuroregeneration and immune response after neurorrhaphy are improved with the use of heterologous fibrin biopolymer in addition to suture repair alone. Muscle Nerve. 2023 Jun;67(6):522-36.
14. Buchaim DV, Cassaro CV, Shindo JVTC, Coletta BBD, Pomini KT, Rosso MPO, Campos LMG, Ferreira Jr RS, Barraviera B, Buchaim RL. Unique heterologous fibrin biopolymer with hemostatic, adhesive, sealant, scaffold and drug delivery properties: a systematic review. J Venom Anim Toxins incl Trop Dis. 2019;25:e20190038.
15. Page MJ, McKenzie JE, Bossuyt PM, Boutron I, Hoffmann TC, Mulrow CD, Shamseer L, Tetzlaff JM, Akl EA, Brennan SE, Chou R, Glanville J, Grimshaw JM, Hróbjartsson A, Lalu MM, Li T, Loder EW, Mayo-Wilson E, McDonald S, McGuinness LA, Stewart LA, Thomas J, Tricco AC, Welch VA, Whiting P, Moher D. The PRISMA 2020 statement: an updated guideline for reporting systematic reviews. BMJ. 2021 Mar;372(71).
16. Barbizan R, Castro MV, Barraviera B, Ferreira Jr RS, Oliveira AL. Influence of delivery method on neuroprotection by bone marrow mononuclear cell therapy following ventral root reimplantation with fibrin sealant. PLoS One. 2014;9(8):e105712.
17. Buchaim RL, Andreo JC, Barraviera B, Ferreira Junior RS, Buchaim DV, Rosa Junior GM, Oliveira ALR, Rodrigues AC. Effect of low-level laser therapy (LLLT) on peripheral nerve regeneration using fibrin glue derived from snake venom. Injury. 2015 Apr;46(4):655-60.
18. Cartarozzi LP, Spejo AB, Ferreira RS, Barraviera B, Duek E, Carvalho JL, Góes AM, Oliveira ALR. Mesenchymal stem cells engrafted in a fibrin scaffold stimulate Schwann cell reactivity and axonal regeneration following sciatic nerve tubulization. Brain Res Bull. 2015 Mar;112:14-24.
19. Buchaim DV, Rodrigues AeC, Buchaim RL, Barraviera B, Ferreira Jr RS, Rosa Junior GM, Bueno CRS, Roque DD, Dias DV, Dare LR, Andreo JC. The new heterologous fibrin sealant in combination with low-level laser therapy (LLLT) in the repair of the buccal branch of the facial nerve. Lasers Med Sci. 2016 Jul;31(5):965-72.
20. Rosso MPO, Rosa Júnior GM, Buchaim DV, German IJS, Pomini KT, de Souza RG, Pereira M, Favaretto Jr IA, Bueno CRS, Gonçalves JBO, Ferreira Jr RS, Barraviera B, Andreo JC, Buchaim RL. Stimulation of morphofunctional repair of the facial nerve with photobiomodulation, using the end-to-side technique or a new heterologous fibrin sealant. J Photochem Photobiol B. 2017 Oct;175:20-8.
21. Spejo AB, Chiarotto GB, Ferreira ADF, Gomes DA, Ferreira RS, Barraviera B, Oliveira ALR. Neuroprotection and immunomodulation following intraspinal axotomy of motoneurons by treatment with adult mesenchymal stem cells. J Neuroinflammation. 2018;15(230).
22. Mozafari R, Kyrylenko S, Castro MV, Ferreira RS, Barraviera B, Oliveira ALR. Combination of heterologous fibrin sealant and bioengineered human embryonic stem cells to improve regeneration following autogenous sciatic nerve grafting repair. J Venom Anim Toxins incl Trop Dis. 2018;24:11. Epub 20180412. doi: 10.1186/s40409–018–0147–x.
23. Leite APS, Pinto CG, Tibúrcio FC, Sartori AA, de Castro Rodrigues A, Barraviera B, Ferreira Jr RS, Filadelpho AL, Matheus SMM. Heterologous fibrin sealant potentiates axonal regeneration after peripheral nerve injury with reduction in the number of suture points. Injury. 2019 Apr;50(4):834-47.
24. Kempe PRG, Chiarotto GB, Barraviera B, Ferreira RS, de Oliveira ALR. Neuroprotection and immunomodulation by dimethyl fumarate and a heterologous fibrin biopolymer after ventral root avulsion and reimplantation. J Venom Anim Toxins incl Trop Dis. 2020;26:e20190093. Epub 20200520. doi: 10.1590/1678–9199–JVATITD–2019–0093.
25. Pinto CG, Leite APS, Sartori AA, Tibúrcio FC, Barraviera B, Ferreira Jr RS, Filadelpho AL, Carvalho SC, Matheus SMM. Heterologous fibrin biopolymer associated to a single suture stitch enables the return of neuromuscular junction to its mature pattern after peripheral nerve injury. Injury. 2021 Apr;52(4):731-7.
26. Rodríguez-Sánchez DN, Pinto GBA, Cartarozzi LP, de Oliveira ALR, Bovolato ALC, de Carvalho M, Silva JVL, Dernowsek JA, Golim M, Barraviera B, Ferreira Jr RS, Deffune E, Bertanha M, Amorim RM. 3D-printed nerve guidance conduits multi-functionalized with canine multipotent mesenchymal stromal cells promote neuroregeneration after sciatic nerve injury in rats. Stem Cell Res Ther. 2021 May 29;12(1):303.
27. Kempe PRG, de Castro MV, Khuriyeh VC, Barraviera B, Ferreira RS, de Oliveira ALR. Ultrastructural Evidence of Synapse Preservation and Axonal Regeneration Following Spinal Root Repair with Fibrin Biopolymer and Therapy with Dimethyl Fumarate. Polymers (Basel). 2023;15(15).
28. Zelada D, Bermedo-García F, Collao N, Henríquez JP. Motor function recovery: deciphering a regenerative niche at the neuromuscular synapse. Biol Rev Camb Philos Soc. 2021;96(2):752-66.
29. Jones RA, Harrison C, Eaton SL, Llavero Hurtado M, Graham LC, Alkhammash L, Oladiran OA, Gale A, Lamont DJ, Simpson H, Simmen MW, Soeller C, Wishart TM, Gillingwater TH. Cellular and Molecular Anatomy of the Human Neuromuscular Junction. Cell Rep. 2017 Nov 28;21(9):2348-56.
30. Rodríguez Cruz PM, Cossins J, Beeson D, Vincent A. The Neuromuscular Junction in Health and Disease: Molecular Mechanisms Governing Synaptic Formation and Homeostasis. Front Mol Neurosci. 2020;13:610964.
31. Sanes JR, Lichtman JW. Development of the vertebrate neuromuscular junction. Annu Rev Neurosci. 1999;22:389-442.
32. Hughes BW, Kusner LL, Kaminski HJ. Molecular architecture of the neuromuscular junction. Muscle Nerve. 2006;33(4):445-61.
33. Nishimune H, Shigemoto K. Practical Anatomy of the Neuromuscular Junction in Health and Disease. Neurol Clin. 2018;36(2):231-40.

34. Lepore E, Casola I, Dobrowolny G, Musarò A. Neuromuscular Junction as an Entity of Nerve-Muscle Communication. Cells. 2019;8(8).
35. Iyer SR, Shah SB, Lovering RM. The Neuromuscular Junction: Roles in Aging and Neuromuscular Disease. Int J Mol Sci. 2021;22(15).
36. Bloch-Gallego E. Mechanisms controlling neuromuscular junction stability. Cell Mol Life Sci. 2015;72(6):1029-43.
37. Sugiura Y, Lin W. Neuron-glia interactions: the roles of Schwann cells in neuromuscular synapse formation and function. Biosci Rep. 2011;31(5):295-302.
38. Ko CP, Robitaille R. Perisynaptic Schwann Cells at the Neuromuscular Synapse: Adaptable, Multitasking Glial Cells. Cold Spring Harb Perspect Biol. 2015;7(10):a020503.
39. Jablonka-Shariff A, Lu CY, Campbell K, Monk KR, Snyder-Warwick AK. Gpr126/Adgrg6 contributes to the terminal Schwann cell response at the neuromuscular junction following peripheral nerve injury. Glia. 2020;68(6):1182-200.
40. Patton BL, Miner JH, Chiu AY, Sanes JR. Distribution and function of laminins in the neuromuscular system of developing, adult, and mutant mice. J Cell Biol. 1997;139(6):1507-21.
41. Patton BL. Basal lamina and the organization of neuromuscular synapses. J Neurocytol. 2003;32(5-8):883-903.
42. Engel AG. The neuromuscular junction. Handb Clin Neurol. 2008;91:103-48.
43. Tintignac LA, Brenner HR, Rüegg MA. Mechanisms Regulating Neuromuscular Junction Development and Function and Causes of Muscle Wasting. Physiol Rev. 2015;95(3):809-52.
44. Ruff RL. Neurophysiology of the neuromuscular junction: overview. Ann N Y Acad Sci. 2003;998:1-10.
45. Conti-Fine BM, Milani M, Kaminski HJ. Myasthenia gravis: past, present, and future. J Clin Invest. 2006;116(11):2843-54.
46. Wu P, Chawla A, Spinner RJ, Yu C, Yaszemski MJ, Windebank AJ, Wang H. Key changes in denervated muscles and their impact on regeneration and reinnervation. Neural Regen Res. 2014 Oct 15;9(20):1796-809.
47. Ma J, Shen J, Garrett JP, Lee CA, Li Z, Elsaidi GA, Ritting A, Hick J, Tan KH, Smith TL, Smith BP, Koman LA. Gene expression of myogenic regulatory factors, nicotinic acetylcholine receptor subunits, and GAP-43 in skeletal muscle following denervation in a rat model. J Orthop Res. 2007 Nov;25(11):1498-505.
48. Grosman C, Auerbach A. Kinetic, mechanistic, and structural aspects of unliganded gating of acetylcholine receptor channels: a single-channel study of second transmembrane segment 12' mutants. J Gen Physiol. 2000;115(5):621-35.
49. Naguib M, Flood P, McArdle JJ, Brenner HR. Advances in neurobiology of the neuromuscular junction: implications for the anesthesiologist. Anesthesiology. 2002;96(1):202-31.
50. Unwin N. Nicotinic acetylcholine receptor and the structural basis of neuromuscular transmission: insights from Torpedo postsynaptic membranes. Q Rev Biophys. 2013;46(4):283-322.
51. Gordon T. Peripheral Nerve Regeneration and Muscle Reinnervation. Int J Mol Sci. 2020;21(22):8652.
52. Lubińska L. Patterns of Wallerian degeneration of myelinated fibres in short and long peripheral stumps and in isolated segments of rat phrenic nerve. Interpretation of the role of axoplasmic flow of the trophic factor. Brain Res. 1982;233(2):227-40.
53. Lindborg JA, Mack M, Zigmond RE. Neutrophils Are Critical for Myelin Removal in a Peripheral Nerve Injury Model of Wallerian Degeneration. J Neurosci. 2017;37(43):10258-77.
54. Gomez-Sanchez JA, Carty L, Iruarrizaga-Lejarreta M, Palomo-Irigoyen M, Varela-Rey M, Griffith M, Hantke J, Macias-Camara N, Azkargorta, Aurrekoetxea I, De Juan VG, Jefferies HBJ, Aspichueta P, Elortza F, Aransay AM, Martínez-Chantar M, Bass F, Mato JM, Mirsky R, Woodhoo A, Jessen KR. Schwann cell autophagy, myelinophagy, initiates myelin clearance from injured nerves. J Cell Biol. 2015;210(1):153-68.
55. Gaudet AD, Popovich PG, Ramer MS. Wallerian degeneration: gaining perspective on inflammatory events after peripheral nerve injury. J Neuroinflammation. 2011;8:110.
56. Moalem G, Xu K, Yu L. T lymphocytes play a role in neuropathic pain following peripheral nerve injury in rats. Neuroscience. 2004;129(3):767-77.
57. Zigmond RE, Echevarria FD. Macrophage biology in the peripheral nervous system after injury. Prog Neurobiol. 2019;173:102-21.
58. Cattin AL, Burden JJ, Van Emmenis L, Mackenzie FE, Hoving JJ, Garcia Calavia N, Guo Y, McLaughlin M, Rosenberg LH, Quereda V, Jamecna D, Napoli I, Parrinello S, Enver T, Ruhrberg C, Lloyd A. Macrophage-Induced Blood Vessels Guide Schwann Cell-Mediated Regeneration of Peripheral Nerves. Cell. 2015 Aug 27;162(5):1127-39.
59. Gordon T. Nerve Regeneration: Understanding Biology and Its Influence on Return of Function After Nerve Transfers. Hand Clin. 2016;32(2):103-17.
60. Rishal I, Fainzilber M. Axon-soma communication in neuronal injury. Nat Rev Neurosci. 2014;15(1):32-42.
61. Fu SY, Gordon T. The cellular and molecular basis of peripheral nerve regeneration. Mol Neurobiol. 1997;14(1-2):67-116.
62. Ma CH, Omura T, Cobos EJ, Latrémolière A, Ghasemlou N, Brenner GJ, van Veen E, Barret L, Sawada T, Gao F, Coppola G, Gertler F, Costigan M, Geschwind D, Woolf CJ. Accelerating axonal growth promotes motor recovery after peripheral nerve injury in mice. J Clin Invest. 2011 Nov;121(11):4332-47.
63. Sakuma M, Gorski G, Sheu SH, Lee S, Barrett LB, Singh B, Omura T, Latremoliere A, Woolf CJ. Lack of motor recovery after prolonged denervation of the neuromuscular junction is not due to regenerative failure. Eur J Neurosci. 2016 Feb;43(3):451-62.
64. Rios R, Jablonka-Shariff A, Broberg C, Snyder-Warwick AK. Macrophage roles in peripheral nervous system injury and pathology: Allies in neuromuscular junction recovery. Mol Cell Neurosci. 2021;111:103590.
65. Su HL, Chiang CY, Lu ZH, Cheng FC, Chen CJ, Sheu ML, Sheehan J, Pan HC. Late administration of high-frequency electrical stimulation increases nerve regeneration without aggravating neuropathic pain in a nerve crush injury. BMC Neurosci. 2018 Jun 25;19(1):37.
66. Chao T, Frump D, Lin M, Caiozzo VJ, Mozaffar T, Steward O, Gupta R. Matrix metalloproteinase 3 deletion preserves denervated motor endplates after traumatic nerve injury. Ann Neurol. 2013 Feb;73(2):210-23.
67. Palispis WA, Gupta R. Surgical repair in humans after traumatic nerve injury provides limited functional neural regeneration in adults. Exp Neurol. 2017;290:106-14.
68. Cisterna BA, Cardozo C, Sáez JC. Neuronal involvement in muscular atrophy. Front Cell Neurosci. 2014;8:405.
69. Guarino SR, Canciani A, Forneris F. Dissecting the Extracellular Complexity of Neuromuscular Junction Organizers. Front Mol Biosci. 2019;6:156.
70. VanSaun M, Humburg BC, Arnett MG, Pence M, Werle MJ. Activation of Matrix Metalloproteinase-3 is altered at the frog neuromuscular junction following changes in synaptic activity. Dev Neurobiol. 2007;67(11):1488-97.
71. Martins RS, Siqueira MG, Da Silva CF, Plese JP. Overall assessment of regeneration in peripheral nerve lesion repair using fibrin glue, suture, or a combination of the 2 techniques in a rat model. Which is the ideal choice? Surg Neurol. 2005;64(Suppl 1):S1:10-6.
72. Ray WZ, Mackinnon SE. Management of nerve gaps: autografts, allografts, nerve transfers, and end-to-side neurorrhaphy. Exp Neurol. 2010;223(1):77-85.
73. Wanner R, Gey M, Abaei A, Warnecke D, de Roy L, Dürselen L, Rasche V, Knoll B. Functional and Molecular Characterization of a Novel Traumatic Peripheral Nerve-Muscle Injury Model. Neuromolecular Med. 2017 Sep;19(2-3):357-74.
74. Sulaiman W, Gordon T. Neurobiology of peripheral nerve injury, regeneration, and functional recovery: from bench top research to bedside application. Ochsner J. 2013;13(1):100-8.
75. Jiang BG, Han N, Rao F, Wang YL, Kou YH, Zhang PX. Advance of Peripheral Nerve Injury Repair and Reconstruction. Chin Med J (Engl). 2017;130(24):2996-8.
76. Faroni A, Mobasseri SA, Kingham PJ, Reid AJ. Peripheral nerve regeneration: experimental strategies and future perspectives. Adv Drug Deliv Rev. 2015;82-83:160-7.
77. Viterbo F, Brock RS, Maciel F, Ayestaray B, Garbino JA, Rodrigues CP. End-to-side versus end-to-end neurorrhaphy at the peroneal nerve in rats. Acta Cir Bras. 2017;32(9):697-705.

78. Sameem M, Wood TJ, Bain JR. A systematic review on the use of fibrin glue for peripheral nerve repair. Plast Reconstr Surg. 2011;127(6):2381-90.
79. Rosso MPO, Buchaim DV, Kawano N, Furlanette G, Pomini KT, Buchaim RL. Photobiomodulation Therapy (PBMT) in Peripheral Nerve Regeneration: A Systematic Review. Bioengineering (Basel). 2018;5(2).
80. Bayer IS. Advances in Fibrin-Based Materials in Wound Repair: A Review. Molecules. 2022;27(14).
81. Isaacs JE, McDaniel CO, Owen JR, Wayne JS. Comparative analysis of biomechanical performance of available "nerve glues". J Hand Surg Am. 2008;33(6):893-9.
82. Ferreira RS, de Barros LC, Abbade LPF, Barraviera SRCS, Silvares MRC, de Pontes LG, dos Santos LD, Barraviera B. Heterologous fibrin sealant derived from snake venom: from bench to bedside - an overview. J Venom Anim Toxins incl Trop Dis. 2017;23:21. Epub 20170404. doi: 10.1186/s40409–017–0109–8.
83. Peretti GM, Randolph MA, Zaporojan V, Bonassar LJ, Xu JW, Fellers JC, Yaremchuk MJ. A biomechanical analysis of an engineered cell-scaffold implant for cartilage repair. Ann Plast Surg. 2001 May;46(5):533-7.
84. Ringe J, Kaps C, Burmester GR, Sittinger M. Stem cells for regenerative medicine: advances in the engineering of tissues and organs. Naturwissenschaften. 2002;89(8):338-51.
85. de Barros CN, Miluzzi Yamada AL, F Junior RS, Barraviera B, Hussni CA, de Souza JB, Watanabe MJ, Rodrigues CA, Alves ALG. A new heterologous fibrin sealant as a scaffold to cartilage repair-Experimental study and preliminary results. Exp Biol Med (Maywood). 2016 Jul;241(13):1410-5.
86. Buchta C, Dettke M, Funovics PT, Höcker P, Knöbl P, Macher M, Quehenberger P, Treiti C, Worel N. Fibrin sealant produced by the CryoSeal FS System: product chemistry, material properties and possible preparation in the autologous preoperative setting. Vox Sang. 2004;86(4):257-62.
87. Whitlock EL, Kasukurthi R, Yan Y, Tung TH, Hunter DA, Mackinnon SE. Fibrin glue mitigates the learning curve of microneurosurgical repair. Microsurgery. 2010;30(3):218-22.
88. Owusu A, Mayeda B, Isaacs J. Surgeon perspectives on alternative nerve repair techniques. Hand (N Y). 2014;9(1):29-35.
89. Tse R, Ko JH. Nerve glue for upper extremity reconstruction. Hand Clin. 2012;28(4):529-40.
90. Abbade LPF, Barraviera SRCS, Silvares MRC, Lima ABBC, Haddad GR, Gatti MAN, Medolago NB, Carneiro MTR, dos Santos LD, Ferreira Jr RS, Barraviera B. Treatment of Chronic Venous Ulcers With Heterologous Fibrin Sealant: A Phase I/II Clinical Trial. Front Immunol. 2021 Feb 23;12:627541.
91. Abbade LPF, Ferreira RS, Dos Santos LD, Barraviera B. Chronic venous ulcers: a review on treatment with fibrin sealant and prognostic advances using proteomic strategies. J Venom Anim Toxins incl Trop Dis. 2020;26:e20190101. Epub 20200622. doi: 10.1590/1678–9199–JVATITD–2019–0101.
92. Ortiz AC, Fideles SOM, Pomini KT, Bellini MZ, Pereira ESBM, Reis CHB, Pilon JPG, de Marchi MA, Trazzi BFM, da Silva WS, da Cunha MR, Buchaim WS, Cunha MR, Buchaim DV, Buchaim RL. Potential of Fibrin Glue and Mesenchymal Stem Cells (MSCs) to Regenerate Nerve Injuries: A Systematic Review. Cells. 2022 Jan 10;11(2):221.
93. Bueno CRS, Tonin MCC, Buchaim DV, Barraviera B, Ferreira Junior RS, Santos PSDS, Reis CHB, Pastori CM, Pereira ESBM, Nogueira DMB, Cini MA, Rosa Jr GM, Buchaim RL. Morphofunctional Improvement of the Facial Nerve and Muscles with Repair Using Heterologous Fibrin Biopolymer and Photobiomodulation. Pharmaceuticals (Basel). 2023 Apr 27;16(5):653.
94. Cassaro CV, Justulin LA, de Lima PR, Golim MA, Biscola NP, de Castro MV, Oliveira ALR, Doiche DP, Pereira EJ, Ferreira Jr RS, Barraviera B. Fibrin biopolymer as scaffold candidate to treat bone defects in rats. J Venom Anim Toxins incl Trop Dis. 2019 Nov 4;25:e20190027. Epub 20191104. doi: 10.1590/1678–9199–JVATITD–2019–0027.
95. Gasparotto VP, Landim-Alvarenga FC, Oliveira AL, Simões GF, Lima-Neto JF, Barraviera B, Ferreira Jr RS. A new fibrin sealant as a three-dimensional scaffold candidate for mesenchymal stem cells. Stem Cell Res Ther. 2014;5(3):78. Epub 20140610. doi: 10.1186/scrt467.
96. Orsi PR, Landim-Alvarenga FC, Justulin LA, Kaneno R, de Assis Golim M, Dos Santos DC, Creste CFZ, Oba E, Maia L, Barraviera B, Ferreira Jr RS. A unique heterologous fibrin sealant (HFS) as a candidate biological scaffold for mesenchymal stem cells in osteoporotic rats. Stem Cell Res Ther. 2017 Sep 29;8(1):205.
97. Muller KS, Tibúrcio FC, de Barros JWF, Matsumura CY, Matheus SMM. Statin exposure during pregnancy promotes neuromuscular junction alterations in postpartum Wistar rats. Muscle Nerve. 2023;67(6):537-47.
98. Zhang RC, Du WQ, Zhang JY, Yu SX, Lu FZ, Ding HM, Cheng YB, Ren C, Geng DQ. Mesenchymal stem cell treatment for peripheral nerve injury: a narrative review. Neural Regen Res. 2021 Nov;16(11):2170-6.
99. Hsu YC, Chen SL, Wang DY, Chiu IM. Stem cell-based therapy in neural repair. Biomed J. 2013;36(3):98-105.
100. Modrak M, Talukder MAH, Gurgenashvili K, Noble M, Elfar JC. Peripheral nerve injury and myelination: Potential therapeutic strategies. J Neurosci Res. 2020;98(5):780-95.
101. Lopes B, Sousa P, Alvites R, Branquinho M, Sousa AC, Mendonça C, Atayde LM, Luís AL, Varejão ASP, Maurício AC. Peripheral Nerve Injury Treatments and Advances: One Health Perspective. Int J Mol Sci. 2022 Jan 14;23(2):918.
102. de Freitas Dutra Júnior E, Hidd SMCM, Amaral MM, Filho ALMM, Assis L, Ferreira RS, Barraviera B, Martignago CCS, Figueredo-Silva J, Oliveira RA, Tim CR. Treatment of partial injury of the calcaneus tendon with heterologous fibrin biopolymer and/or photobiomodulation in rats. Lasers Med Sci. 2022 Mar;37(2):971-81.
103. Reis CHB, Buchaim RL, Pomini KT, Hamzé AL, Zattiti IV, Duarte MAH, Alcade MP, Barraviera B, Ferreira Jr RS, Pontes FML, Grandini CR, Ortiz AC, Fideles SOM, Eugênio RMC, Rosa Jr GM, Teixeira DB, Pereira ESBM, Pilon JPG, Miglino MA, Buchaim DV. Effects of a Biocomplex Formed by Two Scaffold Biomaterials, Hydroxyapatite/Tricalcium Phosphate Ceramic and Fibrin Biopolymer, with Photobiomodulation, on Bone Repair. Polymers (Basel). 2022 May 19;14(10):2075.
104. Buchaim DV, Andreo JC, Pomini KT, Barraviera B, Ferreira RS, Duarte MAH, Alcade MP, Reis CHB, Teixeira DB, Bueno CRS, Detregiachi CRP, Araujo AC, Buchaim RL. A biocomplex to repair experimental critical size defects associated with photobiomodulation therapy. J Venom Anim Toxins incl Trop Dis. 2022 Feb 14;28:e20210056. Epub 20220214. doi: 10.1590/1678–9199–JVATITD–2021–0056.
105. Paes SM, Castro MV, Barbosa RM, Politti Cartarozzi L, Coser LO, Kempe PRG, Decarli MC, Moraes AM, Barraviera B, Ferreira Jr RS, Oliveira ALR. Human dental pulp stem cell monolayer and spheroid therapy after spinal motor root avulsion in adult rats. Brain Res. 2023 Mar 1;1802:148229.
106. Ferreira RS, Morales MM, Barretti P, Barraviera B. Launching a CDMO in Brazil aiming to develop biopharmaceuticals for clinical trials. J Venom Anim Toxins incl Trop Dis. 2022;28:e20220017. Epub 20220606. doi: 10.1590/1678-9199-JVATITD-2022-0017.